

**DEVELOPMENT OF INJECTION MOULDED SELF-  
LUBRICATING SHORT-FIBRE REINFORCED  
COMPOSITES FOR USE AS PLAIN BEARING LINER  
MATERIALS IN AEROSPACE APPLICATIONS**

**Grant Dennis**

Thesis submitted in candidature  
for the degree of Doctor of Philosophy  
at Cardiff University

Cardiff School of Engineering  
Cardiff University

2016

---

## Declaration

This work has not previously been accepted in substance for any degree and is not being concurrently submitted in candidature for any degree.

Signed \_\_\_\_\_ (candidate)

Dated \_\_\_\_\_

### Statement 1

This thesis is being submitted in partial fulfilment of the requirements for the degree of PhD.

Signed \_\_\_\_\_ (candidate)

Dated \_\_\_\_\_

### Statement 2

This thesis is the result of my own independent work / investigation, except where otherwise stated. Other sources are acknowledged by explicit references.

Signed \_\_\_\_\_ (candidate)

Dated \_\_\_\_\_

### Statement 3

I hereby give consent for my thesis, if accepted, to be available for photocopying and for inter-library loan, and for the title and summary to be made available to outside organisations.

Signed \_\_\_\_\_ (candidate)

Dated \_\_\_\_\_

---

## Summary of Thesis

This thesis is concerned with the development of short fibre and particle reinforced polymer composites for plain bearing liners for aerospace applications. Detailed experimental investigations of the tribological and mechanical characteristics of these materials has been completed. The thesis culminates with the identification of two possible materials that have the potential for direct injection moulding of a bearing liner.

### **1. Developing an Injection moulding process**

A thorough understanding of the capability of injection moulding PEEK composites was achieved through experimental investigation. Knowledge of the impact of varying injection moulding parameters on the final material was identified.

### **2. Friction and wear testing**

A bespoke test rig, in line with aerospace standards, was developed to allow the investigation of composite materials. Testing was conducted at room and high temperatures. A full analysis of the impact of the selected bulk material, short fibres and fillers was completed. Key parameters such as coefficient of friction, wear and fatigue life were identified. Further testing using optical microscopy was completed to enhance the understanding of the wear process and to support the findings of the detailed friction and wear testing program.

### **3. Mechanical testing**

The mechanical performance of PEEK materials was investigated through experimental analysis and available data. Again the impact of differing ratios of fillers and short fibres was determined. In addition static testing was used to investigate instantaneous strain and creep of selected materials.

### **4. Development of PEEK blends**

A final testing programme of two identified blends was completed that aimed to optimise for wear, friction and mechanical performance. The materials selected were successful in matching aspects of the established design criteria but further work on the blends needs to be completed. However one of the selected materials is being proposed for an in service aerospace application.

---

## Acknowledgements

Firstly I would like to acknowledge my supervisors Dr Rhys Pullin and Professor Sam Evans of Cardiff University. They have been a source of knowledge and inspiration throughout this project, and always had an open door when I wanted bounce ideas off them. Thanks especially to Rhys for his support through the thesis writing process, it has been invaluable. I look forward to our continued collaborations.

My thanks also to the Technology Strategy Board who joint funded the Knowledge Transfer Partnership with SKF from which this thesis arises. Thanks to KTP advisers Howard Nicholls and Neil Grice, who's guidance through the KTP ensured the successful completion of the project. I would also like to thank SKF, the Aerospace Technology and Product Development team and particularly Andrew Bell and Neil Tolson for initiating and supporting the KTP project and my PhD studies. Furthermore, I would like to thank Michael Colton for his support throughout the project and for allowing me the time away from day today work to complete my thesis. Thanks finally to Paul Hancock for his support with the practical aspects of the project and to Johnpaul Woodhead for his kind words and advice through the latter stages of this work.

A special thanks to my friends Russell Gay and Michael Bryant for making my experience in Cardiff much more enjoyable, our days in S3.17E will not be easily forgotten. Thanks also to Amjad Al-Hamood, Igor Berinskii and Sergey Khaustov.

Finally I would like to thank family and friends who have been a part of this journey, giving me encouragement and welcome distraction along the way. In particular I would like to thank my parents who have always supported me and ensured that I had the opportunity to achieve my goals.

---

## Contents

<b>Declaration</b>	i
<b>Summary</b>	ii
<b>Acknowledgements</b>	iii
<b>Chapter 1: Introduction</b>	
1.1. Background	1
1.2. Aims & Objectives	5
1.3. Thesis Structure	7
<b>Chapter 2: Theory and review of relevant literature</b>	
2.1. Tribology	10
2.1.1. Friction	12
2.1.2. Wear	14
2.2. Bearings	17
2.3. Self-lubricating plain bearings	18
2.3.1. Qualification and design standards	20
2.4. Composite Materials	20
2.5. Review of relevant literature	22
<b>Chapter 3: Material Selection</b>	
3.1. Outline of material Requirements	32
3.2. Selection of materials	36
3.2.1. Bulk Polymer	37
3.2.2. Structural fillers	42
3.2.3. Tribological fillers	47

---

3.3.	Selected materials for characterisation	50
3.4.	Hypotheses	56
<b>Chapter 4: Developing the injection moulding process</b>		
4.1.	Injection moulding theory and process impact	57
4.2.	Injection moulding equipment	62
4.3.	Experimental design	66
	4.3.1. Process mapping	69
	4.3.2. Experimental Design	72
	4.3.3. Results	74
	4.3.4. Conclusions	78
<b>Chapter 5: Experimental methods – friction and wear testing</b>		
5.1.	Ring on Disc Testing	80
5.2.	Test Rig Design	83
5.3.	High Temperature Testing	90
5.4.	Test Procedure	96
5.5.	Coefficient of Friction Calculation	97
5.6.	Test Parameters	99
	5.6.1. Counterface and material roughness	100
5.7.	Results and Discussion	103
5.8.	Conclusions	133
<b>Chapter 6: Experimental Methods – material characterisation</b>		
6.1.	Optical microscopy	136
6.2.	Results and discussion	140
6.3.	Conclusions	151

---

---

**Chapter 7: Experimental methods – mechanical testing**

7.1.	Mechanical properties of selected compositions	152
7.2.	Static load testing method	157
7.3.	Results and Discussion	159
7.4.	Conclusions	164

**Chapter 8: Developing PEEK composite blends**

8.1.	Summary discussion of experimental work	165
8.2.	PEEK composite blends	167
8.3.	Results and discussion	169

**Chapter 9: Conclusions**

9.1.	Summary of conclusions	173
9.2.	Future work	175

**Chapter 10: References** 177**Appendix A: Process Flow for Injection Moulding Experiment**

# 1. Introduction

This thesis focusses on the tribological and mechanical characterisation of short fibre and particle reinforced polymer composite materials as sliding contact surfaces. The composites are assessed and optimised for their use as plain bearing liners for aerospace applications. This chapter outlines the need to be addressed and the aims of the research. It also introduces the background to the investigation and the relevant fields of engineering, namely tribology, materials science, polymer technology and composite materials.

## 1.1. Background

SKF is a global organisation which offers five technology platforms,

- Bearings and units
- Seals
- Mechatronics
- Services
- Lubrication systems

The business comprises of three divisions within which there are separate business units addressing specific market demands. These divisions are as follows,

- Industrial market – strategic industries (IM-SI)
- Industrial market – regional sales and service (IM-RSS)
- Automotive

Aerospace is a business unit within IM-SI and offers solutions for both fixed wing and helicopter applications. SKF offer high precision self-lubricating plain bearings to the aerospace market.

Aerospace bearing products are broadly divided into two categories, airframe and aeroengine. Aeroengine bearings are typically rolling element bearings with engine and gearbox applications. Predominantly these rolling element bearings are grease or oil lubricated and are best suited to very high speed rotating applications and high temperature applications. There are very few self-lubricating applications within the aeroengine area.

Airframe bearings predominantly comprise plain bearings, more specifically spherical plain bearings; journal bearings; thrust washers and friction surfaces. There are many solutions for aerospace plain bearings including greased metal to metal bearings and self-lubricating plain bearings – often termed maintenance free.

The current SKF Aerospace market offering for self-lubricating plain bearings consists of fabric composite lined spherical plain bearings, bushes and friction surfaces in many configurations. The most commonly selected fabric liner, X1-40, is a composite material consisting of a woven fabric – PTFE and glass fibres – impregnated with a phenol-formaldehyde resin using a laminating process. The liner system is presented and discussed in the work of Dr Russell Gay (Gay 2013).

Self-lubricating bearings tend to find applications in aircraft components where continuous lubrication is not possible and regular maintenance, for example regreasing of components, is difficult or uneconomical. A good example of this is in a helicopter main rotor swashplate bearing. This type of component rotates at high speed during flight in an environment where continuous lubrication would prove difficult and greased bearings would require a regular maintenance. Maintenance of this type of bearing would require disassembly of the main rotor from the aircraft, meaning significant aircraft downtime. It is suggested that the cost of grounding a military rotorcraft for maintenance of bearing components can be of the order of €35,000 and put the aircraft

out of action for a number of days. This example of disassembly and cost can be seen in many applications across the aerospace industry.

Other applications where self-lubricating plain bearings are commonly used can include helicopter main rotor and tail rotor pitch control, fixed wing flight control surface actuation, airframe structure in airframe rods and struts and aircraft landing gear (SKF, 2015).

Each application has a unique set of operating requirements. The loads, sliding velocities, dynamic cycles and environment vary significantly, often in the same aircraft. Furthermore, from a design perspective each application has a unique set of constraints on the physical geometry of the bearing. As each bearing must form part of a larger system it is often not feasible to select standard geometry components from a catalogue and therefore it is not uncommon to have bearings designed per application. Also, particularly for less dynamic applications such as structural bearings in fixed wing aircraft, the expected life of the bearing can be significant – in some cases longer than the service life of the aircraft.

For these reasons, the demand for a particular part number can be discontinuous. Therefore it is typical for aerospace plain bearings to be batch manufactured, with batch sizes ranging from one off special products or up to several hundred which is more commonly found on aircraft components such as track rollers for control surface actuation on fixed wing aircraft.

The Current manufacturing processes for a fabric lined bearing involve manufacture of a glass-PTFE woven fabric which is then laminated with a phenolic resin infused woven glass prepreg. This is then cut to fit the profile of the bearing outer ring before cold forming. The liner material is then bonded to the outer ring, which is a totally manual

process which is both time and labour intensive. The liner and adhesive is then cured after cold forming. The increased cost is balance by market leading performance, however some applications which do not require such high performance may be more driven by cost. By utilising an injection moulded liner there is scope to significantly reduce the time and labour required in the manufacture of plain bearings, allowing them to be more cost competitive for standard parts.

The current liner system employs a phenol formaldehyde base resin. Phenolic resins are considered to be at risk of control and potentially banned through REACH regulations. Developing a new liner system offers the opportunity to move away from unsustainable materials and move towards a sustainable alternative

Due to external pressures, both from customer requests and new competitor technologies, there is a requirement within the business to develop a novel bearing liner material. The material must offer some advantage over the current technology both that of SKF and competitor technology. It is expected that the material developed will complement the current fabric liner technologies rather than be a direct replacement. There are a number of business and customer drivers for the new technology, these include: -

- Lower overall product cost
- Reduced manufacturing time
- Lower friction than current technology
- Low wear
- High compressive strength
- Extreme temperature resistance
- Machinable liners

In addition to the business and customer drivers the liner material should meet the qualification standards for aerospace bearings. The key qualification for this application is the SAE AS81820-C standard (SAE 2008). This sets out the minimum requirements for aerospace bearings and the testing procedures used to determine them. The primary parameter is wear resistance, which will be a key focus of this project.

## *1.2. Aims & Objectives*

The long term objective of this work is to develop a range of aerospace standard self-lubricating plain bearings utilising injection moulded composite liner materials developed within the project, which can complement the current product ranges within SKF. It is expected that the self-lubricating material will be formed of a matrix composite. This is because traditional self-lubricating materials, for example PTFE, offer good tribological performance however do not offer adequate structural performance in high load aerospace applications. Conversely, traditional structural polymers, both thermoplastic and thermosetting such as Nylon (thermoplastic) and Epoxy resin (thermosetting) can offer vastly improved structural performance, however this is to the detriment of tribological performance.

The designed materials shall form a low friction, low wear, high strength sliding surface for lining of plain bearings and bushes. The application of these bearings will be primarily in Aerospace – helicopter and fixed wing – however, may be relevant in other applications. In order to achieve this, a number of objectives must be fulfilled.

Firstly, it is necessary to understand the key performance parameters that a liner material must have. This will drive the investigation of materials, and will largely influence the material selection and test methods used to evaluate them.

Once the key parameters have been identified, it is expected that a number of methods for evaluating materials will be developed. This will be in the form of experimental testing, which will include mechanical and tribological testing. It will also be necessary to characterise the macro structure of the composite material and understand the relationship to the structural and tribological performance.

Once a test plan has been defined, the aim is to identify suitable materials beginning with identifying suitable base resins and then identifying appropriate fillers and their ratios. Initially material performance will be taken from literature in order that the most appropriate materials are selected for testing. The first stage of testing will evaluate off-the-shelf materials.

Experimental data and literature will be used to develop an understanding of which materials create the most optimal composites. It will also aid the understanding of the effect of each constituent material on the composite system and its bulk properties, including performance. This understanding from literature and from experimentation will form part of an iterative process whereby candidate materials are refined to create optimum materials.

Alongside the material development there is a need to develop an understanding of the manufacturing process which will take the final materials and integrate them into full bearings and bushes. The manufacturing process can have a direct effect on the bearing performance. It is necessary to gain an understanding of how performance can be affected, and the causes. It is expected that an understanding of the benefits and limitations of the processes will also be gained.

Finally it is expected that this new knowledge will enable the development of a range of matrix composite lined plain bearings suitable for aerospace applications. Furthermore, it is expected that the understanding of how the composite system and manufacturing processes interact will enable a scientific approach to material selection and process parameters to create an optimal liner solution. The long term ambition is to have the ability to optimise these inputs on a 'per application' basis whereby performance is maximised for each solution. The technical feasibility of this will come from the new understanding however the economic feasibility will not be studied.

### *1.3. Thesis Structure*

This thesis is split into nine distinct chapters. Chapter 2 discusses theory and literature relevant to the project. It incorporates knowledge from a number of engineering fields, including tribology, materials science, polymer technology and composite materials. The knowledge gained in this review guides the selection of materials studied within the thesis.

Chapter 3 outlines the selection of materials analysed within the work and the justification for their use. The requirements of the material are discussed and therefore materials selection is based upon the demands of the final application. The novelty of the work is also described whereby the current body of knowledge for the tribological properties of PEEK composites has been derived from fundamental friction and wear tests, whereas there is little knowledge of the performance at the high loads and low speeds seen in typical aerospace applications. A number of commercially available materials were selected and are presented within this chapter for analysis by experimental work described in Chapters 5 to 8.

Chapter 4 is concerned with developing an understanding of the injection moulding process. The injection moulding process is defined and the injection moulding equipment used for the experiment is described. An experimental design for assessing the impact of moulding parameters upon final part quality is described. The experiment was performed on a variety of thermoplastic materials to understand whether the impact of moulding parameters was material specific or common to the process.

Chapter 5 describes the experimental approach to friction and wear testing applied to the materials selected in Chapter 3. The test method and rig design are described and subsequent modifications are discussed. A calculation for friction coefficient is derived for the test method used. Finally, results from the experiment are described alongside a comprehensive discussion before conclusions are drawn.

Chapter 6 discusses the material characterisation with respect to fibre alignment and orientation. The use of optical microscopy is described and images collected from this are shown. The assumptions concerning random orientation and even dispersion are proved on the large scale, meaning that bulk properties can be assumed for the materials which can be considered isotropic.

Chapter 7 describes the static tests employed to understand the mechanical and viscoelastic response of the PEEK composites under representative loads. A survey of mechanical properties from manufacturer data is presented. Instantaneous strain and creep response is presented in the results section and discussed with respect to its impact upon tribological performance.

Chapter 8 summarises the findings from Chapters 5 to 8 from which two optimised material blends arise. These compositions are then tested for tribological performance, for which the results are presented and discussed.

Chapter 9 outlines the conclusions which have been drawn from this thesis based upon both the investigative research and experimental aspects of the work. Future work is also suggested in order to build upon the knowledge gained in this thesis.

## **2. Theory and review of relevant literature**

As discussed in Chapter 1, this thesis incorporates elements of a number of fields of engineering and science, namely tribology, materials science, polymer technology and composite materials. The following chapter discusses the relevant literature in each field before bringing them together to the most relevant work in the field.

### *2.1. Tribology*

Tribology is the study of friction, wear and lubrication. The word tribology is derived from the Greek word 'Tribos', which means to rub, however contrary to the common misconception, the name in the context of the scientific discipline does not have its roots in Greek. In fact, the name tribology only appeared in this context in the 1960s. Many papers and texts credit Mr Peter Jost, a British engineer, with having first coined the term Tribology in his report, for the Department of Education and Science, on industrial lubrication in the United Kingdom (Dowson 1998; Williams 1994; Jost 1966). The report defined tribology as: -

“The science and technology of interacting surfaces in relative motion and  
the practices related thereto.”

This became widely accepted in the scientific world and led to the formalisation of a new branch of academic study into the fields of friction, wear and lubrication, albeit with its foundations in long existing scientific and practical concerns.

The understanding of tribological phenomena, however, has existed since early man. A basic understanding, for example, of the effects of friction can be seen in man developing the means to create fire. By rubbing two pieces of wood together, heat is created due to friction to the point where the heat energy generated is sufficient to ignite the fuel, often dry grass or leaves. Dowson discusses the understanding of tribological phenomena from prehistoric times through to present day in his book, *The*

History of Tribology (Dowson 1998). Dowson discusses how tools were developed in these early times in order to improve the creation of fire by making tools such as the Egyptian bow-drill as shown in Figure 2.1.

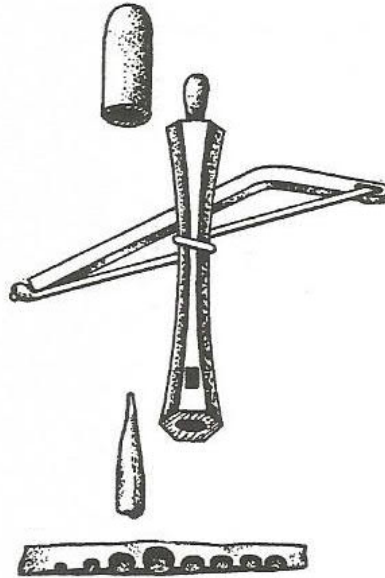


**Figure 2.1 - Ancient Egyptian bow drill for making fire (Dowson, 1998)**

This exemplifies the fact that Ancient Egyptians had an appreciation of the relation of friction and heat generation, whereby increasing the pressure and velocity exerted on the wood increases the work done and ultimately the heat generation and creation of fire.

Dowson goes on to discuss the works of Layard (1853) and Newberry (1893) and Engelbach (1923), discussing the Ancient Egyptian transportation of large stones and blocks for statues and building of pyramids and palaces. The classical view has been that large wooden rollers were used to transport the stones, much like a rolling element bearing arrangement, however the evidence of Newberry suggests that wooden planks were used, lubricated by water to reduce the frictional resistance. Dowson goes on to roughly calculate a friction coefficient ( $\mu$ ) of 0.23 based on evidence from ancient

paintings, which is compared to modern day values for wood-on-wood friction coefficient given by Bowden and Tabor (1950), 0.2 wet and 0.25-0.5 clean and dry.

### **2.1.1. Friction**

Friction is the resistance to motion of an object sliding relative to another and can apply to many interactions. Friction can occur within solids and fluids and at solid-fluid and solid-solid interfaces.

The resistance to motion between solids is referred to as dry friction. It is caused by a number of phenomena, adhesive forces, asperity contact, elastic deformation and contamination by a third body.

Dry friction can be seen as static or dynamic friction and often have different values. Static friction is typically greater than dynamic friction. Static friction is equal to the force required to move an object which is at rest relative to another object. Dynamic friction is the force required to keep an object moving relative to another at constant velocity

Static friction, i.e. the force required to initiate motion between two objects, is typically greater than the dynamic friction of the same materials in relative motion. The difference between these values varies between material pairs. Material pairs which have a significant difference between static and dynamic friction are known to exhibit 'stick-slip' characteristics.

Dry friction is governed by a number of laws. Amontons's first law dictates that dynamic friction is proportional to the normal load applied to an object. The ratio of friction force to normal force is known as the friction coefficient and is given as: -

$$\mu = \frac{F_f}{F_n}$$

**Equation 2.1**

Where  $\mu$  is friction coefficient,  $F_f$  is force due to friction parallel to the sliding direction and  $F_n$  is the normal load perpendicular to the sliding direction.

All materials pairs have a different friction coefficient. When selecting materials in sliding dry contact, knowledge of their friction characteristics can make for easy comparison.

Friction creates a thermodynamic system which respects the conservation of energy. The work done due to friction, i.e. the energy required to overcome friction, is converted to heat energy. If the sliding contact region remains stationary, such as the interface between a rotating shaft and a bush, this can be shown as a heat source. The heat generated at the contact surface then dissipates through the contacting materials. In polymer materials, thermoplastics in particular, this local increase in temperature can have a significant impact upon the mechanical properties as they reach and exceed the glass transition temperature up to the melting point. This can in turn affect the wear performance which has been shown by Archard (1956) to be proportional to the material hardness. As the hardness of the material reduces the wear rate increases. This will be discussed in more detail in following sections

An alternative to selecting materials with a low friction coefficient is to utilise a lubricant. Alternatively, the total resistance to motion can be reduced by reducing the relative sliding between two objects by creating a system of rolling contact. This involves the use of a third body such as a roller or a ball as seen in rolling element bearings.

### 2.1.2. Wear

Wear is defined as the damage and loss of material at the surface of a component in relative sliding contact with another surface (Williams 1994). Theoretical analysis carried out by Archard (1953) reduced the problem to what he considered to be the key characteristics of wear given as: -

$$Q = \frac{KW}{H}$$

**Equation 2.2**

Where Q is volume of material removed per unit sliding distance and K is the wear coefficient, a dimensionless constant, W is the load applied normal to the contact surface and H is the hardness of the material. This is often referred to as the 'Archard wear equation'.

Archard originally developed his wear analysis for metallic components, considering the wear mechanisms that are predominant in these materials. Further work by Archard and Hirst (1956) develops this understanding, hypothesising that the wear of metals in sliding contact is proportional to the load applied and independent of area of contact. This is because the true area of contact is dependent on the load applied causing plastic deformation at the surface roughness scale.

Whilst the work of Archard is applicable to metallic materials, the wear of other materials such as polymers is influenced by many other factors. Hutchings (1992) suggests that when wear testing it is important to consider the factors isolated by Archard and additionally factors such as temperature, contact geometry and atmospheric condition. This suggests that wear is a function of many parameters and can be expressed as:-

$$q = f(W, V, S, H, T, RH, \dots)$$

**Equation 2.3**

Where  $q$  is the volume of material removed,  $W$  is the normal load applied to the surface by the counterface,  $V$  is the sliding velocity,  $S$  is the sliding distance,  $H$  is the indentation hardness of the wearing surface,  $T$  is temperature,  $RH$  is relative humidity. Furthermore, it is hypothesised that the nature of the contact is highly important and can influence the rate of wear. For example, a closed contact which traps the wear debris will behave differently to one which allows removal of wear debris in each wear cycle. A closed contact will retain a third body which depends on its nature will cause a change in wear rate. Hard third body particles under high load may gouge material from the softer surface; material of similar hardness may create microscopic rolling elements reducing wear; a softer material may smear across the surface of the wearing material increasing the true area of contact or acting as a viscous lubricant.

By manipulating the Archard wear equation it is possible to derive a number of relationships. Firstly, where  $K$ ,  $W$  and  $H$  remain constant throughout the wear process then Equation 2.2 can be reduced to:

$$Q = 1$$

**Equation 2.4**

And therefore:

$$\frac{q}{S} = 1$$

**Equation 2.5**

Furthermore:

$$q \propto S$$

**Equation 2.6**

Equations 2.4 to 2.6 imply that wear volume is directly proportional to sliding distance. Where hardness cannot be readily determined, or in those materials where hardness is influenced by external factors, such as the temperature dependent mechanical

properties exhibited by polymers, specific wear rate can be referred to. This is expressed as:

$$k = \frac{K}{H} = \frac{Q}{W}$$

**Equation 2.7**

Where  $k$  has the units  $\text{mm}^3/\text{Nm}$ . Therefore, the Archard wear equation can be further expressed as:

$$q = kWL$$

**Equation 2.8**

In sliding applications, such as plain bearings, maximum allowable wear is generally quoted as a maximum backlash within the component. Within a self-lubricating plain bearing, for example, there will be a consumable liner material with a defined thickness. This limits the operating life to a maximum wear depth. Equation 2.8 can be rewritten as:

$$h = kpS$$

**Equation 2.9**

Where  $h$  is the wear depth and  $p$  is the contact pressure where  $p=F/A$ .  $A$  is the apparent area of contact.

Often the factors of pressure and velocity are described as a coupled effect termed 'pv', the product of contact pressure and sliding velocity. In many materials, specific wear rate is derived experimentally and over a range of 'pv' values. Lancaster (1971) aims to estimate the limiting 'pv' values for thermoplastic materials in dry sliding contact. The limiting 'pv' is defined as the value above which specific wear rate increases rapidly. Lancaster suggests that extrapolation of limiting 'pv' values to different bearing geometries or extremes of pressure and velocity is difficult. This is particularly the case for thermoplastic materials which are much more susceptible to temperature effects than metallic materials considered by Archard (1953). Meng and Ludema (1995) argue

that the 'pv' criterion is rarely useful for estimating bearing life and Rhee (1970) suggests that p and v are independently proportional to wear.

If considering the 'pv' criterion in material selection, Equation 2.9 can be further rearranged to:

$$h = k.(pv).t$$

**Equation 2.10**

Where v is the sliding velocity and t is the running time.

## **2.2. Bearings**

A bearing can be defined as two surfaces in contact which transmit load and provide constraint in at least one degree of freedom. Several bearing solutions have been developed throughout time. Plain bearings present the most simple bearing type. They comprise two surfaces in sliding contact and can be unlubricated, using low friction and low wear materials, or lubricated, generally by oil or grease. Rolling element bearings comprise two surfaces separated by rolling elements. This is done to eliminate sliding by introducing rolling contact. This reduces the frictional losses in the bearing, however the high contact pressures between non conformal contacts mean that their load carrying capacity is lower than that of plain bearings.

For aerospace bearings, plain bearings tend to comprise the majority of structural bearings within fixed wing aircraft. They are also used in the airframe of helicopters as well as in dynamic controls such for pitch control in main rotors. Typical application conditions for plain bearings in aerospace are illustrated in Figure 2.2.

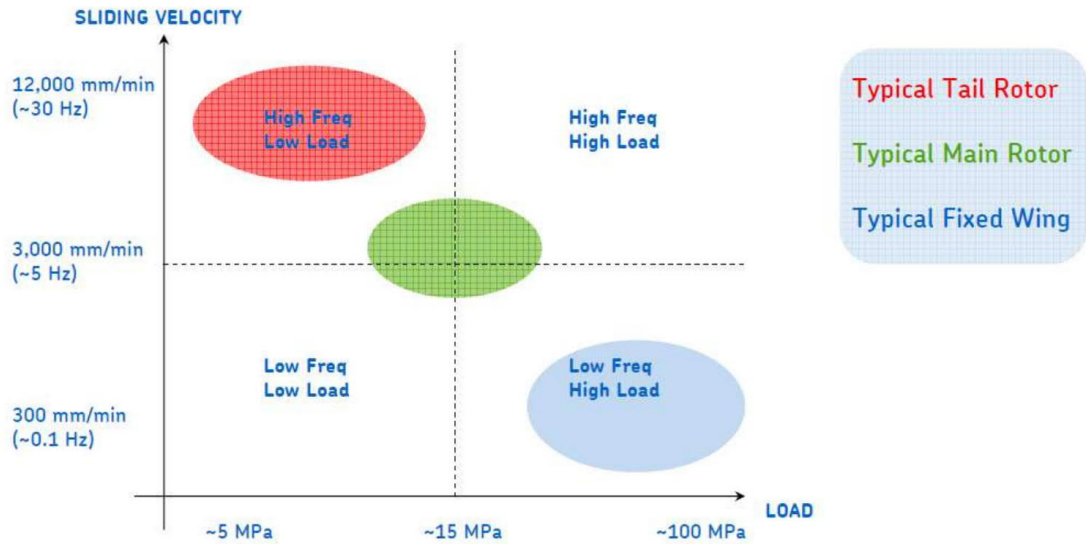


**Figure 2.2 - Typical application conditions for aerospace self-lubricating bearings (Bell 2009)**

For aerospace applications, rolling element bearings are typically used in very high speed applications such as within engine compressors, high temperature areas and low load applications where lubrication is straightforward.

### 2.3. Self-lubricating plain bearing

Self-lubricating plain bearings have been used for many centuries in a variety of applications. Traditional materials include wood and bronze. Bronze exhibits very good tribology and has low friction and wear properties. Traditionally these materials would have been lubricated by oil or grease.

Polymer based dry sliding bearings are a more modern design, however have been used for many years, particularly where lubrication is not possible (Lancaster n.d.). These type of bearings are often described as maintenance free and are considered consumable products. The polymer liner material is consumable and is removed through the process of wear. The materials used are selected for their low friction

properties and low wear rates, with properties satisfying the wear equations described in section 2.2.

Liner materials typically comprise a woven fabric reinforced polymer composite, which incorporates both structural and self-lubricating fibres. An example of this is the X1-40 liner supplied to aerospace applications by SKF. For aerospace applications these liner materials are typically approximately 300µm thick and utilise a phenolic resin as the bulk material (Lancaster n.d.). One advantage of the fabric liner is the ability to alter the weave pattern and materials used to tailor the mechanical and tribological properties as well as to impart anisotropy in the material. This has been described for X1-40 by the work of Gay (2013). This work models the fabric liner and describes the evolution of contact pressures through the wear processes. Furthermore, a friction model is proposed and the basis of a wear model is developed.

Injection moulded, short fibre reinforced bearings exist amongst the wider bearing industry. SKF offer an industrial product, marketed as the F-liner, which comprises a moulded PTFE bulk containing bronze particles. Such materials are not commonplace within aerospace products. Kamatics offer their Karon range which typically comprises a short fibre reinforced thermoset matrix such as a methacrylate resin. Thermoplastic base injection moulded liner materials are not used for aerospace applications.

Short fibre and particle reinforced bearing liners and surfaces exist in a wide range of aerospace applications such as spherical bearing liners, lined bushes, friction surfaces and track rollers. Kamatics are the only manufacturer offering such technology. The Karon range comprises the short fibre and particle reinforced technologies. Across the range of technologies, Kamatics are utilising a thermoset bulk resin with a range of fillers to suit various application conditions.

### **2.3.1. Qualification and design standards**

Aerospace self-lubricating plain bearings are subject to rigorous testing to establish their performance before they can enter service on aircraft.. They are tested in many aspects including wear performance, dynamic and static load performance as well as for resistance to fluid contamination (SAE 2008). The common bearing standard for aerospace bearings is SAE AS81820, which assesses self-lubricating spherical plain bearings against several criteria. Most relevant to this work is the analysis of the wear performance of the liner material. The standard AS81820 describes a test methodology for fully assembled spherical plain bearings in order to assess their tribological and mechanical performance, resistance to chemicals and general geometric limits. An average contact pressure of 272MPa is applied radially to the bearings and the inner ring is rotated  $\pm 25^\circ$  at 10 cycles per minute. This is an accelerated test which assesses the performance at an extremely high load but at very low sliding speed, more typical of structural applications in fixed wing aircraft. This test favours very high strength materials, however as the loads are not representative of application conditions, described in Figure 2.2, it can mean that material which are better suited to lower load conditions are overlooked.

### **2.4. Composite Materials**

Composites have been used in aerospace engineering for several decades; in fact many modern composite materials were first developed for aerospace applications. Individually, materials have a given set of properties. Materials can be chosen for their suitability for an application and in many cases that material will satisfy the needs of that application without modification. In some circumstances, however, a material may have a deficiency in some area, for example physical properties, machining properties, mechanical properties, mass, cost or impact upon a system. The system impact can

include impact of using a particular material on energy consumption, as well as environmental impact of using such a material. It is possible to enhance the performance of a single material through the use of manufacturing processes, which can include heat treatment of metallic components or surface treatments, or through intelligent design. However when considering all aspects of material selection, it is possible that no material can meet the requirements given and no existing single material can be modified in such a way that it can meet the needs of the application. In this case it may be possible to engineer a material which closely matches the requirements of the application through composite design. A composite material can be loosely described as a combination of two or more materials with distinct properties, which when combined create a useful material with some desired material property. This covers a broad range of materials including woven fabric reinforced polymers, steel reinforced concrete, bone, wood and short fibre reinforced polymer matrices. A more accurate definition of a composite material is described as:

“Composite Material. A substance consisting of two or more materials, insoluble in one another, which are combined to form a useful engineering material possessing certain properties not possessed by the constituents” (ASTM International 2007)

These composite materials in many cases have far superior properties to traditional materials, or can be more cost effective without compromising performance.

Composite materials occur naturally. Bone is an example of a naturally occurring composite. The constituent materials in bone are soft collagen and brittle apatite (Callister 2006). The combination of these materials produces a composite material which has high mechanical strength, yet can absorb significant impacts without brittle failure.

## 2.5. Review of relevant literature

Early work in the use of polymer based dry sliding materials as bearing liners was carried out by J.K Lancaster, with his paper reviewing polymer materials and the impact of fillers and fibre reinforcement upon the tribology of the composite (Lancaster 1972). This work surveys typical bearing materials and ranks their wear performance, shown in Figure 2.3. Lancaster concludes that PTFE has exceptional friction properties, however the wear performance is very poor compared to other unfilled thermoplastics. PTFE can however be used as a filler material in other polymers to give good friction properties whilst retaining good wear performance.

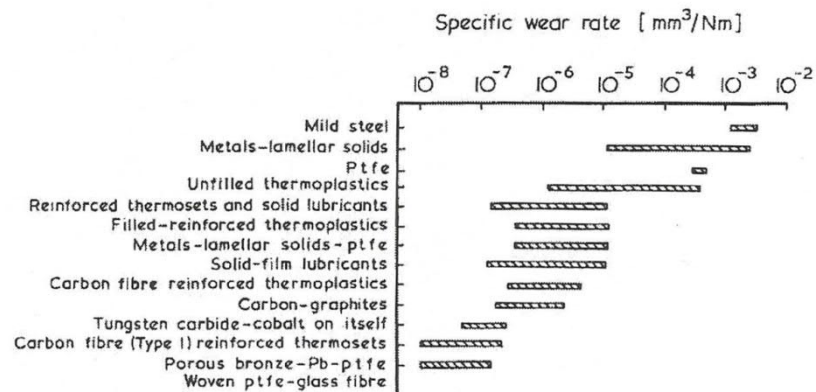


**Figure 2.3 - Specific wear rates of various materials against steel (Lancaster 1972)**

Lancaster (1971) attempts to derive the critical ' $\rho v$ ' for thermoplastic bearing materials. The limiting ' $\rho v$ ' is defined as that above which the wear rate starts to rapidly increase resulting in premature failure of the sliding material. Whilst this work ranks materials, it only aids selection of potential materials as the ' $\rho v$ ' factor does not fully account for the thermal influence upon the tribological system, It also applies no weighting to either pressure or sliding velocity, a point raised by Meng and Ludema (1995) and Rhee (1970), who argue that pressure has a far greater impact upon bearing wear than sliding velocity. Further to this work, there are a number of publications which discuss appropriate polymer materials for self-lubricating sliding contact. Anderson (1982)

surveys available plastic materials to assess their wear performance considering the ' $p\nu$ ' factor described in Section 2.1, concluding that effect of temperature on wear rate makes material selection more complicated than simply considering the limiting ' $p\nu$ '. PTFE containing composites are shown to offer the best wear performance, particularly as a woven fabric liner material.

The predominant work in the field of short fibre reinforced PEEK composites has been carried out by the Institute for Composite Materials (Institut für Verbundwerkstoffe) at the University of Kaiserslautern. The works of Friedrich et al focusses upon understanding the fundamental tribology and mechanical performance of PEEK composites, with early works such as the review of short fibre matrix composites, including PEEK (Friedrich 1985). The influence of microstructure on performance is discussed, including the influence of fibre orientation and alignment, and the volume fraction of filler materials used. This was further investigated by Voss and Friedrich (1987) who studied the wear behaviour of glass fibre and carbon fibre reinforced PEEK composites, concluding that use of carbon fibre fillers offers a superior enhancement to wear performance and mechanical performance than use of glass fibres. Their tests were carried out at contact pressures of 0.2 to 8.4MPa with ' $p\nu$ ' factors of 0.5, 1.7 and 5MPa.m.s<sup>-1</sup>.

Hager and Friedrich (1993) assessed PEEK composites at elevated temperature, 220°C, for their friction and wear performance. PEEK was selected for its high temperature properties, with a glass transition temperature of 143°C and melting temperature of 343°C. Composites contained PTFE, glass fibres, carbon fibres and graphite. Materials were tested in a block on ring setup with contact pressures ranging from 0.25 to 4MPa and sliding speeds of 1 to 4ms<sup>-1</sup>. Inclusion of fibre fillers improves the mechanical properties so that at high temperature, compressive strength remains

higher than the applied load. It is concluded that PEEK composites are a promising solution for temperatures in excess of 150°C.

Friedrich et al (1995) discusses the state of the art in polymer tribology at a time when the behaviour of PEEK was becoming more widely understood. They compare the thermal, mechanical and tribological properties of PAEKs to other commercially available polymers. They show that the PEEK is overall a desirable material for use in sliding contact across these performance criteria, and that use of both structural fillers and solid lubricants can enhance these properties significantly. There is a clear bias towards PEEK composites, which is in line with other works coming from the University of Kaiserslautern.

Lu and Friedrich (1995) concluded that 15-25%w/w carbon fibre reinforcement in PEEK was the optimal composition for wear. Greater than 20% can cause stick-slip, especially at high temperatures. For optimum coefficient of friction, 10%w/w was shown to be optimal.

Flock et al (1999) investigated the influence of PAN and pitch carbon fibre on the tribological performance of PEEK composites. A fibre content of 10% was shown to reduce friction to a minimum of 0.25 and specific wear rate to a minimum of  $7 \times 10^{-6}$  mm<sup>3</sup>/Nm. This represents the optimal fibre content, with increasing friction and wear rate as fibre content increases further. Tests were carried out at 1 to 3MPa contact pressures and a sliding velocity of 1ms<sup>-1</sup>.

Unal et al (2004) studied the impact of addition of glass fibres, bronze particles and carbon fibres on the tribological properties of PTFE. They used a pin-on-disc arrangement with contact pressures ranging from 0.18MPa to 1.06MPa and sliding velocity ranging from 0.32ms<sup>-1</sup> to 1.28ms<sup>-1</sup>. It was concluded that all filled materials

gave a reduced friction coefficient and wear rate when compared to unfilled PTFE. Glass fibres showed a significantly better improvement than that of bronze and carbon fibre, which both showed rather similar levels of improvement. Furthermore it was hypothesised that the poor wear performance of PTFE is due to its poor mechanical properties and that by improving the load carrying capacity by inclusion of high strength fillers the wear properties are improved. They also noted that PTFE and its composites exhibit a reduction in coefficient of friction with increasing load.

Wu (n.d.) developed aramid reinforced Nylon-66 and PPS composites to understand the impact upon wear. The aramid used was Kevlar-49 at a ratio of 20%w/w. These materials were tested alongside unfilled and glass filled versions of the same base materials. Nylon-66 and PPS were filled with 33%w/w and 40%w/w glass fibres respectively. The test setup was a thrust washer type wear test as described by the ASTM D3702 standard. Contact pressures 1.72MPa and 0.276MPa were combined with sliding velocities of  $0.05\text{ms}^{-1}$  and  $0.254\text{ms}^{-1}$  respectively. This gives  $p\nu$  values of  $0.088\text{MPa}\cdot\text{ms}^{-1}$  and  $0.07\text{MPa}\cdot\text{ms}^{-1}$  respectively. Tests showed that 33% glass fibre filled nylon-66 reduced the wear rate by a factor of two at  $p\nu = 0.088$  and a factor of four at  $p\nu = 0.07$ . Kevlar-49 filled Nylon-66 reduced the wear rate by four times at  $p\nu = 0.088$  and eight times at  $p\nu = 0.07$ . For PPS, Kevlar-49 gave a 20 times improvement in wear rate compared to glass fibre reinforcement.

Tribological testing of PEEK composites is typically carried out at low contact pressures in the range of 0.1MPa to 10MPa, and sliding velocities of the order of  $1\text{ms}^{-1}$  (Lu and Friedrich 1995; Davim and Cardoso 2009; Rasheva et al. 2010). At present, insufficient research has been undertaken to understand the tribology of these materials at much higher contact pressures applicable to aerospace type applications. It is not clear whether the tribology observed at these low contact pressures and relatively high sliding velocities is also observed in highly loaded, slow sliding speed conditions.

For a single solid material it is possible to assume that the material is isotropic. This is the case for most polymer materials as the structure is formed on the molecular level. The material properties are driven by the polymer chain structure, the alignment of polymer chains and the degree of crystallinity.

For a composite, the properties of the material can vary significantly in each different component. An example of this is the elastic modulus of a carbon fibre reinforced PEEK composite and its individual components. The elastic modulus of 30%w/w carbon fibre reinforced PEEK is 26GPa (Vitrex 2011). The elastic modulus of carbon fibre is given as 230-400 GPa (Callister 2006). The elastic modulus of unfilled PEEK is given as 3.7 Gpa (Vitrex 2011). In this case, the addition of carbon fibres has the effect of increasing the elastic modulus of the PEEK matrix. The structural properties of the composite material vary significantly at the micro-scale, and on the scale of the geometry of the fibre fillers used. The local properties can vary significantly and the macro properties can vary depending on fibre orientation and dispersion. Figure 2.4 illustrates poor dispersion of fibres whereby there are areas of high concentration of fibres and areas where no fibres are present. The stiffness of the composite through the thickness will be much lower in areas where there are no fibres present and significantly improved in areas of high concentration.

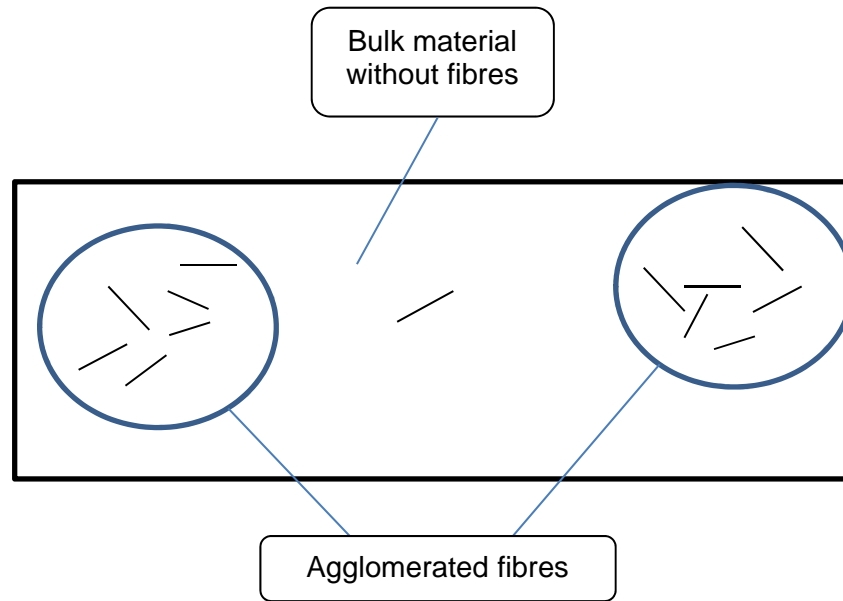


**Figure 2.4 - Illustration of poor fibre dispersion in a matrix composite**

In order to minimise this local variation the idealised solution is to have an even dispersion of fibres as shown in Figure 2.5.

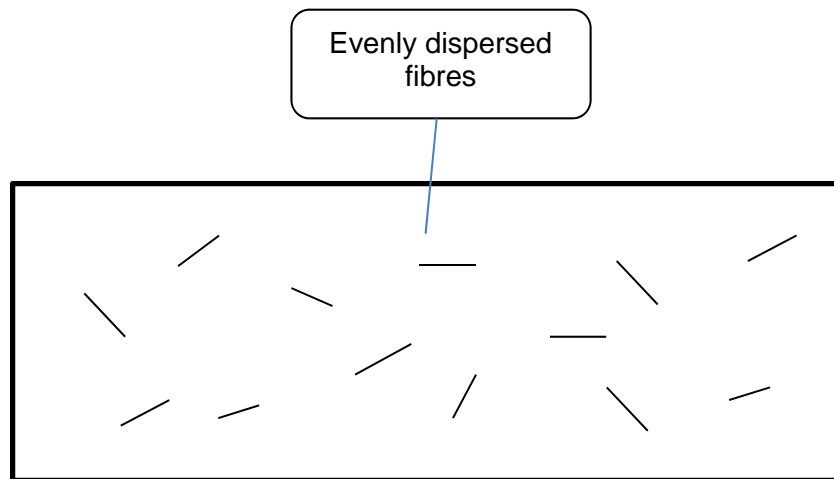


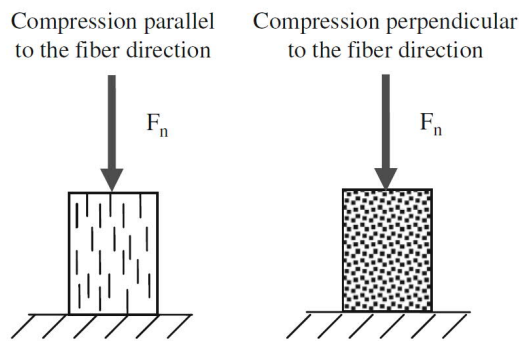
**Figure 2.5 - Illustration of ideal random fibre dispersion in a matrix composite**

Rasheva et al (2010) studied the effect of fibre orientation on mechanical and tribological properties of carbon fibre reinforced PEEK. They evaluated compression modulus, compressive strength and wear resistance for three PEEK composites, shown in Table 2.1.

**Table 2.1 - Material compositions evaluated with respect to fibre orientation (Rasheva et al. 2010)**

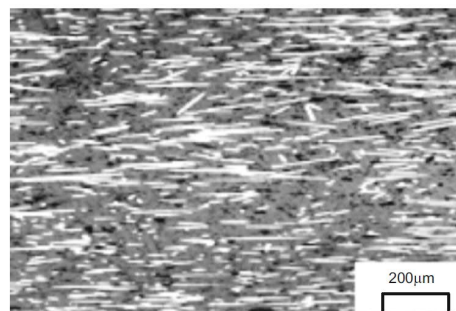
Material code	PEEK (vol%)	PTFE (vol%)	Graphite (vol%)	SCF (vol%)
MA	70	10	10	10
MB	65	10	10	15
MC	75	5	5	15

Samples were loaded parallel and perpendicular to the fibre direction with an apparent contact area of 4 x 10mm with a length of 10mm. Figure 6.3 illustrates the loading direction for the specimen.



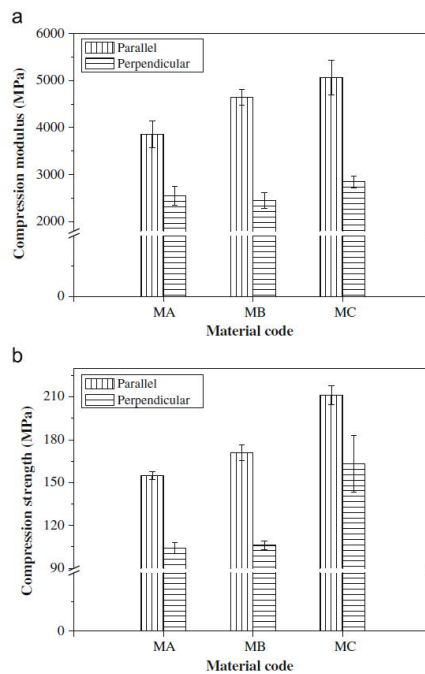
**Figure 2.6 - Fibre orientation in compression experiments carried out by Rasheva et al (2010)**

Figure 2.7 shows an example of fibre filled PEEK exhibiting strong alignment of the carbon fibres.



**Figure 2.7 - Morphology of a polished cross section (Rasheva et al. 2010)**

Figure 2.8 shows the results of the compression tests carried out by Rasheva et al. A significantly higher compressive strength and compressive modulus parallel to the fibre orientation was observed. Conversely a parallel fibre orientation was shown to give improved tribological performance, although the correlation was less strong than for compressive performance.



**Figure 2.8 - Results of compression tests carried out by Rasheva et al (2010)**

Zhang et al (2010) studied the effect of fibre orientation on tribological performance of short carbon fibre reinforced PEEK. They used a block on ring method to test friction and wear performance in three fibre orientations, as shown in Figure 2.9. Tests were carried out at a sliding velocity of 1m/s and contact pressures of 1MPa to 5MPa. Their results show a lower friction coefficient when fibres are oriented in the antiparallel direction, especially for higher contact pressures, 3 to 5 MPa). They conclude that fibre orientation has little effect on wear rate at low contact pressures (1-2 MPa), however at higher contact pressures there is a higher wear resistance in the antiparallel orientation.

Their results for wear are shown in Figure 2.10. Between 3 and 5 MPa contact pressure, there does not appear to be a correlation between fibre orientation and wear rate and there is not an order of magnitude difference between wear rates, therefore the results are inconclusive.

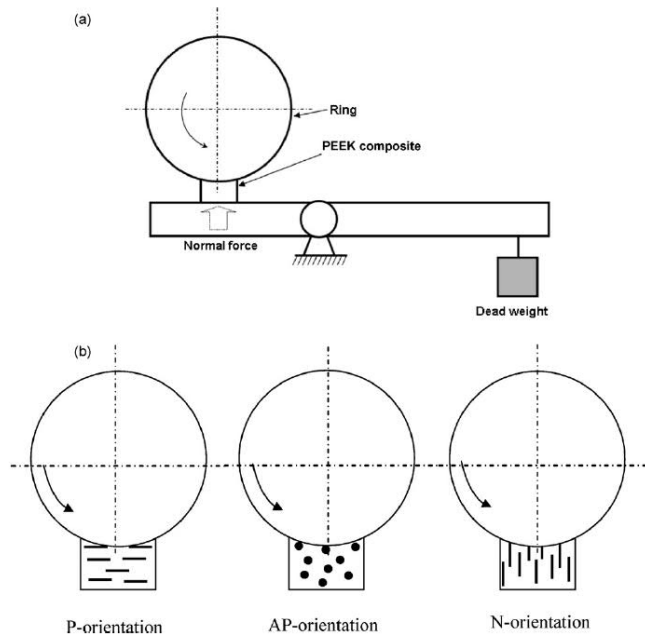


Figure 2.9 - Block on ring test and fibre orientations studied by Zhang et al (Zhang et al. 2010)

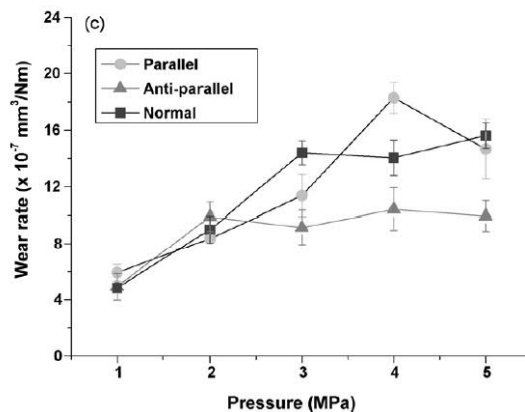


Figure 2.10 - Wear rate against contact pressure for various fibre orientations (Zhang et al. 2010)

In summary, literature suggests that there is a strong correlation between mechanical properties and fibre alignment in short fibre reinforced composites. The impact upon tribological performance is less clear. The results from Chapter 5 show that the wear performance of the PEEK composites tested are strongly linked to their thermo-mechanical and friction performance. Therefore, a fibre orientation detrimental to the mechanical properties will lead to a reduction in tribological performance due to mechanical failure and plastic deformation.

### **3. Material selection**

This chapter outlines the justification for the composite materials and their individual components selected for the experimental work carried out in this thesis. A description of the material requirements is discussed and a comparison of available candidate materials against these requirements is given.

#### *3.1. Outline of material requirements*

In order to define appropriate materials for evaluation as a self-lubricating bearing liner, it is necessary to understand the requirements of the final product and how the performance with respect to these requirements can be characterised.

As a self-lubricating sliding contact material, the chosen polymer must offer excellent tribological performance in order to compete with the liner systems currently in application, which comprise either a fabric reinforced or short fibre reinforced thermoset based composite. The material must possess good friction properties in order to reduce the energy lost within the components, reducing the actuation load in aircraft systems and to allow for retrofitting into existing applications where actuation systems are already defined. As the self-lubricating material forms the contact surface it is subject to wear. The chosen material must offer excellent wear properties in order that the life of the product is sufficient. This is determined by the level of backlash within a part, meaning that there is a limit on maximum clearance between the liner material and its counter surface. The consequence of a high wear rate can be an increase in inspection intervals of parts. In the case of extremely high or unpredictable wear it could be possible that all of the liner material is removed and the part becomes damaged or unusable due to seizing when it runs metal to metal. This would not be acceptable in

the majority of applications, particularly in those applications critical to aircraft performance.

Typical aerospace application conditions for self-lubricating bearings are illustrated in Figure 3.1. These are the typical sliding speed and average contact pressure conditions seen in applications from highly dynamic helicopter tail rotor bearings to quasi-static structural bearings in fixed wing airframes. The selected material must be capable of operating at the extremes described and therefore capable of carrying dynamic loads of in excess of 100MPa. Qualification tests often seek to apply even higher loads for the purpose of accelerating wear tests. Typical bench test loads can be as high as 250MPa in aerospace specifications such as SAE AS81820 (SAE 2008). The selected material must therefore have excellent mechanical properties and be capable of carrying the high loads observed. Thermoplastic materials in particular suffer from high levels of creep; therefore the selected material must have good creep resistance properties.

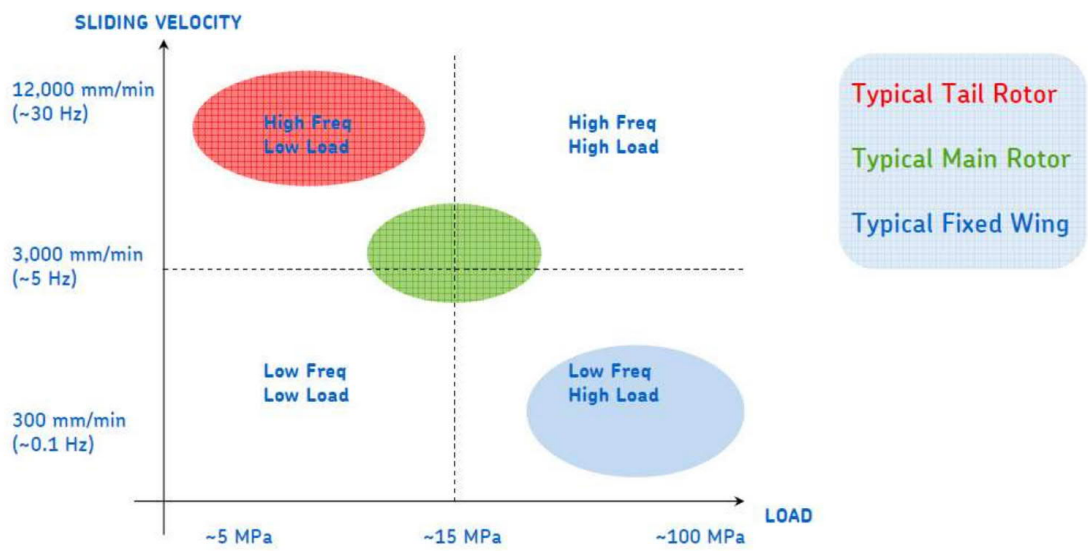


Figure 3.1 - Typical application conditions for aerospace self-lubricating bearings (Bell 2009)

Aircraft are typically exposed to harsh environmental conditions. They can be subjected to extreme ambient temperatures, for example aircraft operating in polar regions or at high altitude will experience very low temperatures, as low as  $-54^{\circ}\text{C}$ . Conversely, aircraft can be operating in desert conditions where temperatures can typically exceed  $+50^{\circ}\text{C}$ . In addition, depending upon the location of a bearing within an aircraft, it can be exposed to higher than ambient temperatures, for example in areas close to the outlet of a jet engine on a fixed wing aircraft. Capability to operate at temperatures of  $+130^{\circ}\text{C}$  is often requested and the AS81820 specification requires testing at  $+163^{\circ}\text{C}$  to establish extreme temperature performance. Furthermore, a bearing on an aircraft can see a wide range of temperatures in one duty cycle, for example a fixed wing commercial aircraft may fly from an ambient ground temperature of  $-30^{\circ}\text{C}$  to an ambient ground temperature of  $+60^{\circ}\text{C}$ . Aircraft structures are typically designed to withstand low temperatures of  $-54^{\circ}\text{C}$  (National Research Council 1996). A bearing will then also experience additional heating due to friction when in motion. It is therefore important that the selected material is capable of performing at the temperature extremes described without significant detriment to performance or risk of failure.

Finally, aerospace bearings can be exposed to many contaminants, many of which are aggressive chemicals which can affect the stability of the bearing materials. The selected liner material must have good chemical resistance, in particular to typical contaminants that may be encountered. It is beyond the scope of this project to test the selected materials' resistance to contamination, however it is recommended as future work.

In summary the material should:

- Possess good friction properties, comparable to existing fabric liner technology

- Have good wear performance, capable of achieving aerospace qualification standards
- Be able to operate in extreme temperature conditions
- Be resistant to typical aerospace contaminants

### 3.2. Selection of materials

Section 3.1 describes a broad range of material requirements, the combination of which is not available in any single material. This is evident by the use of composite materials for self-lubricating bearing liners which are subject to arduous applications. It is therefore necessary to define a composite material which can be optimised to suit these requirements, which can have far superior properties to the constituent materials.

Figure 3.2 illustrates the approach taken in this project when considering appropriate materials for evaluation. Constituent materials of the composite can be separated into three categories. The base resin is that which forms the basis of the composite and will generally form the largest component. The additional materials are those which are added to the composite in order to improve some characteristic. In this case these can be broadly defined as structural fillers and tribological fillers. The structural fillers are those which can be considered to improve the mechanical properties of the composite. The tribological fillers can be considered to be those which improve the friction or wear properties of the material. It is feasible that there are materials which can be beneficial for both structure and tribology, which for the purpose of this research study will be the most attractive. Initially materials are considered for their known benefit, findings which show additional benefit are discussed.

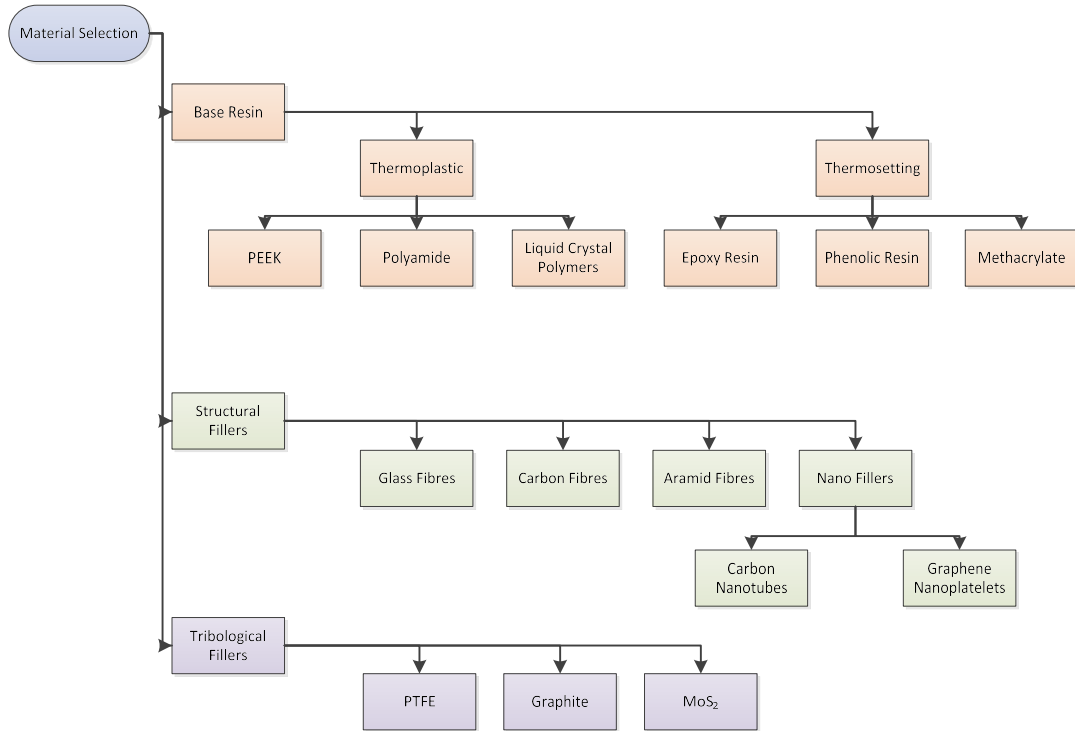


Figure 3.2 - Material Selection Approach

### 3.2.1. Bulk Polymer

This study aims to develop an understanding of the suitability of polymer based liner materials for use as a sliding surface in aerospace bearing applications. Currently, short fibre reinforced and tribologically enhanced thermoset based composites already exist for this purpose. Thermoplastic based composites do not exist in aerospace applications for the purpose of comprising a self-lubricating plain bearing liner material. Thermoplastic materials offer a number of benefits for these types of products over thermosetting solutions, which are summarised in Table 3.1, and present an interesting field to be researched and understood.

**Table 3.1 - Summary of advantages and disadvantages of thermoplastic and thermoset polymers for sliding contact**

Thermoplastics	Thermosets
<ul style="list-style-type: none"> <li>• Strength improvement through structural reinforcement</li> <li>• Good impact resistance</li> <li>• Well understood tribological performance</li> <li>• High performance thermoplastics have excellent thermal properties – continuous use temperatures &gt;200°C</li> </ul>	<ul style="list-style-type: none"> <li>• High strength</li> <li>• Poor impact resistance leading to brittle failure</li> <li>• More complex processing for short fibre reinforced materials</li> <li>• Well suited to fabric reinforced technologies</li> </ul>

The project does not seek to develop new base polymers and therefore a polymer resin has been selected from commercially available thermoplastic materials. There is a vast range of thermoplastic materials available, and so selection has been based on the most extreme properties required acknowledging the fact that some properties can be significantly enhanced by the inclusion of filler materials.

A predominant requirement of the self-lubricating material is high temperature performance. The material must be capable of continuous use at temperatures of 163°C as well as additional heat generated due to friction. The melting temperature ( $T_m$ ) must clearly be far in excess of this and the glass transition temperature ( $T_g$ ) must be close to this temperature or in the best case higher. It is the case with thermoplastic materials that due to their often amorphous nature they lose their mechanical properties with increasing temperature. The chosen material must remain reasonably stable up to high temperatures as the load requirements will remain the same as at ambient temperature.

Table 3.2 shows the glass transition and melting temperatures for a range of polymer materials. Nylon is a traditional polymer base material for bearings in both PA6 and PA6,6 forms.  $T_g$  for PA6,6 is 57°C and the melting point is 265°C, evidently much lower than the required glass transition temperature. A survey of potential materials reduces the choice to a limited selection of candidate materials; polyimide (PI) and polyamide-imide (PAI) in their thermoplastic states with exceptionally high  $T_g$ , in excess of 275°C; Polycarbonates (PC) with a  $T_g$  of 150°C and  $T_m$  of 265°C; Polyetheretherketone (PEEK) with a  $T_g$  of 143°C and  $T_m$  of 334°C.

**Table 3.2 - Glass transition ( $T_g$ ) and melting ( $T_m$ ) temperatures for common polymer materials (Callister 2006)**

Polymer	Glass Transition Temperature [°C (°F)]	Melting Temperature [°C (°F)]
Aramid	375 (705)	~640 (~1185)
Polyimide (thermoplastic)	280–330 (535–625)	<i>a</i>
Polyamide-imide	277–289 (530–550)	<i>a</i>
Polycarbonate	150 (300)	265 (510)
Polyetheretherketone	143 (290)	334 (635)
Polyacrylonitrile	104 (220)	317 (600)
Polystyrene		
• Atactic	100 (212)	<i>a</i>
• Isotactic	100 (212)	240 (465)
Poly(butylene terephthalate)	—	220–267 (428–513)
Poly(vinyl chloride)	87 (190)	212 (415)
Poly(phenylene sulfide)	85 (185)	285 (545)
Poly(ethylene terephthalate)	69 (155)	265 (510)
Nylon 6,6	57 (135)	265 (510)
Poly(methyl methacrylate)		
• Syndiotactic	3 (35)	105 (220)
• Isotactic	3 (35)	45 (115)
Polypropylene		
• Isotactic	–10 (15)	175 (347)
• Atactic	–18 (0)	175 (347)
Poly(vinylidene chloride)	–17 (1)	198 (390)
• Atactic	–18 (0)	175 (347)
Poly(vinyl fluoride)	–20 (–5)	200 (390)
Poly(vinylidene fluoride)	–35 (–30)	—
Polychloroprene (chloroprene rubber or neoprene)	–50 (–60)	80 (175)
Polyisobutylene	–70 (–95)	128 (260)
cis-Polyisoprene	–73 (–100)	28 (80)
Polybutadiene		
• Syndiotactic	–90 (–130)	154 (310)
• Isotactic	–90 (–130)	120 (250)
High density polyethylene	–90 (–130)	137 (279)
Polytetrafluoroethylene	–97 (–140)	327 (620)
Low density polyethylene	–110 (–165)	115 (240)
Polydimethylsiloxane (silicone rubber)	–123 (–190)	–54 (–65)

<sup>a</sup> These polymers normally exist at least 95% noncrystalline.

PEEK belongs to a group of polymers called polyaryletherketones (PAEK). PAEKs are made up of ether and ketone groups in their polymer chains and can be tailored to vary

the glass transition and melting temperatures (Friedrich et al. 1995). The glass transition and melting temperatures of various PAEKs are shown in Table 3.3.

**Table 3.3 -  $T_g$  and  $T_m$  for various PAEKs (Victrex 2011)**

	$T_g$	$T_m$
PEEK	143°C	343°C
PEK	152°C	373°C
PEKEKK	162°C	387°C

Of the high temperature candidate materials, PEEK offers good baseline mechanical properties in its unreinforced state, as shown in Table 3.4. By addition of structural filler materials such as carbon fibres or glass fibres it is possible to significantly improve these properties, for example the addition of 30%w/w carbon fibres to PEEK increases the tensile strength,  $\sigma$ , from 98MPa to 265MPa, whilst the elastic modulus,  $E$ , is increased from 4GPa to 28GPa (Victrex 2011).

**Table 3.4 - Mechanical properties of high temperature thermoplastics (Matweb 2016)**

	Tensile strength, $\sigma$ (MPa)	Modulus of Elasticity, $E$ (GPa)
Thermoplastic Polyimide (PI)	58.6 – 92.2	2.41 – 4.5
Polyamide-imide (PAI)	62.1 – 150	3.03 – 5.52
Polycarbonate (PC)	46.1 – 93.1	1.8 – 3
Polyetheretherketone (PEEK)	54.5 - 150	2.2 - 12

Figure 3.3 shows a comparison of specific wear rate and friction coefficient for a selection of high temperature thermoplastic materials at a  $pv$  of 1MPa.m/s and at

ambient temperature (Friedrich et al. 1995). PEEK has good wear properties relative to polyimide (PI) and has a friction coefficient of approximately 0.4 in this test setup. Both of these properties can be significantly improved by addition of filler materials such as PTFE and graphite.

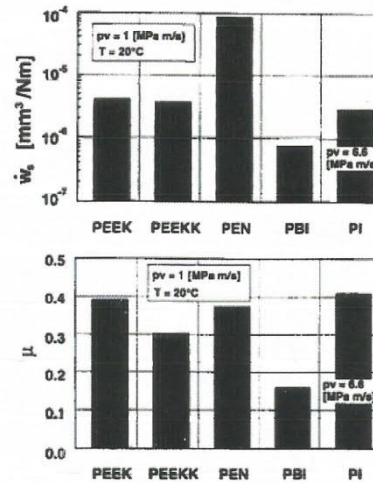


**Figure 3.3 - Specific wear rate and friction coefficient of various high temperature polymers tested at  $p=1\text{MPa}$  and  $v=1\text{ms}^{-1}$  (Friedrich et al. 1995)**

PEEK also has the benefit of being highly chemically inert and composite materials are readily available with enhanced mechanical and tribological properties.

There have been many studies into the performance of filled thermoplastics, in particular PEEK, to characterise the tribology in unlubricated sliding contact conditions. The work of the Institute for Composite Materials (Institut für Verbundwerkstoffe) at the University of Kaiserslautern, and particularly the work of Friedrich et al, has put significant focus on the development of PEEK based composites for tribological applications over the past 30 years (Friedrich 1985). A good body of knowledge has been developed and data has been generated for friction and wear properties of short fibre and particle filled thermoplastics, with significant test data generated. This has been predominantly in standard tribological tests such as the pin-on disc test setup.

The tests have been typically carried out at low contact pressures in the range of 0.1MPa to 10MPa, and sliding velocities of the order of  $1\text{ms}^{-1}$  (Lu and Friedrich 1995; Davim and Cardoso 2009; Rasheva et al. 2010). At present, insufficient research has been undertaken to understand the tribology of these materials at much higher contact pressures applicable to aerospace type applications. It is not clear whether the tribology observed at these low contact pressures and relatively high sliding velocities is also observed in highly loaded, slow sliding speed conditions. The experimental work in this thesis seeks to build an understanding of the tribology in these conditions, which is detailed in Chapter 6.

PEEK possesses mechanical, tribological and chemical properties that are well suited to the arduous conditions experienced by self-lubricating plain bearings in aerospace applications. By incorporation of various filler materials into a composite matrix these properties can be tailored further to achieve the performance required for use in application. Furthermore, a wide and varied selection of PEEK based composites are readily available in the market meaning that many filler materials and blend ratios can be characterised with relatively low material and development costs. PEEK composites will form the basis of the experimental work with the aim of understanding the impact of types and quantities of filler materials upon the properties outlined.

### **3.2.2. Structural fillers**

Structural fillers can be defined as those which are incorporated principally to have a positive impact upon the mechanical properties of the composite matrix. Typically these comprise high modulus and high strength materials which are resistant to deformation and fundamentally increase the load carrying capacity of the bulk material. In the case of woven fabric, continuous fibre reinforced composites, such as SKF X1-40, they add

a defined structure to the composite by the repeating and ordered nature of the fibre alignment. This creates directionality to the properties and creates an anisotropic composite material. When considering short fibre reinforced composites, the fibres can be considered as discrete particles suspended within the bulk resin. Depending upon how they are manufactured, a single fibre can assume an orientation independent of the other fibres in the matrix. It is possible to assume then that all fibres will be randomly oriented and therefore, on the scale of the bulk material, properties should be equal in all directions. If this assumption is correct then the matrix can be considered as a homogeneous isotropic material, and thus be treated as a bulk material. In reality this is an idealised solution as, particularly for injection moulding, the flow characteristics of the material, the mould design, the thickness of the part relative to the fibre length and the injection moulding parameters will all have an impact upon the orientation. It is possible that the fibres can tend to align creating directionality similar to that of the continuous fibre reinforced composite. This will create an anisotropic material, either by chance or through considered design. The validity of this assumption is investigated in Chapter 6.

Chopped carbon fibres are a commonly used filler material to improve the mechanical properties of polymer materials. Carbon fibres exhibit very high strength, up to 6GPa, and high Young's modulus, up to 800GPa (Callister 2006). Most commonly they are used in long fibre woven fabrics impregnated with a resin. They are also available in short-fibre form and are often used as structural fillers in moulded polymers. They exhibit higher stiffness and strength than glass fibres, however they are usually more expensive (De and White 1996).

Significant research has been undertaken to understand the impact of short carbon fibres on the tribological and mechanical characteristics of PEEK. Davim and Cardoso

(2006) used statistical techniques to investigate the effect of  $pv$ , temperature and sliding distance upon the tribological characteristics of 30%w/w carbon fibre filled PEEK. The analysis of variance (ANOVA) design of experiments technique was used with three factors at three levels. They carried out a full design of experiments covering all permutations of all factors which are shown in Table 3.5. They concluded that the friction coefficient was highly influenced by sliding distance and to a lesser extent the  $pv$  factor. They also concluded that the weight loss, or wear, was predominantly influenced by temperature and sliding distance.

**Table 3.5 - Variables for ANOVA experiment carried out by Davim and Cardoso (2006)**

Assignment of the levels to the factors			
Level	Factors		
	$pv$ Factor (MPa m/s)	Temperature (°C)	Sliding distance (m)
1	0.5	60	2500
2	1.5	90	5000
3	3	120	10,000

Lu and Friedrich (1995) concluded that 15-25%w/w carbon fibre reinforcement in PEEK was the optimal composition for wear. Greater than 20% can cause stick-slip, especially at high temperatures. For optimum coefficient of friction, 10%w/w was shown to be optimal.

Similarly to carbon fibres, glass fibres have long been used as a structural component in composite systems. As a continuous fibre reinforcement, it makes up a significant portion of the SKF X1-40 woven fabric bearing liner system. In this respect its purpose is to increase the stiffness of the fabric matrix. It has been shown that the fabric weave with glass fibres exposed at the fabric surface also improves the wear performance in sliding conditions typical of aerospace applications.

Use of short glass fibres in PEEK composites is commonplace. The main advantages of glass fibres for reinforcement is their low cost, high tensile strength and high chemical resistance (Flöck et al. 1999). Glass does exhibit some less desirable properties, such as low fatigue resistance and self-abrasiveness. It is understood that the glass fibres used in Victrex compounds, including 450GL15 and ST45GL30, is chopped E-glass fibres (Ralph et al. 2015). E-glass exhibits a tensile strength of 3450MPa, a similar order of magnitude to carbon fibres, however elastic modulus is much lower at 72.5GPa (Callister 2006).

Unal et al (2004) studied the impact of addition of glass fibres, bronze particles and carbon fibres on the tribological properties of PTFE. They used a pin-on-disc arrangement with contact pressures ranging from 0.18MPa to 1.06MPa and sliding velocity ranging from  $0.32\text{ms}^{-1}$  to  $1.28\text{ms}^{-1}$ . It was concluded that all filled materials gave a reduced friction coefficient and wear rate when compared to unfilled PTFE. Glass fibres showed a significantly better improvement than that of bronze and carbon fibre, which both showed rather similar levels of improvement. Furthermore it was hypothesised that the poor wear performance of PTFE is due to its poor mechanical properties and that by improving the load carrying capacity by inclusion of high strength fillers the wear properties are improved. They also noted that PTFE and its composites exhibit a reduction in coefficient of friction with increasing load.

Voss and Friedrich (1987) investigated the influence of short glass fibre and carbon fibre reinforced PEEK composites. Unfilled PEEK, 20%w/w and 30%w/w glass fibre and 30%w/w carbon fibre filled PEEK were studied. The tests were carried out in a pin-on-ring arrangement with contact pressures from 0.2 to 8.4MPa and sliding velocities of 0.6 to  $3\text{ms}^{-1}$ . They concluded that the addition of short fibres was beneficial to the wear rate in certain  $p$  $v$  conditions when run against a smooth steel counterface. Furthermore,

carbon fibres gave superior improvement to wear resistance when compared to glass fibres. Tests also showed that the friction coefficient was reduced with the inclusion of both glass and carbon fibres. At 0.6MPa and  $3\text{ms}^{-1}$ , unfilled PEEK exhibited a coefficient of friction of 0.27. 20%w/w glass, 30%w/w glass and 30%w/w carbon fibre composites had friction coefficients of 0.26, 0.25 and 0.23 respectively.

Aramid fibres can also be used to add structural reinforcement to self-lubricating composites. Aramid is a synthetic polymer, its name deriving from aromatic polyamide. Its advantages are that it is lightweight, tough and has high strength (Wu n.d.). It has good high temperature stability and is less abrasive than E-glass and carbon fibre. This can improve wear resistance of reinforced composites as the fibres will cause less abrasive wear when they are released from the composite as third body wear. Aramid, specifically Kevlar-49, has a tensile strength of 3.6-4.1GPa and elastic modulus of 131GPa.

Wu (n.d.) developed aramid reinforced Nylon-66 and PPS composites to understand the impact upon wear. The aramid used was Kevlar-49 at a ratio of 20%w/w. These materials were tested alongside unfilled and glass filled versions of the same base materials. Nylon-66 and PPS were filled with 33%w/w and 40%w/w glass fibres respectively. The test setup was a thrust washer type wear test as described by the ASTM D3702 standard. Contact pressures 1.72MPa and 0.276MPa were combined with sliding velocities of  $0.05\text{ms}^{-1}$  and  $0.254\text{ms}^{-1}$  respectively. This gives  $p\nu$  values of 0.088 MPa.ms<sup>-1</sup> and 0.07 MPa.ms<sup>-1</sup> respectively. Tests showed that 33% glass fibre filled nylon-66 reduced the wear rate by a factor of two at  $p\nu = 0.088$  and a factor of four at  $p\nu = 0.07$ . Kevlar-49 filled Nylon-66 reduced the wear rate by four times at  $p\nu = 0.088$  and eight times at  $p\nu = 0.07$ . For PPS, Kevlar-49 gave a 20 times improvement in wear rate compared to glass fibre reinforcement.

The impact of carbon fibres, glass fibres and aramid fibres were tested, the results for which are presented in the experimental chapters of this thesis.

### **3.2.3. Tribological fillers**

Tribological fillers are those materials which when incorporated into a self-lubricating composite can improve the friction or wear performance of the composite. Typically these materials will be dry lubricants which significantly reduce the friction coefficient. By this nature, the heat generated due to friction will also be lower. This can reduce wear in a polymer matrix as the temperature dependent mechanical properties of the bulk polymer will be higher as the temperature seen at the contact and dissipated through the composite is lower. Depending on the tribological filler used there is typically a reduction in mechanical properties, especially if another low modulus polymer is used.

Polytetrafluoroethylene (PTFE) is well known for its low friction coefficient, between 0.05-0.1 (DuPont 2012) It can be used as a filler material in order to lower the coefficient of friction of the composite material. Alone, PTFE is considered to have poor wear properties when compared to other thermoplastic materials, illustrated in Figure 3.4 (Lancaster 1972).

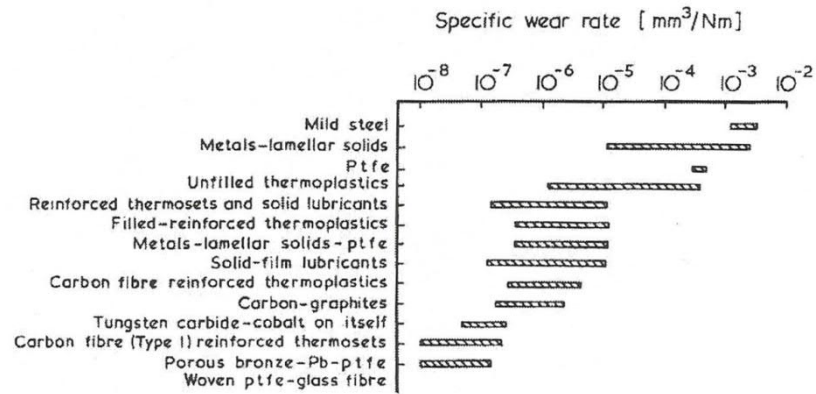


Figure 3.4 - Specific wear rates of various materials against steel (Lancaster 1972)

Inclusion of PTFE into PEEK composites has been shown to improve the wear rate at low concentrations, however it increases as the ratio of PEEK-PTFE approaches a predominantly PTFE concentration. Coefficient of friction is significantly reduced by the inclusion of PTFE, with a 5%v/v filled PTFE exhibiting a friction coefficient half that of its unfilled equivalent. The work of Lu and Friedrich (1995) shows these relationships for PEEK-PTFE composites ranging from 100%v/v PEEK to 100%v/v PTFE. Their tests were carried out at a contact pressure of 1MPa and a sliding velocity of 1ms<sup>-1</sup>. They concluded that the optimum inclusion of PTFE in PEEK was 10%v/v to 20%v/v for both friction and wear improvement. The results are shown in Figure 3.5.

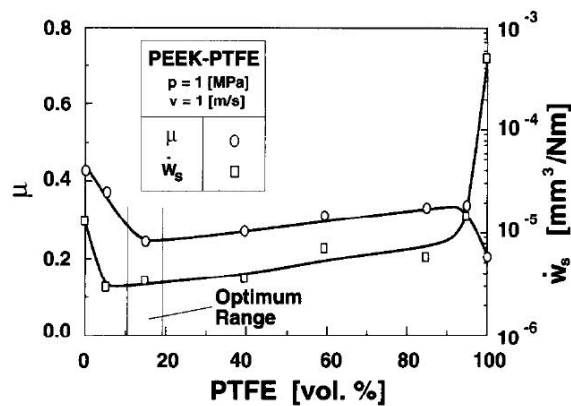


Figure 3.5 - Optimum range of PTFE content in PEEK composites for tribology

PTFE creates a transfer film on the sliding contact counter surface. This transfer layer generates a smoother contact surface on the metal counterface which reduces local asperity stresses. This leads to a reduced wear rate of the PTFE containing composite (Lancaster 1972).

Another form of solid lubricant is classed 'lamellar solids'. These materials have a plate-like crystal structure which has strong interatomic bonding within the crystal planes, but weak bonding between successive planes (Williams 1994). This allows the layers to move easily across each other when subjected to shear stresses. This leads to low friction in these types of materials. The two most commonly used solid lubricants in this class of materials are graphite and molybdenum disulphide, MoS<sub>2</sub>. Similarly to PTFE, these materials create a transfer layer upon the opposing surface after a degree of running in. This development of a transfer film is inefficient as is the transfer process itself (Lancaster 1972). Therefore a content of at least 10%v/v is required to obtain minimum values for coefficient of friction. As graphite is quite stiff, the transfer film on steel exhibits a stiff behaviour when compared to PTFE (Zhang et al. 2004). The mechanical properties of these materials compared to PTFE can also mean that their negative impact upon the mechanical properties the PEEK composite is less severe.

Giltrow (1973) suggests that the inclusion of lamellar solids in self-lubricating composites is mainly seen in high load, 70MPa, and low speed, 0.1ms<sup>-1</sup> reciprocating mechanisms. This is in the range of the application conditions being investigated in this thesis therefore their inclusion in the composite materials being tested is paramount.

### 3.3. Selected materials for characterisation

The ideal scenario would be to manufacture a range of material blends and perform a design of experiments to fully understand the main effects of each constituent material on the performance and the interactions between materials. In order to do this it is necessary either to fully develop the material blending and injection moulding processes, or to work with a polymer processing company who can supply the materials to the required specification. It is not within the scope of this study to develop material compounding process as the required equipment, a twin screw extruder, is not available. Also the cost of developing the number of material blends required for a full design of experiments is cost prohibitive. Due to this commercially available materials are selected in order to develop a first understanding of the composite materials in the test conditions required for this study.

Based upon the understanding of the individual component materials and their influence upon the composite system, as discussed in Section 0, a number of these component materials have been selected for experimental testing. The selected materials and fillers are shown in Table 3.6.

**Table 3.6 - Component materials selected for further analysis**

Base Polymers	Structural Fillers	Tribological fillers
Polyetheretherketone (PEEK)	Aramid fibres	Graphite
Polyetherketone (PEK)	Carbon fibres	Molybdenum disulphide (MoS <sub>2</sub> )
Polyetherketoneetherketoneketone (PEKEKK)	Glass fibres	PTFE

The experimental plan consists of a number of commercially available materials which utilise the selected structural and tribological fillers at varying ratios. These materials were supplied by Victrex and Lehmann & Voss. The Victrex samples were supplied as moulded plaques of 150mm<sup>2</sup> and 4mm thickness. The samples provided by Lehmann & Voss were in the form of tensile test specimens with the dimensions shown in Figure 3.6. The thickness of the samples was 4mm. In order to be tested as described in Chapter 6 it was necessary to cut individual test samples from these as indicated by the red dashed line. The dimensions of these were 24mm x 20mm x 4mm

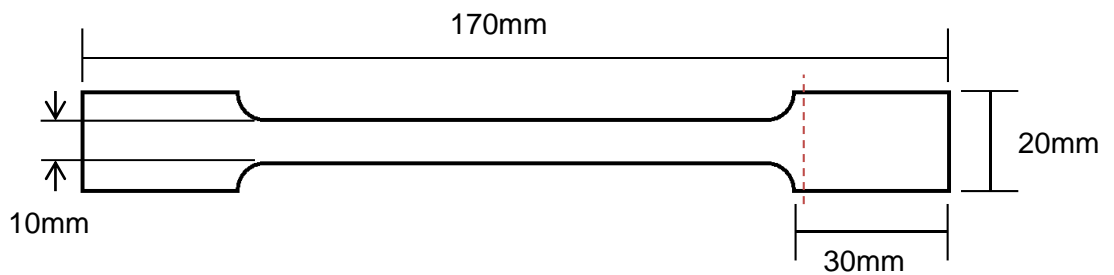


**Figure 3.6 - Sample dimensions of Lehmann & Voss supplied composites**

The aim of Initial coupon tests was to rank each of the selected materials. It gives an understanding of the role that each component plays in the composite system and its effect on the performance of the material as a bearing surface, both in its tribological and structural properties.

The composite materials which have been selected for analysis are shown in Table 3.7. Materials designated 1105-xxxx are those materials supplied by Lehmann & Voss, whereas all others were supplied by Victrex. Each material is broken down by its constituent filler materials and each is shown by its percentage by weight of the total composite. All compositions are PEEK based composites unless shown otherwise. ST45GL30 and ST45CA30 are PEK based. HT22GL30 and HT22CA30 are PEKEKK

based. This is to determine whether there is any tribological performance benefit deriving from the use of these base materials when compared to PEEK owing to their improved thermal properties, as outlined in Section 3.2.1.

Table 3.7 - Selected composite materials and their composition by weight for analysis

Composite	PEEK	Glass fibre	Carbon fibre	Aramid fibre	PTFE	Graphite	MoS <sub>2</sub>	Silicone oil
450G	100%							
450GL15	85%	15%						
450GL30	70%	30%						
HT22GL30 (PEK)	70%	30%						
ST45GL30 (PEKEKK)	70%	30%						
HT22CA30 (PEK)	70%		30%					
ST45CA30 (PEKEKK)	70%		30%					
150FC30	70%		10%		10%	10%		
450FE20	80%				20%			
WG101	Composition Unknown							
1105-8783	55%			20%	10%		15%	
1105-8487	70%			30%				
1105-8403	80%			10%	10%			
1105-8165	50%		10%			40%		
1105-0699	55%		30%		10%	5%		
1105/GR/15/T F/15-2	70%				15%	15%		
1105-8613	60%		10%		20%	10%		
1105-7760	50%		10%		15%	10%	15%	
1105/XCF/15-S	85%		15%					
1105-7714-WE	66%				15%		15%	4%

The ratios shown allow comparison between materials and also the optimum amount of each constituent can be identified.

It is expected that the following relationships can be evaluated with the materials shown in Table 3.7. A comparison can be made of the performance of the three polymer technologies, PEEK, PEK and PEKEKK through comparison of Victrex HT and ST grades with carbon fibre and glass fibre fillers. The key difference between the three polymers is the thermal properties, as discussed in section 3.2.1. Direct comparison of aramid fibre, carbon fibre and glass fibre fillers can be derived from the materials filled only with carbon or glass fibres. Influence of PTFE can be assessed directly and in combination with other fillers. Graphite and MoS<sub>2</sub> can be also assessed in combination with other fillers. Lehmann & Voss provided a material composition containing 4%w/w silicone oil, material 1105-7714-WE. Whilst this is not one of the selected materials, it nevertheless may provide some interesting results.

It is hypothesised that materials with a high volume fraction of hard particle fillers will be more brittle than those with high volume fraction of polymeric fillers. This is due to the stiffness of the fillers being significantly higher than that of the matrix. When loaded, the interfacial bonding between the filler and the PEEK matrix will fail before the filler material will fail. Any internal tensile stresses will be carried by the PEEK matrix and any defect will propagate as cracks through the material. Whilst a high loading of hard particles will be beneficial to load carrying capacity, brittle failure is more likely to occur where defects exist. In order to test this hypothesis it is much clearer to present the selected composites and their components by volume rather than by weight. This is presented in Table 3.8. The percentages have been calculated by using published data for the density of each component material (Victrex 2011; Matweb 2016; Callister 2006; Hexcel 2016).

Table 3.8 - Selected composite materials and their composition by volume for analysis

Composite	PEEK	Glass fibre	Carbon fibre	Aramid fibre	PTFE	Graphite	MoS <sub>2</sub>	Silicone oil
450G	100%							
450GL15	72%	8%						
450GL30	82%	18%						
HT22GL30 (PEK)	82%	18%						
ST45GL30 (PEKEKK)	82%	18%						
HT22CA30 (PEK)	76%		24%					
ST45CA30 (PEKEKK)	76%		24%					
150FC30	79%		10%		7%	6%		
450FE20	87%				13%			
WG101	Composition Unknown							
1105-8783	66%			22%	7%		5%	
1105-8487	72%			28%				
1105-8403	84%			10%	6%			
1105-8165	62%		9%			29%		
1105-0699	64%		25%		7%	3%		
1105/GR/15/T F/15-2	80%				10%	10%		
1105-8613	71%		9%		14%	7%		
1105-7760	66%		10%		12%	8%	5%	
1105/XCF/15-S	89%		11%					
1105-7714-WE	79%				11%		5%	6%

### 3.4. Hypotheses

It is expected that the material compositions being tested will show that there is a compromise between the mechanical and tribological properties of filled materials. This derives from an expectation that the materials with the highest mechanical properties are likely to perform poorly in friction and wear. Conversely, materials with very good friction properties are more likely to be poor mechanically. It is unclear which materials will perform the best in wear, however it is expected that materials with good friction properties will be most likely to exhibit good wear properties. The justification for this hypothesis is that in the dynamic test conditions that the materials are exposed to are of a very high load of 172MPa. With this magnitude of load it is expected that the materials will fail plastically. The inverse proportionality of temperature and compressive strength means that heat generation will be a key factor in the failure of these materials. Therefore with a low friction coefficient, less heat will be generated and hence the mechanical properties will be sustained at a higher level. The balance of tribological fillers to structural fillers is expected to be critical to performance. The experimental chapters seek to address this hypothesis.

Mechanically, it is expected that the creep resistance and compressive strength will be proportional to each other. It is expected that materials with a high volume of structural fillers will exhibit the best creep resistance. This will however be balanced by the expectation that materials with a high volume of structural fillers will be more likely to suffer brittle failure.

## **4. Developing the injection moulding process**

The aim of this chapter was to develop the capability to injection mould PEEK composites and gain an understanding of the injection moulding process. The final aim was to be able to injection mould PEEK composite test samples, as well as to be able to develop a mould for either a standard bush geometry or spherical bearing geometry however this was not feasible within the project due to the level of investment required. Also, the project became more focussed upon the fundamental tribology of PEEK composites as outlined in Chapter 3. Nevertheless, it was valuable to start to develop an understanding of the injection moulding process and the potential impact of the process upon the properties and tribology of the composite materials. It is recommended that this work forms the basis of further study into the manufacturing process in the context of enhancing the tribology of injection moulded self-lubricating bearing liners.

### *4.1. Injection moulding theory and process impact*

Injection moulding is a common manufacturing process for producing plastic parts. Crudely, the process involves taking a polymer based feedstock from solid to liquid form and injecting the liquid material into a cavity at high pressure. The material is then solidified by either cooling below the melting temperature for thermoplastics or by crosslinking for thermosets, such that the solid material takes the form of the mould cavity. This process is designed to be repeatable and should produce parts of predictable geometry and consistent quality. Figure 4.1 shows a typical layout for an injection moulder and the components of the machine.

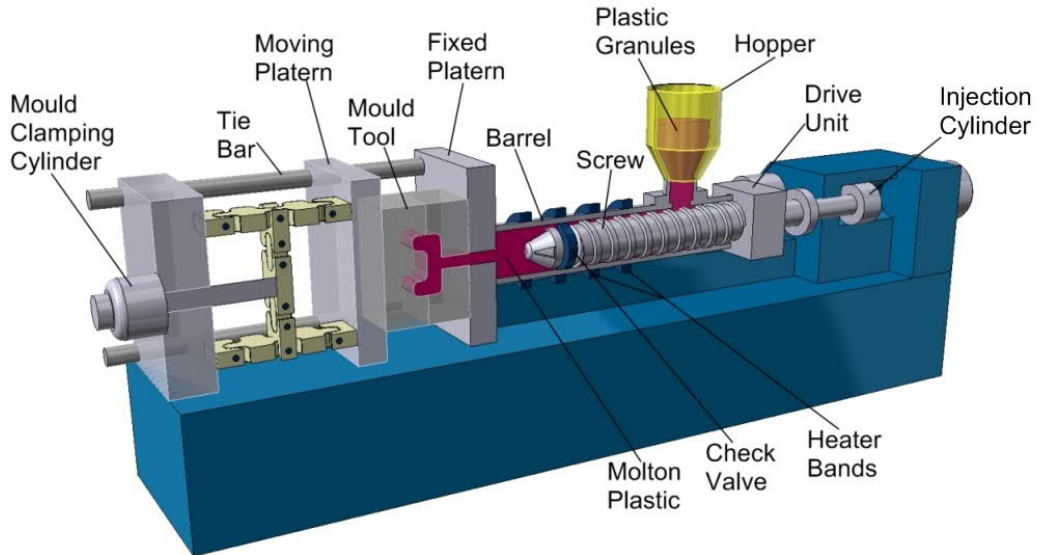


Figure 4.1 - Injection moulding machine (Rutland Plastics Ltd 2016)

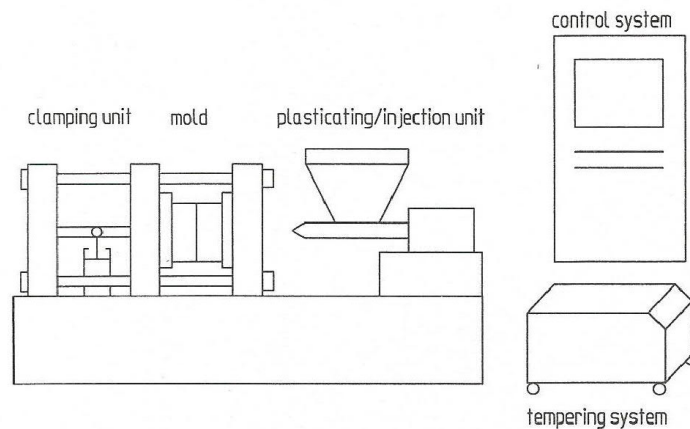
The feedstock for the moulding process is typically in the form of pellets or powder as shown in Figure 4.2. Typically these pellets are formed using a twin screw extruder where any filler materials are added to the base polymer to injection mould. The twin screw extruder creates a homogeneous raw material by thorough mixing of the molten plastic and solid fillers.



Figure 4.2 - PEEK pellets for injection moulding

The basic components of an injection moulder are shown in Figure 4.3. The plasticising unit takes the material in solid form, moves it through a series of heating elements in order to melt the material whilst at the same time increasing the pressure behind the

material in order that it can be forced into the mould cavity. This is typically done with a screw plasticising unit which ensures a homogeneous melt of the material and good mixing. The clamping unit is analogous to a horizontal press which applies a clamping force between the fixed and moving halves of the mould (Pötsch and Michaeli 2008). This clamping force ensures that the molten material is held in the cavity, and is sufficient to react the force of the material being injected under high pressure. Once the material has solidified and is sufficiently cool, the clamping unit retracts in order to release moulded part



**Figure 4.3 - Basic design of an injection moulding machine (Pötsch and Michaeli 2008)**

Figure 4.4 shows a simple two plate injection mould tool. The liquid polymer is injected through the opening in the right hand half of the mould. The material flows through the sprue into the mould cavity. Once solidified, the mould opens at the parting line and the part is ejected either manually or by an ejector system.

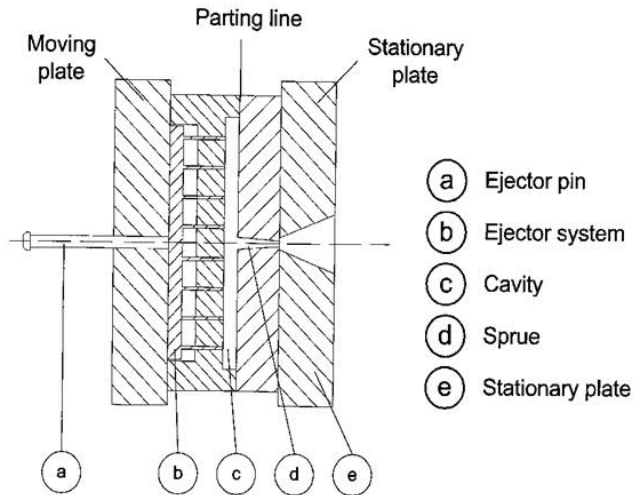


**Figure 4.4 - Simple two-plate injection mould (Goodship 2004)**

Injection moulding is considered to be a high volume process. This is due to the very fast cycle times that can be achieved, particularly in fully automated injection moulding units. It is also most economically viable for large runs of the same part. The cost of tooling is relatively high as the process requires matched metal dies because of the high temperatures and pressures seen in the process (Campbell 2003). This is often of the order of several thousand pounds depending upon the complexity of the mould cavity and the materials used. In high volume manufacturing, this cost is spread over many parts, meaning that the cost per part is acceptable. To balance the high fixed costs, the capability of the injection moulding process to be automated can lead to low cycle times and lower labour costs. The consistent operation of the process can give high quality products with a low reject rate (De and White 1996).

Self-lubricating liner materials conforming to the AS81820 qualification standard are limited to a maximum thickness of 550µm (SAE 2008). Typical fabric liner systems conforming to this standard, such as SKF X1-40, have a thickness of approximately 300µm. This would be considered a very thin section for injection moulding and therefore could pose some difficulty to manufacture. In a thin section, the surface area

of the cavity is very large when compared with the volume of material. As the mould is cooler than the polymer entering the mould, for thermoplastic materials, the large surface area means that cooling of the polymer occurs more rapidly. Rapid and uneven cooling can cause internal stresses in the moulded part, which can cause distortion. Also, rapid cooling coupled with poor mould design can lead to the mould cavity not fully filling before the material freezes off. Finally, the typical length of short fibre fillers observed in this work is approximately 100-200 $\mu\text{m}$ . If the section thickness is of a similar order of magnitude, the fibres will tend to align parallel to the surface. This will cause the material to be anisotropic, this may, however, be a desirable outcome.

The materials being developed will be used as a self-lubricating liner material which will be adhered to a metallic substrate. In order to assemble the metallic components the liner will need to be directly moulded into the part. In the case of bushes, the liner will be moulded into the contact surfaces. For spherical plain bearings, the liner will be directly moulded into the cavity between the inner and outer races of the bearing. For this the inner and outer rings will need to be assembled with the required clearance between the components. The insert moulding technique can allow for in mould assembly of the bearing metallic component and the liner. Insert moulding is a process where a preform component is placed into the mould cavity and the material is injected onto the metallic component (Goodship 2004). At each cycle, a component must be loaded into the mould tool either by hand or using automation. This added step will add time to the injection process. Different rates of thermal expansion are likely between the mould tool, the insert and the polymer. The insert is likely to need to be preheated to enable insertion into the mould whilst respecting the close tolerances needed to ensure the polymer only fills the desired part of the cavity. Also, upon cooling internal stresses can be formed at the material interfaces and can lead to poor bonding of the polymer to the substrate (Pötsch and Michaeli 2008).

## **4.2. Injection moulding equipment**

The injection moulder used for this experimental work was an Arburg Allrounder 270C 400-100 with a 20mm diameter screw injection unit, similar to that shown in Figure 4.5. This machine has a specification typical to that of an industrial standard injection moulder. It is expected that the bearing products described in this thesis will be manufactured using similar equipment. It was therefore deemed necessary to develop an understanding of the process on a machine of this scale. The machine capabilities are summarised in Table 4.1.



**Figure 4.5 - Example of a modern injection moulding unit (Arburg GmbH 2016)**

**Table 4.1 - Arburg Allrounder 270C 400-100 specification summary (Arburg GmbH 2016)**

Maximum injection pressure	2500 bar
Maximum clamping force	400kN
Screw diameter	20mm
Maximum barrel temperature	450°C
Maximum tool temperature	220°C *
Minimum tool temperature	Ambient
Maximum shot volume	31cm <sup>3</sup>

\* From modification of the tooling discussed later

The maximum barrel temperature of 450°C is sufficient for moulding a wide range of thermoplastic materials, including PEEK for which moulding temperatures of approximately 400°C are required (Victrex 2011a).

The mould tool used to create flat samples for tribological tests is shown in Figure 4.6. The mould is an existing piece of tooling which has been used for previous studies. The tool has been manufactured using tooling steel and features a single runner system with a single fill point into the cavity. The dimensions of the moulded part are 120mm x 24mm x 2mm. The cavity uses an ejection system where the back face of the cavity moves outwards to release the moulded part, as indicated in Figure 4.6

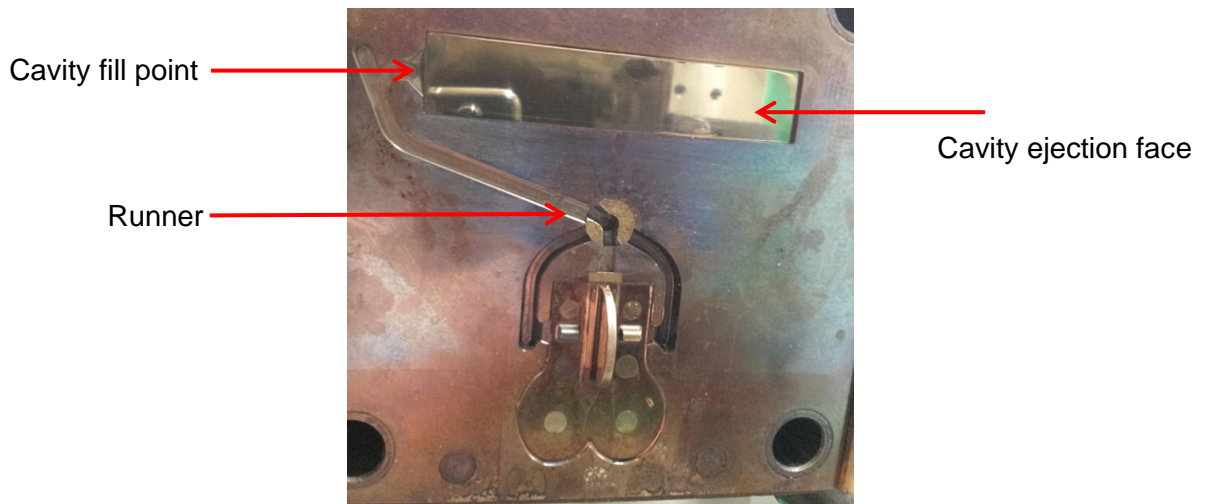


**Figure 4.6 - Mould tool for flat test samples**

PEEK is a high temperature thermoplastic material with thermal properties far higher than typically used high-volume thermoplastics. The melting point of standard grade PEEK is 343°C (Vitrex 2011b) with processing temperatures between 350°C and 420°C (Goodship 2004 p.94). When injection moulding PEEK, it is necessary to utilise a heated mould tool as otherwise the temperature difference between the material flowing into the mould and the mould cavity would be so large as to cause defects in the moulded part. Vitrex (2011a) recommend using a tool temperature of minimum 170°C in order to obtain a crystalline component. Higher temperatures are suggested to aid cavity filling, particularly for filled composites, and to increase dimensional stability.

Prior to this study, the injection moulder did not have the ability to artificially heat the mould. Primarily it did not have the hardware capability to use heating elements; however control of heating elements could be enabled within the software. In order to be able to injection mould PEEK, heating elements were installed into the injection moulder and enabled within the software. The mould had existing cavities for the use of heating elements, therefore was capable of being heated to allow the use of high temperature thermoplastics as well as thermosets which require heat to crosslink. The

mould itself has four cavities, two at either side as shown in Figure 4.7. Due to a limited number of available wiring terminals within the injection moulder control unit a maximum of three heating elements could be installed. The heating elements used were cartridge heaters 10mm diameter and 50mm length, with a power rating of 250W. In addition, thermocouples were installed behind the thermal insulation boards to measure the temperature and give feedback to the control system. This allowed the control system to thermostatically control the mould temperature. In order to verify that the mould cavity had reached the correct temperature measurements were taken using an infrared thermometer. The addition of heating elements meant that the mould was capable of being heated to 220°C, in excess of the requirements for PEEK moulding.

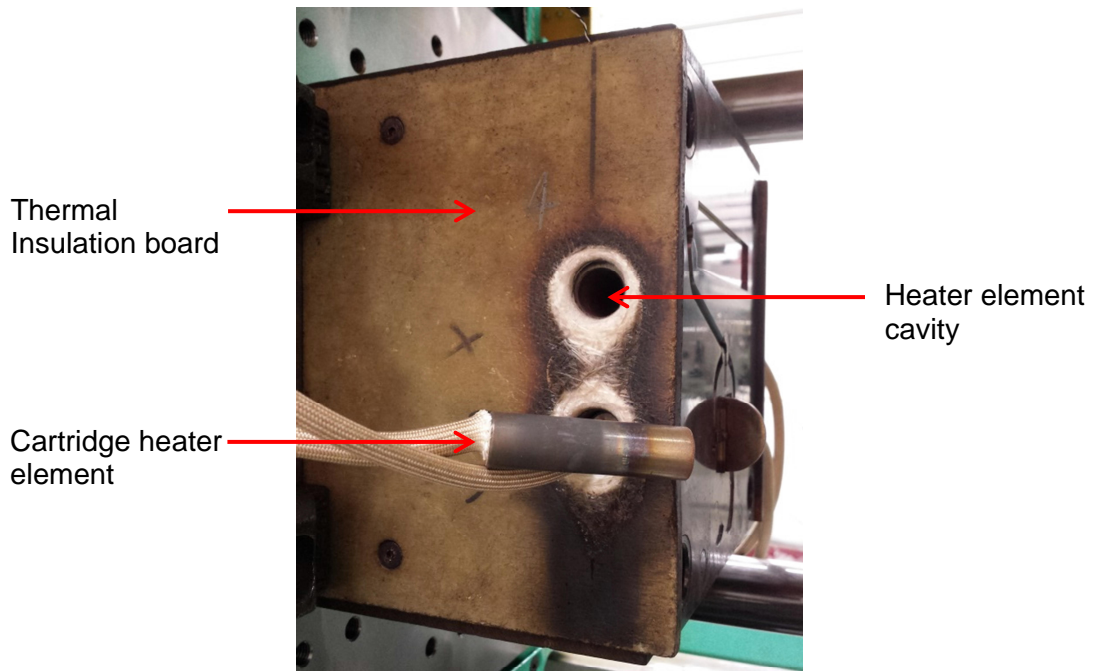


**Figure 4.7 - Mould tool for flat test samples with heater cavities and elements shown**

With this added capability, it was possible to carry out the experiments to investigate the impact of moulding parameters on the final moulded part using PEEK. It also gave the ability to manufacture flat samples for tribological testing.

### *4.3. Experimental design*

In order to gain an understanding of the influence of the injection moulding parameters upon the manufactured parts, a series of experiments were carried out with a range of thermoplastic materials. The initial aim was to develop an understanding of the process with unfilled thermoplastics, starting with available materials before modifying the injection moulder to enable the moulding of PEEK. Due to the focus of the main body of work moving more towards the fundamental tribology of PEEK composites, it was decided to only investigate unfilled materials and to recommend a wider investigation into moulding of filled composites as future work.

A common view of injection moulding is that it is a 'dark art'. It requires specialist knowledge and many years of experience to set up injection moulding parameters to create a desired part free from defects (Basil 2011). When defects are seen, there are a number of parameters that can be varied in the process to eliminate those defects. Whilst one operator may vary one set of parameters to get the desired result, another operator can vary a different set of parameters and get the very same result. The Six Sigma process gives a number of tools to enable process control and improvement. The key aim is to identify the cause of defects and to reduce variability in manufacturing processes. The Six Sigma approach can be used to understand the impact of controlled variables within the manufacturing process upon the finished parts by empirical and statistical means. The steps taken in this approach are shown in Figure 4.8, as are the tools used to develop the understanding at each step.

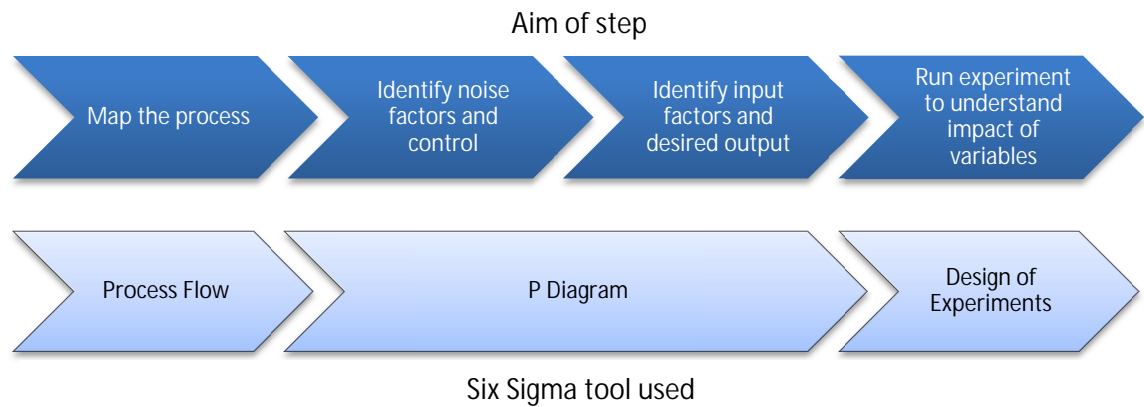


**Figure 4.8 - Six Sigma steps used for process control**

The design of experiments approach has successfully applied to the injection moulding process to understand the influence of processing parameters and to optimise the manufacturing process. The Taguchi method was applied by Sha et al (2007), Erzurumlu and Ozcelik (2006), Tang et al (2007) and Altan (2010) to assess process parameter influence on surface quality and warpage in thin sections and shrinkage. Park and Ahn (2004) argue that whilst the Taguchi approach is effective in identifying main effects of design factors, interactions of factors cannot be considered effectively. For this reason they suggest using a factorial design. The Taguchi method tested factors at three levels, which is advantageous when considering curvilinear responses. A two level approach approximates a linear trend, however this can be adequate for process optimisation as it represents the trend within the range of the high and low values.

Sha et al (2007) considered barrel temperature, mould temperature, injection speed and distance between features for micro-injection moulded parts. They conclude that all three machine parameters have significant influence on cavity filling, however they are not consistent between different polymers. They also conclude that the geometric features have little impact on cavity filling. The polymers used in this study were

polypropylene (PP), polyoxymethylene (POM) and acrylonitrile butadiene styrene (ABS).

Tang et al (2007) studied the influence of factors on warpage in a thin plate with dimensions of 120mm x 50mm x 1mm. The factors considered were melt temperature, filling time, packing pressure and packing time. They conclude that the most influential factor for warpage is the melt time, and that filling time only had a slight influence. Erzumulu and Ozcelik (2006) considered mould temperature, melt temperature, packing pressure in their experiment using a three level Taguchi design. They used a polycarbonate/ABS copolymer, POM and PA66. They showed that packing pressure has the most significant impact in warpage.

Park and Ahn (2004) used the factorial design approach to aid design of a runner system for a two cavity mould. The factors varied were sub-gate position, main gate position, and sub and main runner diameters. The design of experiments approach showed that all factors except sub runner diameter had a strong influence on filling time and injection pressure. They concluded that the factorial design approach was most effective as it enabled two factor interactions to be identified and optimised.

The Six Sigma approach has been used in this work to understand the noise factors in the injection moulding process and to gain an understanding of the moulding parameters on the finished parts. The type of defect that has been focussed upon is short mouldings and excessive shrinkage of the finished part. Both of these will mean that a lower volume of material than desired fills the mould cavity of the injection moulder. This can be characterised by the mass of the part.

### **4.3.1. Process mapping**

In order to identify unwanted noise within the manufacturing process, it is necessary to create a process map for injection moulding of a part. This should include all the process steps to get from raw material to the finished part. The process flow for this experiment can be found in Appendix A. The understandings gained from mapping the process allow a 'P Diagram' to be populated. The 'P diagram' shows the inputs and outputs of the process. The inputs are both desired and undesired, the former being the controlled variables, process constants and process controls, the latter being noise factors. The outputs are the ideal state and the error state.

The 'P Diagram' for the injection moulding process for this experimental work is shown in Figure 4.9. The noise factors have been identified with those which are deemed to have a significant impact upon the volume of material entering the mould becoming the controlled input signals. Those which cannot be controlled or have minimal impact are accepted. The input signals are split into constant and variable inputs. The constant inputs are those which could be varied, however have been assumed to have minimal impact upon the actual volume of the moulding compared to the desired volume. For the experiment, these values have been fixed for each material and are shown in Table 4.2. Conversely, the variable inputs are those which have been assumed to impact the volume of the moulding and will be the parameters investigated in this experiment. These are summarised in Table 4.3.

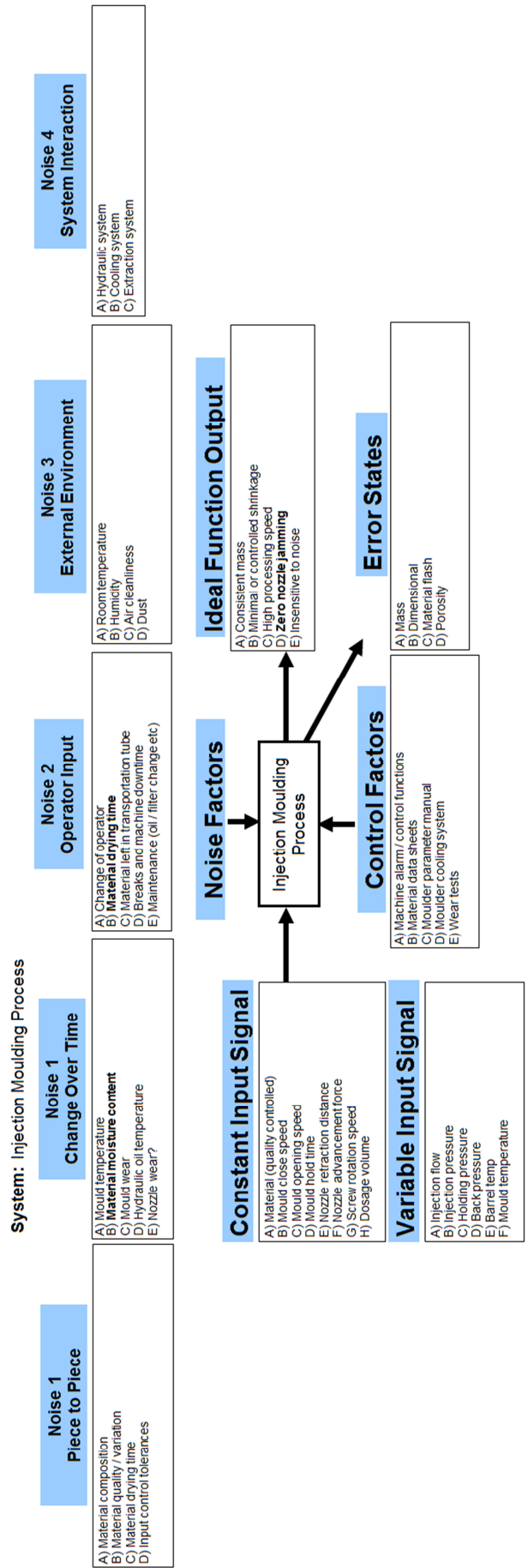


Figure 4.9 - 'P Diagram' for injection moulding

Table 4.2 – Constant input signals for each material in experiment

		Constant Input Parameters							Unit
Input	Identification	HDPE	ABS	Polystyrene	Nylon (PA66)	PEEK			
Mould	Close speed (stage 1)	350	350	350	350	350			mm/sec
	Close speed (stage 2)	250	250	250	250	250			mm/sec
	Opening speed	150	150	150	150	150			mm/sec
Nozzle	Hold time	8.1	8.1	8.1	8.1	8.1			sec
	Retraction distance	20	20	20	20	20			mm
Screw	Advancement force	40	40	40	40	40			kN
	Rotation speed	10	10	10	10	6			m/min
Dosage	Dosage volume	13.5	13.5	13.5	13.5	13.5			ccm
	Mould close time	8	8	8	8	30			sec
Mould temperature		No heating	No heating	No heating	No heating	170			°C

Table 4.3 - Variable input signals for each material in experiment

		Variable Input Parameters										Unit
Input	Identification	HDPE		ABS		Polystyrene		Nylon (PA66)		PEEK		
		Max	Min	Max	Min	Max	Min	Max	Min	Max	Min	
Injection flow	Q305	40	30	40	30	40	30	40	40	20	20	ccm/sec
	p305	1350	600	1550	650	1550	650	1550	450	2500	1250	Bar
	p311 + p312	800	300	900	400	900	350	1050	350	1800	600	Bar
	p403	90	60	80	40	80	40	60	60	60	60	Bar
Barrel temp	Processing temperature	280	190	240	180	250	190	260	230	420	380	°C
	Zone 1	260	190	220	180	230	190	240	230	390	380	
	Zone 2	265	195	225	185	235	195	245	235	400	370	
	Zone 3	270	200	230	190	240	200	250	240	410	380	
	Zone 4	275	205	235	195	245	205	255	245	420	390	
Zone 5	280	210	240	200	250	210	260	250	400	380		

### 4.3.2. Experimental design

The materials selected for the experiment were low density polyethylene (LDPE), polystyrene, acrylonitrile butadiene styrene (ABS), polyamide 66 (PA66) and PEEK. The reason for carrying out the experiment with a wide range of materials was to understand if the significant factors were common across materials.

All materials were dried prior to moulding in accordance with the values shown in Table 4.4. The materials were dried using an Arburg Thermolift material dryer with forced convection heating as shown in Figure 4.1. The material dryer also automatically conveys the dried material to the throat of the plasticising unit in a closed circuit to prevent any moisture reabsorption prior to moulding.

**Table 4.4 - Drying parameters for selected materials (Goodship 2004)**

Material	Drying temperature	Drying time
LDPE	-	-
Polystyrene	-	-
ABS	90°C	3 hours
PA66	100°C	4 hours
PEEK	200°C	4 hours



**Figure 4.10 - Arburg Thermolift material dryer**

When starting the injection moulder or changing the barrel temperature, parts were manufactured until consistent mouldings were observed. This is because all elements of the moulding machine needed to reach a steady temperature so that the time dependent impact was minimised. In particular, the mould tool was sensitive to the temperature of the polymer entering the cavity.

The factors varied for each test are shown in Table 4.5. Initial testing with LDPE, polystyrene and ABS showed that back pressure and injection flow did not show any significance to the mass of the parts produced and therefore became constant input signals for PA66 and PEEK.

**Table 4.5 – System control variables for each material**

Material	Barrel Temperature	Injection Pressure	Holding Pressure	Back Pressure	Injection Flow
LDPE	X	X	X	X	X
Polystyrene	X	X	X	X	X
ABS		X	X	X	X
PA66	X	X	X		
PEEK	X	X	X		

The experimental design used was a fractional factorial design of experiments. For the first experiments using LDPE, polystyrene and ABS,  $2^{5-1}$  factorial design was used. This means that each of the five factors identified were varied at 2 levels, a high and low value for each. Half of the possible combinations were tested, giving a response for all main effects two factor interactions. 16 test runs were carried out for each material. The high and low values were estimated from manufacturers recommended values and are shown in Table 4.3. For experiments using PA66 and PEEK, a  $2^3$  full factorial

design was used. Again, this was a two level design, however all combinations of factors were tested giving eight test runs per material.

### **4.3.3. Results**

Figures 4.11 to 4.14 show the results for polystyrene, ABS, PA66 and PEEK respectively. The graphs have been produced using Minitab®, a statistical software programme with which design of experiments can be designed and analysed. The plots show the Pareto charts for each material, which illustrates the magnitude of each main effect and two level interaction. The red line shows the threshold for which a result can be considered significant. There are also main effects and interaction plots shown, which show the direction of the effect and the interaction crossovers.

Varying the factors for LDPE resulted in full mouldings in all cases. No results are presented as varying all factors between the levels presented in Table 4.3 had no influence on the final moulding. LDPE was straightforward to mould and was forgiving to extremes in moulding parameters.

Polystyrene had significant variation in the filling of the mould cavity. There were both short mouldings and mouldings with significant flash as the material overfilled the mould. Figure 4.11 shows plots for the main effects and interactions of the variables tested. The red line in the Pareto charts shows the threshold for a factor to be considered significant. For polystyrene, the main effects of holding pressure and barrel temperature are significant, as are the two factor interactions of holding pressure-barrel temperature and injection pressure-barrel temperature. Back pressure and injection flow did not show a significant impact upon the filling of the mould, as didn't injection pressure in isolation.

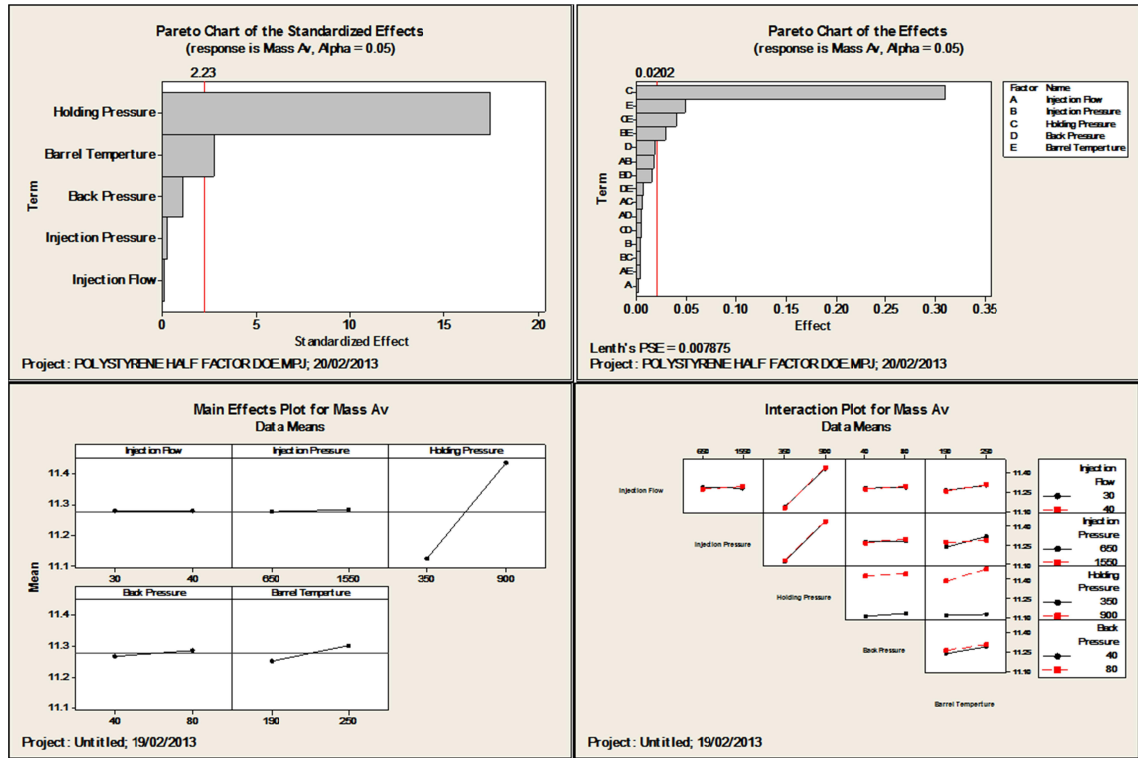


**Figure 4.11 - Pareto charts of effects and main effect and interaction plots for polystyrene experiment**

Similarly to polystyrene, ABS gave significant variation in filling of the mould cavity. The low barrel temperature setting of 180°C at the throat to 200°C at the nozzle was too low for the material to flow into the mould and the material would freeze in the nozzle exit. Only the mouldings at high barrel temperature yielded results.

Figure 4.12 shows the results for ABS. Barrel temperature is not shown as values were zero, however there is clearly a very strong impact of this variable. As for polystyrene, holding pressure has a significant effect as does the holding pressure-injection pressure interaction. For ABS there is also a significant effect of injection pressure. As for polystyrene, injection flow and back pressure have an insignificant impact.

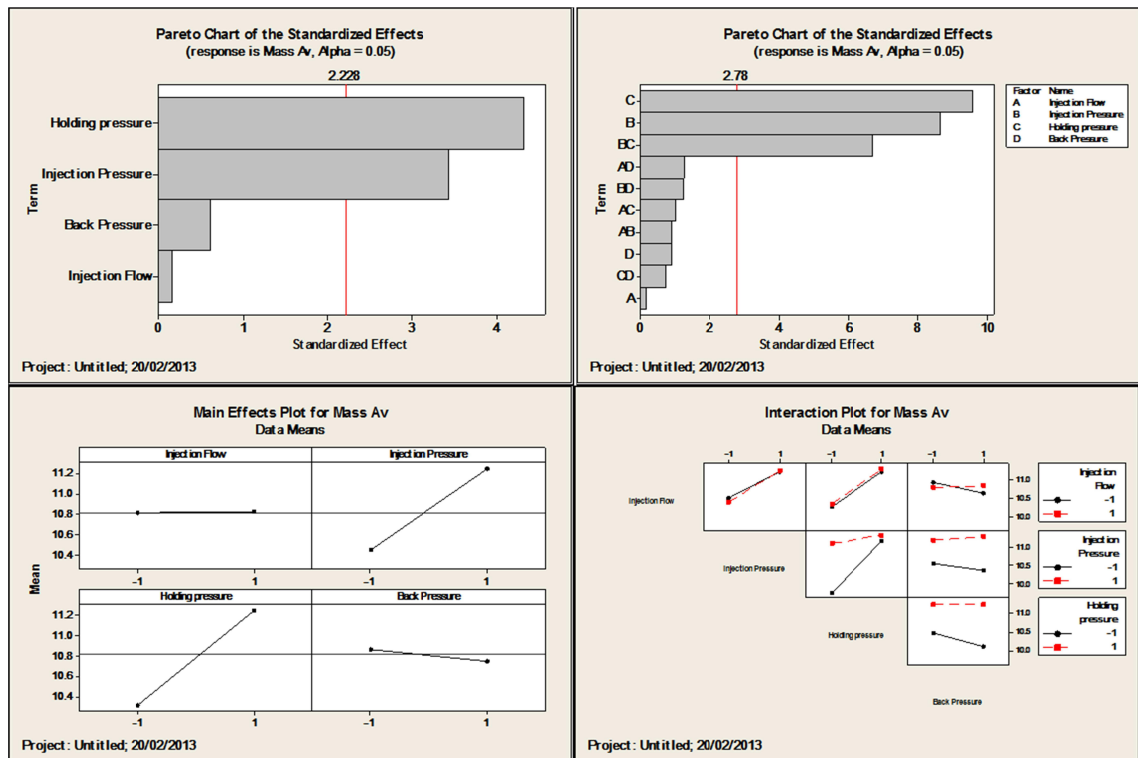


**Figure 4.12 - Pareto charts of effects and main effect and interaction plots for ABS experiment**

The results from both polystyrene and ABS showed that injection flow and back pressure did not have a significant impact upon mould filling. For the experiments with PA66 and PEEK, these have been fixed and will not be tested.

PA66 was the most problematic material to process. Even after drying for more than four hours as recommended by literature, there was still significant moisture present. This was evident as steam was exiting the nozzle and the expansion of the steam within the plasticising unit was causing the PA66 material to leak from the nozzle whilst it was retracted from to mould tool. The material was prone to freezing off at the nozzle outlet meaning that continuous moulding was not possible. The results for PA66 are shown in Figure 4.13. Holding pressure is the only significant factor shown for this material. Injection pressure showed a small effect, but not significant. Barrel temperature did not have a significant impact and no two factor interactions showed an

impact. Due to the difficulties faced injection moulding PA66, it should be considered that these results are not fully conclusive.

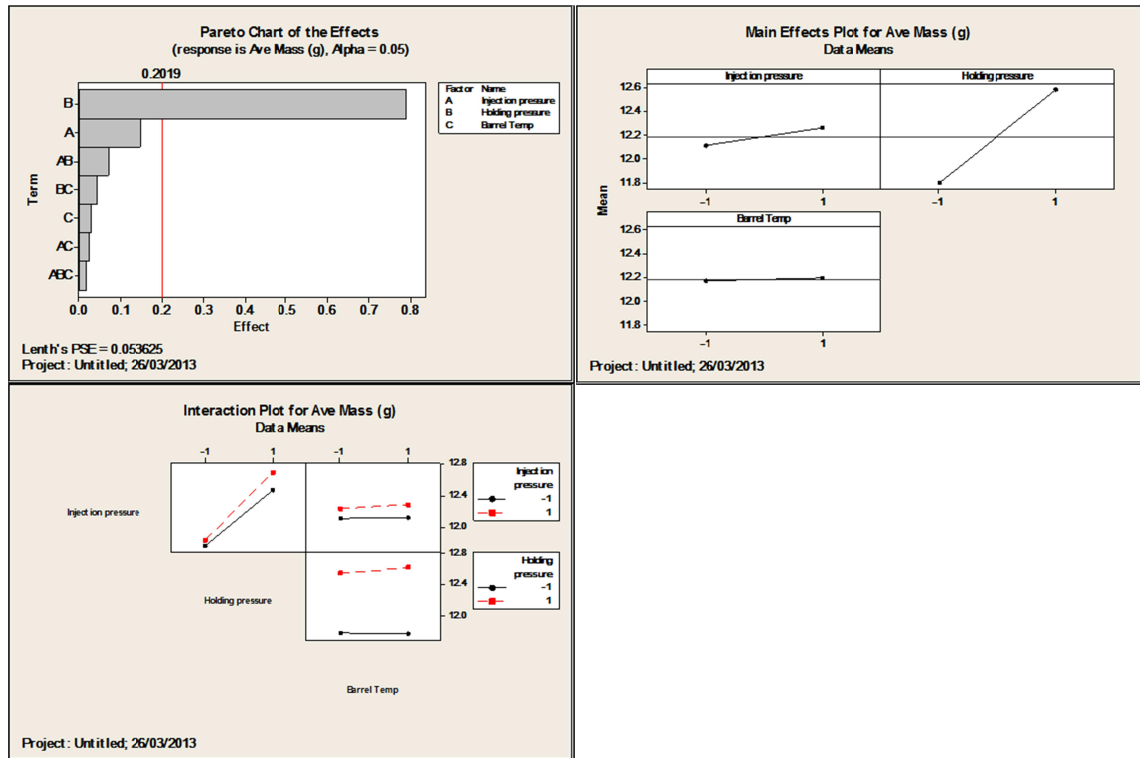
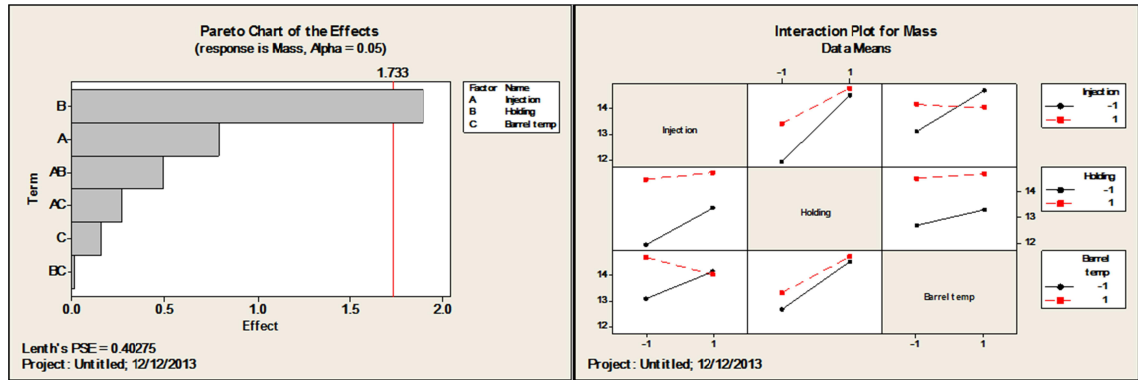


Figure 4.13 - Pareto charts of effects and main effect and interaction plots for PA66 experiment

PEEK gave a good range of mouldings, but was much more consistent than polystyrene, ABS and PA66. Due to the high temperature of the moulding, the holding time was increased to ensure that the material temperature was reduced sufficiently to allow easy release from the mould tool. The holding time was increased from 8.1 seconds to 30.1 seconds. Unlike the other materials the mould tool was heated to 170°C as recommended by the manufacturer (Victrex 2011b). The results for PEEK are shown in Figure 4.14. There was a strong effect shown by holding pressure. A weak effect was shown by injection pressure and a weak two factor interaction between injection and holding pressures.



**Figure 4.14 - Pareto charts of effects and main effect and interaction plots for PEEK experiment**

#### 4.3.4. Conclusions

All materials showed that holding pressure had the biggest impact on the mass of the part produced. The mass of the part takes into account to some extent part shrinkage, although the dominant factor is the level of cavity filling to produce a complete moulding.

The injection pressure and barrel temperature show a small impact across tests. Barrel temperature only shows as a significant factor for polystyrene. This is most likely to be due to the sensitivity of the material to the melt temperatures chosen, whereas in other materials the selected temperatures are within a more normal processing range. Injection pressure is only significant.

The injection flow, i.e. volume of material injected per second, was not shown to have a significant impact upon mould filling. This conflicts with the results shown by Sha et al (2007) who show that it has significant effect. The difference is likely due to the values attributed to the factor levels as, for this study, the variations in holding pressure, injection pressure and barrel temperature are large and at the extremes of common processing parameters, whereas injection flow is within a normal range for each material. The determination of these levels can have a large impact upon the

significance of individual factors shown. For this reason, the relative impacts of each factor largely depend upon the experimental design and are difficult to compare between non-identical experiments.

Comparison between materials does show some correlation between factors with significant and insignificant impact. As the high and low values were arbitrarily chosen for each material, it makes it more difficult to draw analogies between them. Nonetheless, holding pressure is the most significant factor across materials.

The design of experiments method has given a good indication of parameter impact for each material. It is recommended that this work forms the basis of a deeper investigation into the injection moulding process to include material morphology and fibre and filler orientation and dispersion.

## **5. Experimental methods – friction and wear testing**

This chapter describes the test methodology developed and used for material screening and benchmarking tests throughout this study. It describes the test rig design and modifications carried out over the course of the experimental work. The results from the tests carried out using this methodology are presented and discussed.

### *5.1. Ring on disc testing*

For aerospace bearing applications, there are a number of common benchmark standards for self-lubricating bearings, including the SAE AS81820-C specification as well as many aircraft manufacturer specific qualification standards. When developing a new liner technology for plain bearings it is important that the materials can perform in accordance with these standards as well as in the specific applications in which the components will be used. By not achieving one or more of these standards, aircraft manufacturers will be less likely to consider using these products, significantly reducing the potential market. This is because typically they will select bearings against a procurement specification which will be common to all bearing manufacturers. This allows them to source parts from multiple manufacturers, reducing their procurement risks. Due to competition in the market, particularly for standard bearing technologies, manufacturers will qualify to the aerospace standards in order to be considered as a potential supplier.

The bearing standard AS81820-C describes a test methodology for fully assembled spherical plain bearings in order to assess their tribological and mechanical performance, resistance to chemicals and general geometric limits. It is not within the scope of this project to consider the materials used for the ball and outer race. These will be manufactured from 440C stainless steel, a commonly used and well understood

bearing material and likely counterface material for the developed liner material in application, through hardened to 56 Rockwell C minimum.

In order to test to AS81820 standard to determine performance of selected materials, it would be necessary to manufacture the liner materials into spherical plain bearings. This would require a well-developed and robust manufacturing process in order that performance is based predominantly upon the material being tested and all other potential noise factors are minimised. Several factors mean that this is not feasible within this research project. Firstly, the manufacturing process for a fully assembled bearing would use the injection moulding process outlined in Chapter 4. This would involve the use of insert moulding techniques and the capability to mould very thin sections to be compatible with the bearing geometries required for AS81820 standard bearings. These typically use fabric liner materials with a thickness of approximately 0.3mm, such as the SKF X1-40 liner system. This would require significant knowledge of the process to be gained, reducing the time available to carry out performance tests. Secondly, a significant amount of raw material would be required to optimise the process, several material compositions would be required to manufacture sufficient samples to adequately understand the influence of fillers on the performance of the composite. Each material has its own flow characteristic, meaning that mould tools may not be optimally designed for all compositions. The cost to manufacture mould tooling and obtain sufficient material for all tests would be high and require significant investment. This is not feasible for this study as the technology is at very low technology readiness level (TRL) and there is a high risk that the performance of the materials will not be adequate. It is also not feasible to develop a manufacturing process for fully assembled bearings prior to full development of the liner material as the final material properties will have a significant impact upon this. Predominantly the aim of this part of the study is determine the tribological and mechanical properties of

the candidate materials in a relevant environment in order to assess their suitability for use in the applications described.

The standard sets out how the test must be carried out for an assembled bearing. This is not feasible at this stage of the project as a part cannot be developed without some prior knowledge of the material behaviour. The test will only be comparative, allowing the rig design and methodology to be an interpretation of the standard, rather than the exact test (SAE 2008). In order that samples can be easily evaluated, a ring-on-disc test method will be employed. Firstly this allows a direct comparison of materials including, as a benchmark, materials which have already passed the standard in the full bearing test. It also enables easy procurement or manufacture of candidate material test samples, and enables the use of standard testing equipment rather than bespoke bearing test rigs. Previous testing has taken place within SKF on their fabric liners, which is similar to the test methodology set out in Section 5.4. For the purpose of this benchmarking activity, the amount of wear at a given set of test parameters at both room temperature and at the high temperature of +163°C (SAE 2008) is being considered as the pass-fail criteria. For room temperature applications the allowable wear depth is 0.045" (115.3µm).

Initial commissioning of the test apparatus for the ring-on-disc test showed that the system could not control the load when 25kN was requested, which gives the required contact pressure for the AS81820 test standard. This meant that the applied load was not constant which could impact the performance of the materials being tested as well as cause noise in the displacement measurements. This is as a result of the test bench control parameters leading to instability in the axial load as it reached the limit of the machine capabilities. There was no observed instability in rotation, therefore in order to yield reliable results under constant load the applied load was reduced. As previous testing had been carried out by SKF it was decided that the load should be reduced to

suit this as it was a very similar test setup. The load was reduced to 17.2kN giving a contact pressure of 172MPa over the designed area of contact. Aside from this, all other interpretations of the AS81820 test were employed. This change can be justified as it has been designed as a comparative test of tribology at relatively high load. It is assumed that the ranking of materials will be representative of what would be expected in full bearing tests at AS81820 loads.

## 5.2. Test rig design

Test materials were either injection moulded at Cardiff University or purchased as plaques from material manufacturers. Any test rig design had to be capable of assessing both manufactured and purchased materials. Figure 5.1 shows an injection moulded sample manufactured using an existing mould tool. The test rig has been designed primarily around these ruler samples as this represents the most straightforward method of manufacturing new materials. The ideal solution for testing would be to develop a mould which can mould directly into a bearing assembly and testing in accordance with current testing and standards. This is not feasible at this stage as designing such a complex mould would be both costly and time prohibitive. In order to develop a suitable mould a good deal of knowledge of the materials is required which this body of work will seek to gain.

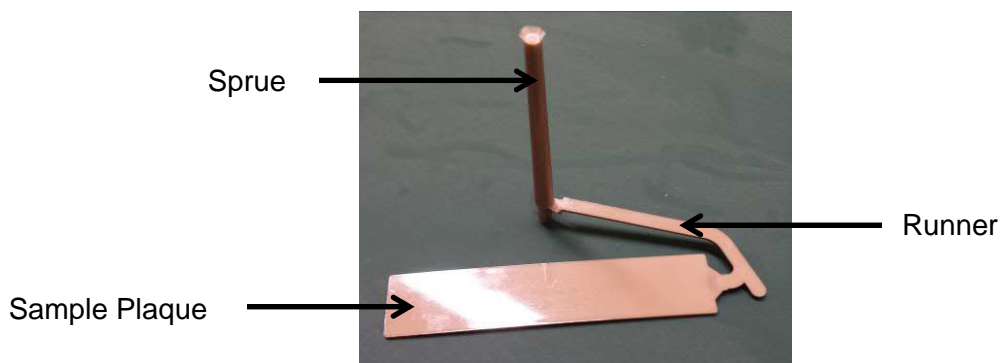


Figure 5.1 – Injection moulded test sample

Figure 5.1 shows the sample as moulded and shows the sprue and runner. The test sample has a width of 24mm and a depth of 2mm, corresponding to the recess in the bottom plate of the rig design. The length is 120mm. The test apparatus has been designed in such a way that any length sample can be tested. This allows pre-moulded samples, such as those materials supplied by Victrex and Lehmann & Voss, to be tested without modifying the test apparatus. These pre-moulded samples are 150mm squares of varying thickness. These are then cut to the corresponding sample width in order to be tested, as shown in Figure 5.2.



**Figure 5.2 - Machined PEEK samples (Victrex)**

In order to benchmark the materials against the current fabric liners, a sample of X1-40 was manufactured. The liner itself is 24mm in width, 100 mm in length and 0.3mm in thickness. In order to test this in the rig the liner material was bonded to a steel substrate with a width of 24mm and a depth of 4mm as shown in Figure 5.3.



**Figure 5.3 - X1-40 sample bonded to steel substrate**

The basis of the testing apparatus is the MTS 858 Mini Bionix II tension-torsion apparatus as shown in Figure 5.4. The apparatus is capable of applying up to 25kN load and up to 225Nm of torque.



**Figure 5.4 - MTS 858 Mini Bionix II Test Apparatus**

The apparatus has been modified such that it can hold the test sample within the fixed half and apply an axial contact pressure of 172MPa across the area of a counterface, as described later. Figure 5.5 shows the fixed half of the apparatus. This incorporates a load cell and has eight fixing points to attach fittings specific to the test being carried out.

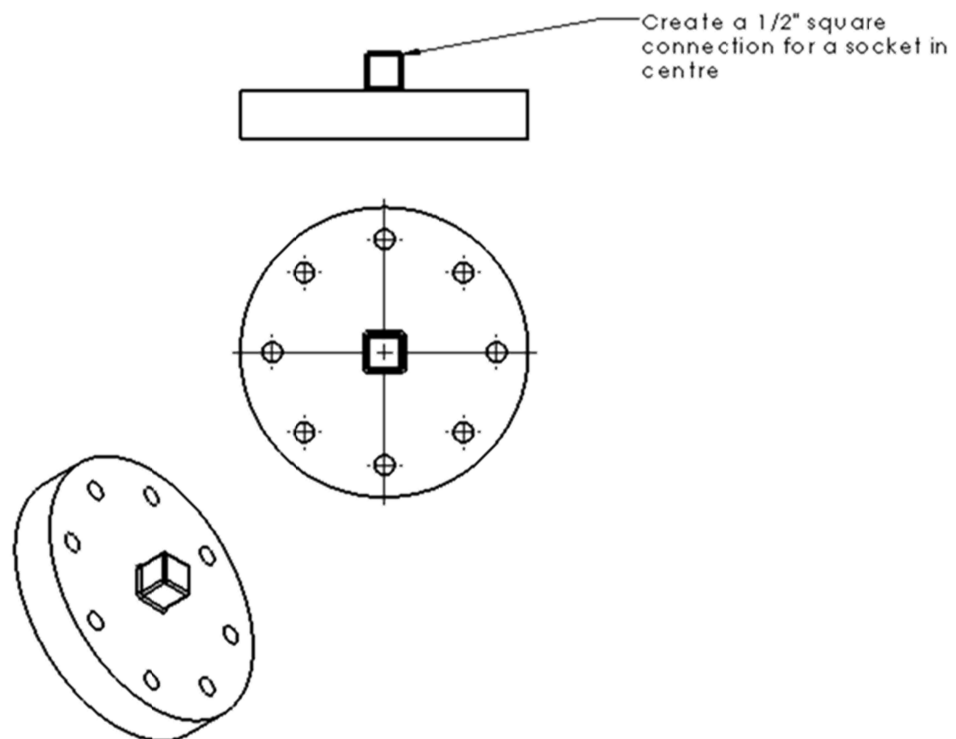


**Figure 5.5 - MTS 858 Mini Bionix II Fixed Half & Load Cell**

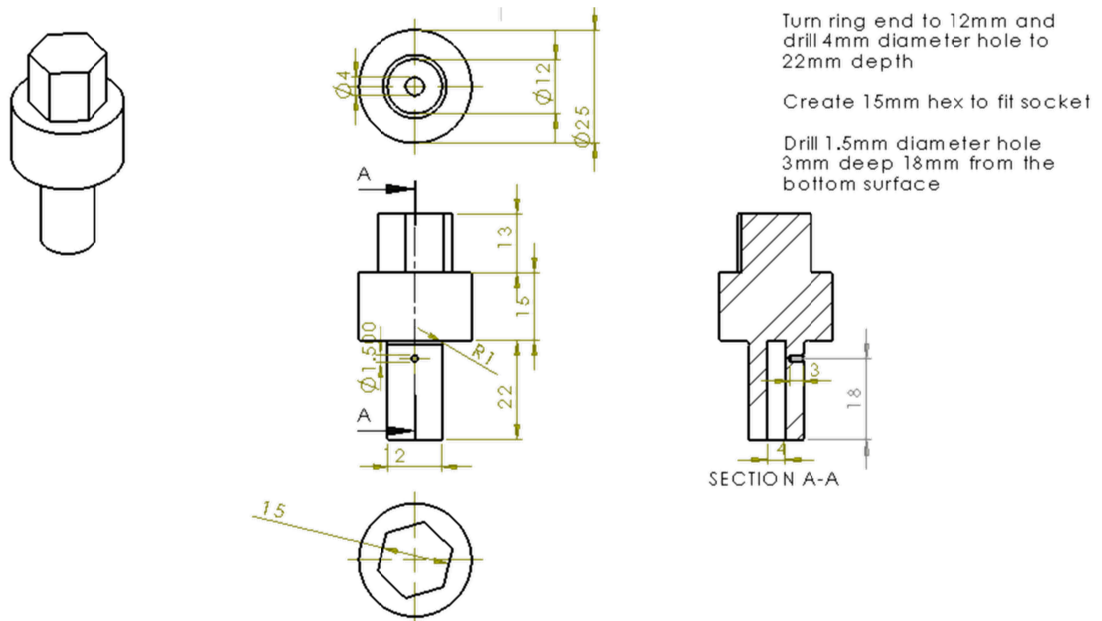
Figure 5.6 shows the fitting designed to be used for the experimental work. The fitting consists of a cylindrical steel block with a milled recess to 1.9mm for the test piece. The fitting picks up on all eight fixing points of the fixed half and uses countersunk hex bolts in order that they do not interfere with the test sample. The recess depth is undersized compared to the standard moulded sample thickness to enable effective clamping. Hence a clamping piece with drilled guide hole has been incorporated. The clamping piece covers a 24mm<sup>2</sup> test area, and oversized by 10mm either side so that it can be screwed into the bottom plate. There is a guide hole of 15mm diameter in the clamp to prevent excessive lateral movement of counterface and load shaft. This is most necessary when using an extension arm for use within a heating unit, as small lateral deviation will produce a larger moment about the pivot point at the base of the actuator.



Figure 5.8 shows the upper fitting for the experimental work. A top plate was manufactured which holds the counterface and will be required to transfer the axial and shearing loads to the contact area. Given the need for a  $\pm 25^\circ$  rotational oscillation, in accordance with the AS81820 standard (SAE 2008 p.15), it is necessary to secure the counterface accordingly. It would not be possible to use a threaded counterface as this would only secure effectively in one direction of rotation. A chuck would be a suitable solution, however cost and ease of incorporation when compared to other options is prohibitive. The simplest solution is to create a ring counterface with a hexagonal head. This can then be held using a standard hexagonal socket, which will provide constraint in the positive and negative rotational directions. A  $\frac{1}{2}$ " square socket connection has been inserted into the centre of the top plate. This will allow a hexagonal socket to be connected to the top plate which will constrain the upper section of the counterface as shown in Figure 5.9.



**Figure 5.8 - Test Rig Top Plate Design**



**Figure 5.9 - Test Rig Counterface design**

The contact surface was machined to a diameter of 12mm and has a central bore with a diameter of 4mm. This gives a contact area of 100mm<sup>2</sup>, which applies the required contact pressure of 25,000 psi (172 MPa) at a load of 17.2kN. The counterface has been manufactured from 440C stainless steel hardened to 56 Rockwell C minimum. This is the standard bearing material. Measuring the contact temperature is clearly difficult, as the contact area is completely enclosed. In order to approximate the contact temperature in a repeatable manner so that all tests can be accurately compared there is a 1mm diameter hole in the side of the shaft 18mm away from the contact area. During the test, a thermocouple is inserted and adequately secured. The thermocouple is connected to a microprocessor unit which is in turn connected as an auxiliary input to the PC based control software. This allows accurate recording for the duration of the test.

Figure 5.10 shows the completed test rig modifications for the basic ring-on-disc screening tests at ambient temperature.

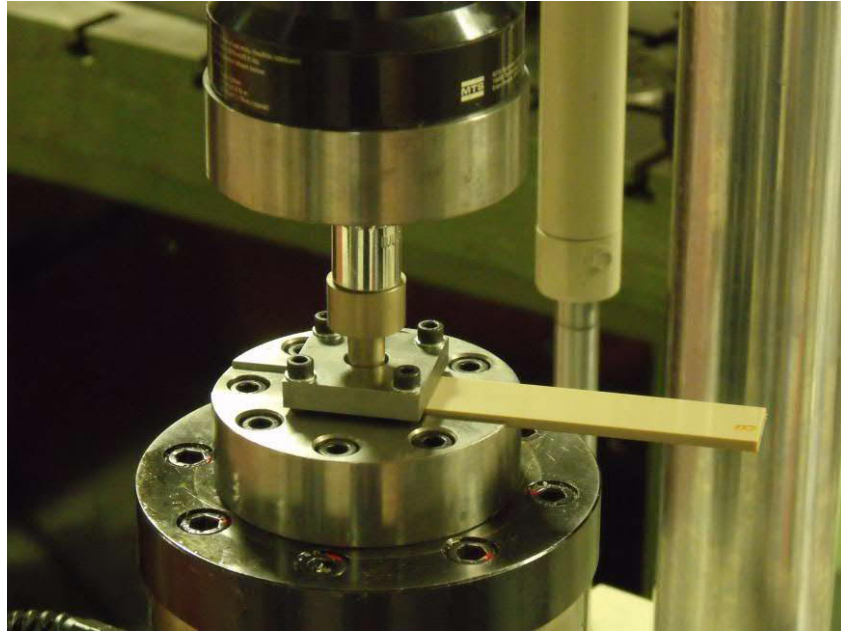


**Figure 5.10 - Test rig for ring-on-disc screening tests**

### *5.3. High Temperature Testing*

Many applications require bearings to perform at elevated temperature. Many helicopter applications, for example, request a maximum service temperature of +90°C and in some cases +130°C. The temperature requirement is based upon the position of the bearing in the application and the environment in which the aircraft will likely be used.

In addition to the ambient temperature testing outlined in the AS81820 qualification standard, there is a requirement to carry out high and low temperature tests (SAE 2008). The test method for high temperature tests is fundamentally the same as for ambient, with the corresponding loads and rotational speed. The test requires the contact surface to be heated to 163°C +6°C/-0°C (SAE 2008). The allowable wear at the high temperature is 0.006" (152.4µm) (SAE 2008). This is a higher allowance than at ambient temperature where the wear limit is 0.045" (115.3 µm).

The test method for the high temperature tests remained the same, however a number of modifications were made to the test apparatus. Figure 5.11 shows the test apparatus with an Instron environmental chamber installed. The Instron chamber can be temperature controlled to 200°C by a forced convection heater and thermostat. It is also capable of chilling controlled to -70°C by use of liquid nitrogen. The dosage is controlled by a valve and the thermostat. The scope of this investigation is limited to high temperature testing, although it will be necessary in the future to carry out low temperature tests.



**Figure 5.11 - Test rig with high temperature modifications**

In order to use the environmental chamber with the current fixings it has been necessary to further adapt them. The reason for this is that the load cell and hydraulic ram diameters are too large to fit through the entry points at the top and bottom of the oven. The solution to this has been the design and incorporation of upper and lower

extensions. The extensions have been manufactured as shafts with a flange at each end. The shafts have been manufactured using 1¼" solid stainless steel bar. In order to allow simple disassembly the flanges must be removable, rather than simply welding them to the shaft. The flanges are bolted to the solid shaft with four countersunk hex bolts once the shaft has been inserted through the entry point. The flanges have eight holes which pick up on the attachment points on the load cell and hydraulic ram. The top and bottom test fixings can then be bolted to the opposite flanges.

Figure 5.12 shows the test fittings within the environmental chamber. An LVDT was incorporated in order to obtain a more accurate axial displacement measurement. The displacement measurement taken from the test rig is between the top of the hydraulic ram and the load cell. As the test rig carries the compressive load, a strain is induced in the fitting. When the rotational oscillation is underway heat is developed at the contact due to friction which diffuses predominantly into the shaft. Heat is also developed at the upper portion of the shaft due to conduction from the hydraulic fluid. When considering the displacement due to strain over the length of the fittings and thermal expansion over the length of the fittings, an error of tens of microns is induced. The displacements due to wear are of the same order of magnitude, therefore the results become unreliable. By using the LVDT between these two points, the bottom and the top plate, a reduction in the error of the overall measurement to the order of microns, which is acceptable, can be achieved. The LVDT was connected to a signal processor which amplifies the output voltage. This was connected to the controller as an auxiliary input and shown in the PC based software where it was recorded as a displacement channel.

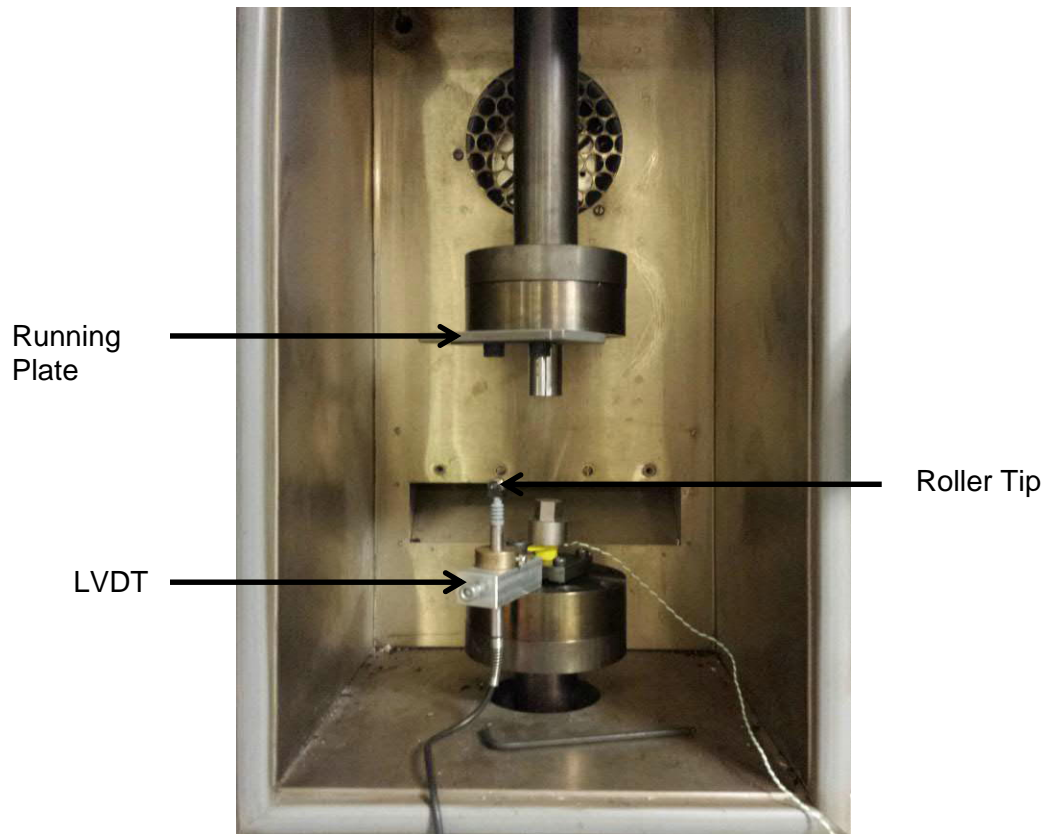


**Figure 5.12 - High temperature modifications and LVDT**

The environmental chamber is only capable of controlling the overall temperature within the test environment and not at the counterface and specimen interface. During the test heat is developed at the contact interface due to friction. The interface temperature is higher than the temperature of the surroundings as the heat does not instantly diffuse. A visual illustration is shown in Figure 5.13, where heat is generated at the interface and diffuses through the steel counterface and the sample material. This means that the true interface temperature can be much higher than the required 163°C, highest in those materials with the highest friction coefficient. This poses some difficulty when attempting to characterize the materials. In standard bearing tests the interface is maintained at 163°C rather than the environment. Figure 5.13 has been created from a basic Abaqus thermal model. It shows that the majority of the heat flows through the conductive steel counterface with some flowing into the low thermal conductivity polymer. The true division of heat energy is determined by the relative

conductivities of the contacting materials, and the temperature of each will be determined by their specific heat capacities.

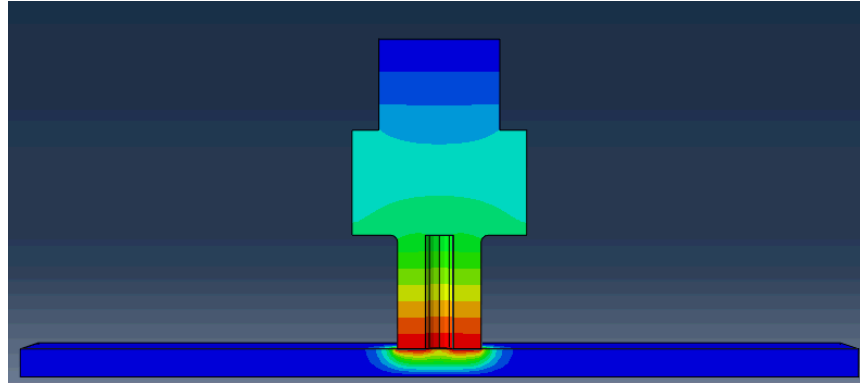


**Figure 5.13 - Visualisation of frictional heat generation (Gay 2014)**

The thermoplastic materials being tested lose mechanical strength with increasing temperature. At their glass transition temperature ( $T_g$ ) PEEK and PEEK composites will have lost approximately 50% of their strength compared to room temperature. Above the  $T_g$  there is a steep change in tensile strength. Above this and as they tend towards their melting point ( $T_m$ ), the tensile strength continues to reduce in a linear fashion. For PEEK the  $T_g$  and  $T_m$  are 143°C and 343°C respectively. Figure 5.14 shows the change in tensile strength of PEEK composite with increasing temperature (Victrex 2011).

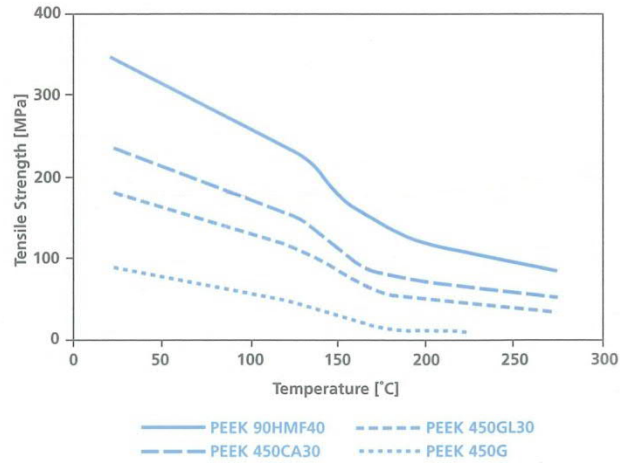


**Figure 5.14 - Tensile strength versus temperature of various Victrex materials (Victrex 2011)**

The qualification standard does not state whether it is the interface or the environment which should be held at 163°C. By ensuring that the environment is kept at this temperature, it is inevitable that the contact temperature will be further increased due to frictional heat generation. This would mean that the mechanical properties would be reduced more than if the interface temperature was held at 163°C. Therefore, for the materials being tested it is detrimental to the material properties to test at higher temperatures above the prescribed 163°C. Whilst it would be more ideal to maintain the interface temperature, the available equipment prohibits this not least because true and accurate measurement of the interface temperature is extremely difficult as it is impractical to place a sensor within the contact region, as described by Bhushan (2000). Given that all of the materials will be tested in the same way, it is expected that the results will be representative of the standard qualification test. The wear rates and failure loads will be somewhat exaggerated similarly to accelerated wear testing, however it is expected that the results will yield the same ranking of materials as the standard test.

## 5.4. Test procedure

In order to replicate, as far as is practicable, the SAE AS81820C standard test to determine wear resistance of bearing liner materials, the following test parameters were used. The ring was oscillated between  $\pm 25^\circ$  from zero, travelling through  $100^\circ$  per cycle. Rather than using a typical sinusoidal oscillation for rotation a triangle wave has been chosen. The aim of this is to achieve a relatively constant velocity throughout the cycle. The cycle frequency should not be less than 10 cycles per minute. In order to accelerate testing, this was carried out at 1Hz (60 cpm), which is the maximum stable oscillation frequency for this test set up. The applied load, and consequential pressure over the contact area, was representative of the application. For this reason, the initial testing was run under a 17.2kN load, with a 12mm diameter - 4mm bore ring counterface giving a contact pressure of 172MPa. This is in line with previous testing of fabric liner, with a similar methodology. The failure threshold was set at not more than 0.0045" (115.3 $\mu$ m) wear after 25000 cycles at ambient temperature, rising to .006" (152.4 $\mu$ m) at high temperature (163 $^\circ$ c) (SAE 2008 p.15).

### Methodology

- 1) Secure top and bottom plates on test rig (Figure 5.6 - Figure 5.8)
- 2) Insert thermocouple into ring counterface (Figure 5.9)
- 3) Locate socket and ring counterface head on the top plate
- 4) Identify test areas on sample
- 5) Insert sample into recess and clamp in position.
- 6) Lower the top arm and ensure that the ring locates within the guide hole
- 7) Apply the required load of 17.2kN
- 8) Hold the load at 17.2kN for 15 minutes before commencing oscillations
- 9) Oscillate the ring  $\pm 25^\circ$  at 1Hz

- 10) Run test to material failure at the material thickness or 3mm, whichever is smaller.
- 11) Record parameters through the test using the MTS multipurpose testware PC based software.

### 5.5. Coefficient of friction calculation

In order to compare the resistance due to friction in sliding motion a calculated parameter was created within the software. This is proportional to the torque applied to the counterface which causes the relative sliding motion.

Due to the design of the counterface there is a variation in force applied at radius  $R$ , as shown in Figure 5.15, according to Equation 5.1.

$$R = r_0 + \Delta r$$

Equation 5.1

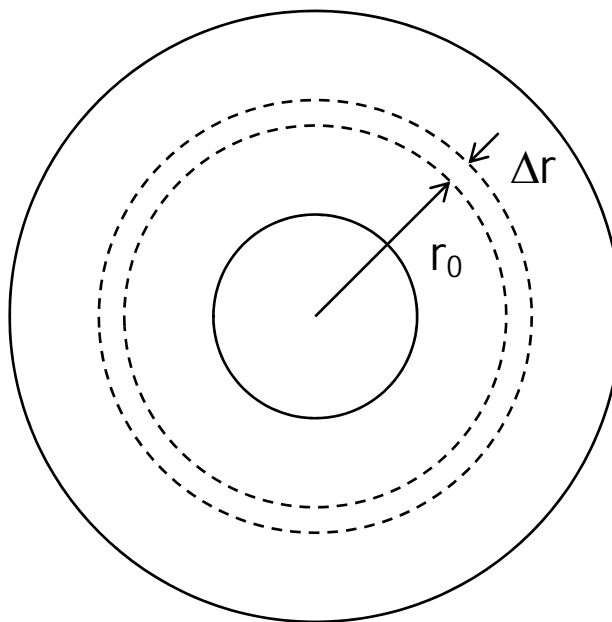


Figure 5.15 - Schematic of Ring Counterface Contact Area

The equation for torque is shown in Equation 5.2, where T is torque applied; F is the force applied, in this case equal to the frictional resistance; D is the distance from the axis of rotation, in this case equal to R. This gives the relationship shown in Equation 5.3. This shows that the torque required to overcome the frictional resistance varies with radius.

$$T = F \times D \quad \text{Equation 5.2}$$

$$T = F_R \cdot (r_0 + \delta r) \quad \text{Equation 5.3}$$

The applied torque is a known variable, where the instantaneous torque value is read by a load cell within the test apparatus and given as a readout channel in the test software. Therefore rearranging the equation for friction, Equation 5.4 can be obtained. This shows that the frictional resistance varies with the radius.

$$F_R = \frac{T}{(r_0 + \delta r)} \quad \text{Equation 5.4}$$

An equivalent radius for calculating friction coefficient from the applied torque has been derived as shown in the Equations 5.5 to 5.14

$$p = \frac{F}{A} \quad \therefore \quad F = pA \quad \text{Equation 5.5}$$

$$F = [\Delta r \times 2\pi r]p = p2\pi r \Delta r \quad \text{Equation 5.6}$$

$$T = F_{friction} \cdot r \text{ and } F_{friction} = \mu F_{normal} \quad \text{Equation 5.7}$$

$$\therefore T = 2\mu\pi r^2 p \Delta r \quad \text{Equation 5.8}$$

$$T = \int_{r_1}^{r_2} (2\mu\pi r^2 p) \delta r = \frac{2\mu\pi p}{3} [r_2^3 - r_1^3] \quad \text{Equation 5.9}$$

$$\therefore \mu = \frac{3T}{2\pi p [r_2^3 - r_1^3]} = \frac{3TA}{2\pi F [r_2^3 - r_1^3]} \quad \text{Equation 5.10}$$

$$\therefore \mu = \frac{3T(r_2^2 - r_1^2)}{2F(r_2^3 - r_1^3)} \quad \text{Equation 5.11}$$

$$r_1 = 2mm, r_2 = 6mm \quad \text{Equation 5.12}$$

$$\therefore \mu = \frac{T}{4.33F} \quad \text{Equation 5.13}$$

$$\therefore r_{equivalent} = 4.33mm \quad \text{Equation 5.14}$$

Equations 5.1 to 5.14 show how the equivalent radius to calculate friction from torque was determined.

## 5.6. Test parameters

There are a significant number of variables that can be considered when evaluating these materials and applying them to a design. The materials themselves will be composites made up from an injection moulded base material with fillers added to improve performance. This represents a significant area for research in the future in selecting the right mix of materials, as well as optimising the ratios of each constituent material within the mix. The understanding of the benefits and drawbacks of each constituent material, how each material interacts with and enhances the composite and how this knowledge can enable the optimal composite to be developed for each application is key to the long term research goal. The initial testing stage gave an indication of some of these properties as each material had a different composition. The variability in material used for the bearing surface in contact with the liner will also have an effect.

As each application will have differing demands, the liner material will need to be able to cope with a wide range of external variables. These include load; torque; contact pressure; frequency of motion; amplitude of motion; impact loading; application temperature; presence of chemical substances to name a few.

All of the above variables represent known factors for the testing environment, and all can be controlled aside from ambient temperature. The initial tests will be conducted in an ambient workshop. It is assumed that the ambient temperature will remain reasonably constant during tests, and any fluctuations will be minimal and thus have minimal effect on the results.

Unknown and uncontrolled variables will be measured and recorded during the test in order to develop an understanding of these materials and how they perform. These will be wear depth over time, coefficient of friction and counterface temperature.

In the future, more of these parameters will be varied so that a more complete understanding can be gained.

### **5.6.1. Counterface and material roughness**

It is necessary to ensure that there is minimal variation in surface finish of the steel counterface between tests. This will ensure that the counterface roughness is controlled and does not impact the results. Also, there must be no contaminants on the counterface from previous tests, for example any material transfer. In order to ensure that the counterface has the same surface finish for each test and is free of contaminants the counterface must be prepared according to a strict regime prior to each test.

In order to get a consistent surface finish, the samples were prepared using a grinding and polishing machine as shown in Figure 5.16. The machine has an automatic head which applies a load which ensures that the contact surface remains flat. Polishing by hand would not ensure a consistent and even load distribution. As the counterface has a relatively high centre of gravity, it could not be held directly by the automatic head

and would become dislodged, therefore a boss was manufactured which the counterface is held in for polishing giving it stability.



Figure 5.16 - Struers Rotopol 31 with Rotoforce 4

Table 1 shows the surface preparation method used for the steel counterface. It shows the consumables used and the time and load required for each step.

Table 1 - Surface preparation method for steel counterface

Step	Polishing Disc	Polishing Fluid/ lubricant	Time /mins	Load /N
1	MD Piano	Water	7.5	100
2		Water	7.5	100
3	Mol	Struers MD Mol (3 $\mu$ m) Struers DP Blue Lubricant	10	100
4	Nap	Struers NapB (1 $\mu$ m) Struers DP Blue Lubricant	5	80

Figure 5.17 and Figure 5.18 were obtained using a Talysurf surface profilometer. They show a two and three dimensional profile of a polished counterface respectively. The  $R_A$  value of the corresponding counterface is 8.15 nm, which is of the order of roughness of a highly superfinished steel surface. This is typically the finishing process for a steel inner ring of a SKF spherical plain bearing. As can be seen, there is not a significant variation in height.

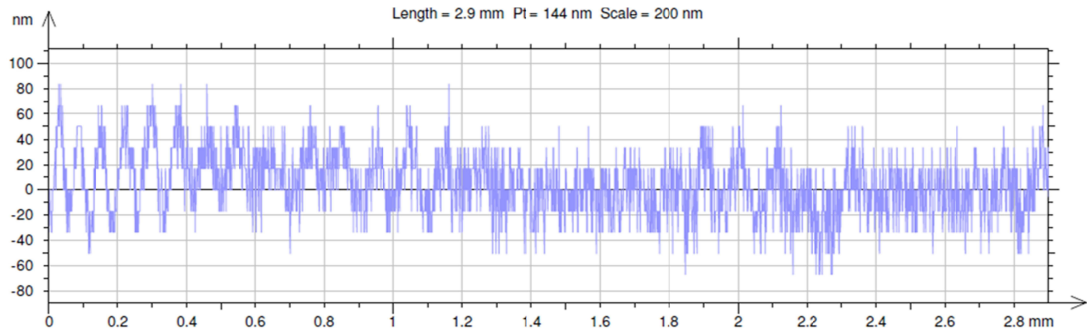


Figure 5.17 - Surface profile of a polished steel counterface

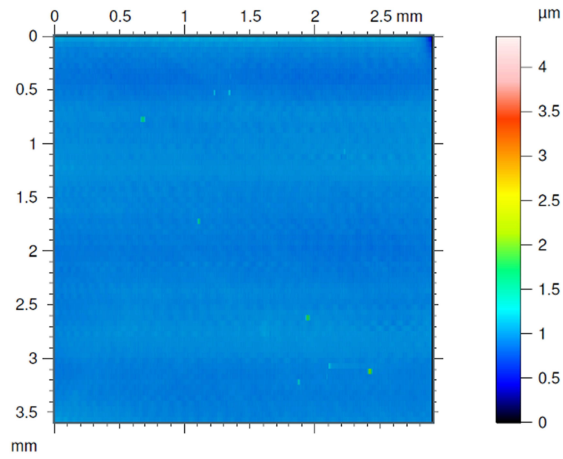


Figure 5.18 - 3D surface profile of a polished steel counterface

## **5.7. Results and Discussion**

This section presents and discusses the results of the dynamic testing described in Sections 5.1 to 5.4. The friction and axial displacement results for each material are first shown individually. The purpose of this is to understand the characteristic failure mode for each material as well as to understand the repeatability in the results for each.

As has been discussed in Section 5.3 the axial displacement measurement is a composite of several factors which includes the elastic deformation and creep quantified in Chapter 7, as well as the wear and plastic deformation of the materials.

Figure 5.19 shows the dynamic friction and temperature data for PEEK composite containing 10% weight fraction each of PTFE, graphite and carbon fibres. The graph shows the evolution of temperature 18mm away from the contact area in the steel counterface, as described in Section 5.2 and the evolution of friction through the test until 3mm axial displacement. The temperature and coefficient of friction vary together which is particularly illustrated between 2000 and 4000 cycles where both the temperature and coefficient of friction decrease together. This is an expected phenomenon as heat is generated at the contact as energy is transferred from work done. The reducing friction in the initial stages is due to running in and the initial build-up of the PTFE transfer film on the counterface. During this period there is less heat energy input into the system due to friction and so there is net heat flow out of the system. As the friction coefficient increases the net heat flow is into the system as more heat is generated than can be expelled to the environment through thermodynamic heat transfer.

The relationship between temperature close to the contact and the coefficient of friction is seen for all materials tested.

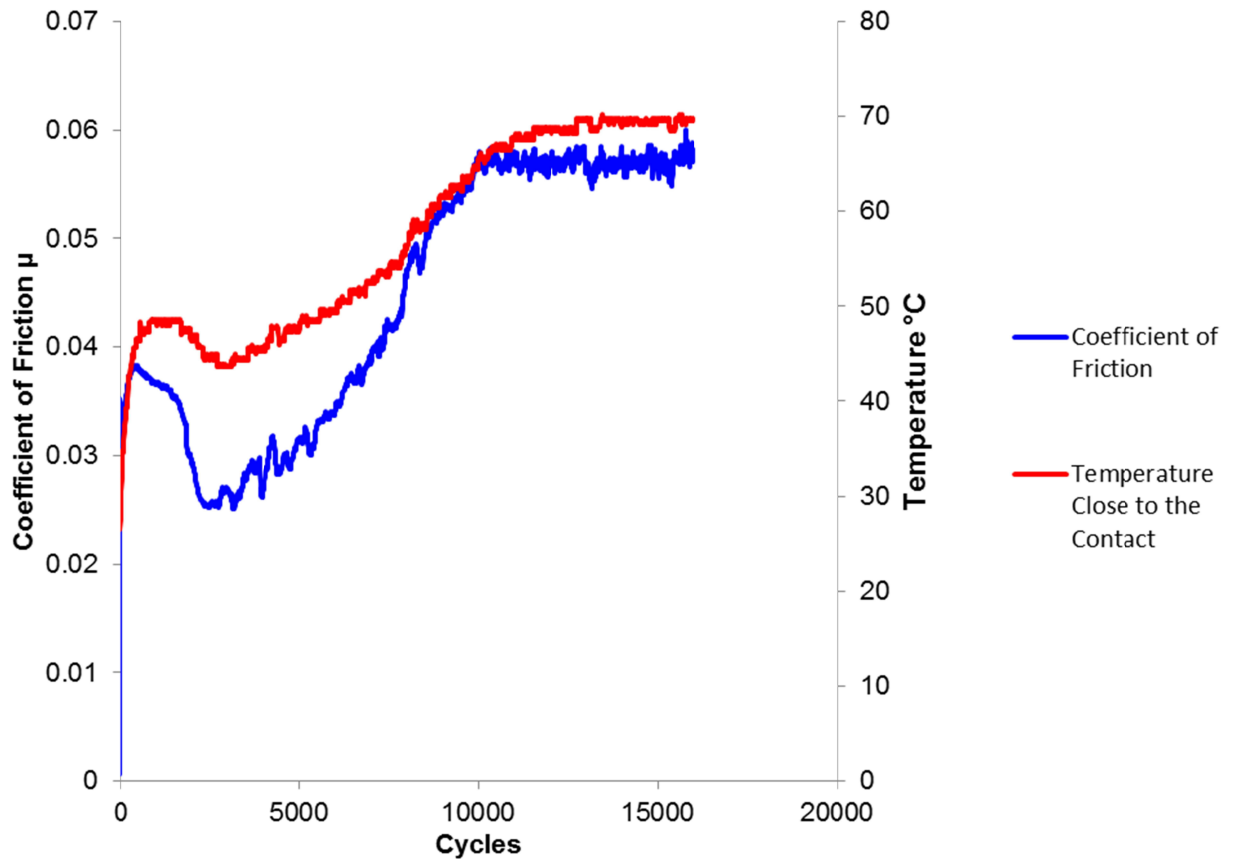


Figure 5.19 - Dynamic friction and contact temperature data for 150FC30

The contact temperature for all materials is defined by the thermodynamics of the system, the thermal properties of the contacting materials and the work done to overcome friction between the contacting surfaces. The thermodynamics of the test bench overall remain relatively consistent for all tests, the main influence being the variation of laboratory temperature. This temperature did not vary significantly during testing with a typical ambient temperature of approximately 18-21°C. As is shown in Figures 5.20 to 5.42 there is a significant variation in friction coefficient dependent upon the type and quantity of fillers utilised within each composite. The division of heat energy between the counterface and composite is a product of the heat generated at the interface and the thermal properties of the materials.

Figures 5.24 to 5.46 show the dynamic test friction and wear data for the PEEK composites presented in Section 3.3. All materials were tested to 3mm axial displacement. Whilst the maximum wear criteria described in Section 3.1 is 115.3 $\mu$ m (0.0045”), materials were tested to 3mm axial displacement in order to observe the evolution of friction and wear through the sample thickness. A number of materials suffered brittle failure, with the test ending abruptly, for example for PEEK filled with 30%w/w carbon fibre, 5%w/w graphite and 10%w/w PTFE shown in Figure 5.36. In these cases, the axial displacement shown in the graph does not reach 3mm as failure occurred between measurements. PEEK filled with 20%w/w PTFE, shown in Figure 5.29, did not reach 3mm axial displacement in any tests as the wear rate was extremely low. These tests were ended before 3mm was reached as the time to reach maximum displacement would have reduced the time available to test further materials.

Figure 5.20 shows the data for unfilled PEEK, Figure 5.21 and Figure 5.22 shows tests 1, 3, 4 and 5 at a higher resolution so that the friction and wear evolution can be easily compared between tests. Unfilled PEEK was tested in order to establish a baseline performance from which it would be possible to understand the impact of adding filler materials to the dynamic performance of the composite.

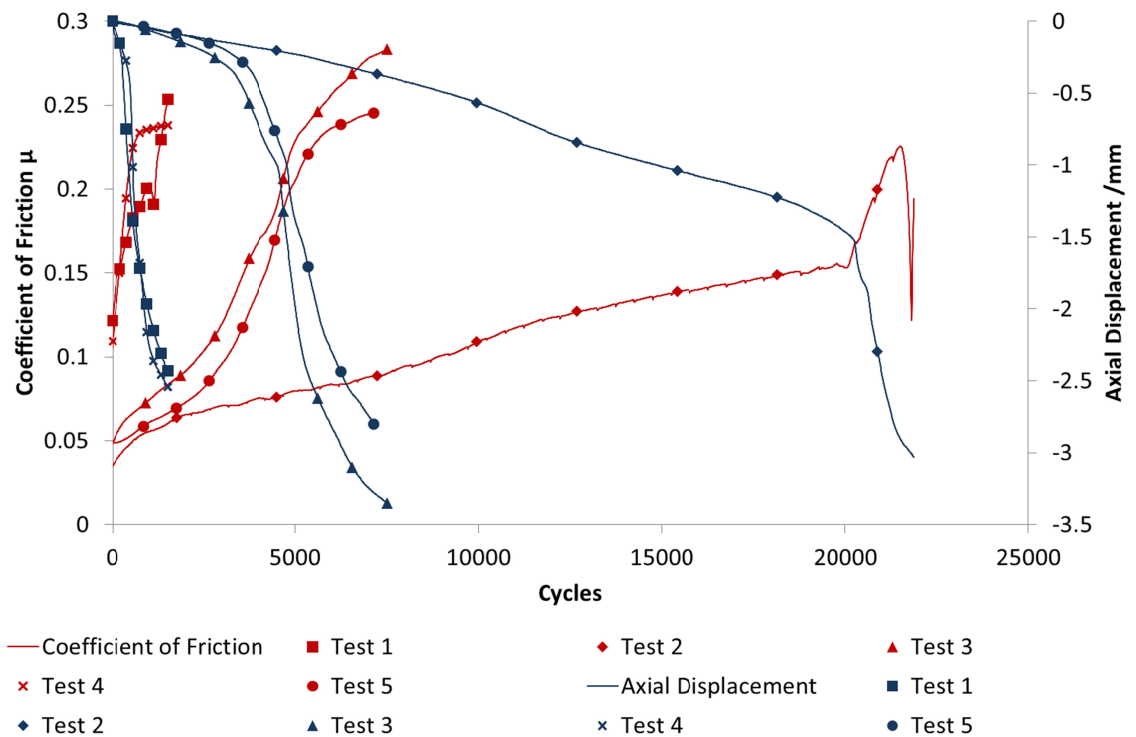


Figure 5.20 - Ring on disc test data for unfilled PEEK

The results for unfilled PEEK were inconsistent. Tests 1 and 4 had the shortest failure time at 1520 and 1580 cycles respectively. The friction coefficient at the beginning of the tests was 0.11 increasing to 0.25 at the end of life. Tests 3 and 5 failed at 7520 and 7210 cycles respectively. The friction coefficient for these tests was initially 0.05 increasing to in excess of 0.25 at end of life. Test 2 showed a far longer life with failure occurring at 22880 cycles. The friction coefficient in this test started at 0.04 increasing to 0.23 at the end of life.

Figure 5.21 shows the results for tests 1 and 4 at higher resolution with respect to dynamic cycles completed, whilst Figure 5.22 shows the results for tests 3 and 5. In all tests the same pattern can be seen in the failure mode. It can be observed that there is a correlation between the rate of change of friction coefficient and axial displacement. The samples which have a rapidly increasing friction coefficient show a corresponding

rapid increase in wear rate. There is an initial period of steady and low gradient change in axial displacement followed by a significant increase in the rate of change of displacement into a second phase which then decreases towards the end of life. It is suggested that this represents an initial phase of wear at a steady state where heat energy is being generated due to friction. As the material heats up the compressive strength of the sample is reducing and at a critical point the material fails due to plastic deformation, leading to catastrophic failure, which agrees with the mechanical properties published by Victrex for compressive strength against temperature (Victrex 2011). The material morphology could have an impact upon the wear rate as the material at the surface is likely to be more amorphous due to rapid cooling in the mould, whereas the material at the centre cools more slowly giving a more crystalline structure. Hedayati et al (2012) showed that the wear rate of amorphous PEEK is higher than that of semi-crystalline PEEK by between 25% and 75% depending on the applied load. A higher friction coefficient was also observed for amorphous PEEK. Figures 5.21 to 5.23 show that the wear rate at the material core is much higher than at the surface. Furthermore, the surface friction coefficient is lower than is observed at the core. If material morphology were to impact the friction and wear performance it would be expected that the higher hardness of the crystalline material would exhibit a lower wear rate in addition to a lower friction coefficient. Reduction of mechanical properties is a more probable explanation for the failure of this material. This is a dominant failure mode exhibited by the majority of PEEK composites shown in Figure 5.23 to Figure 5.42.

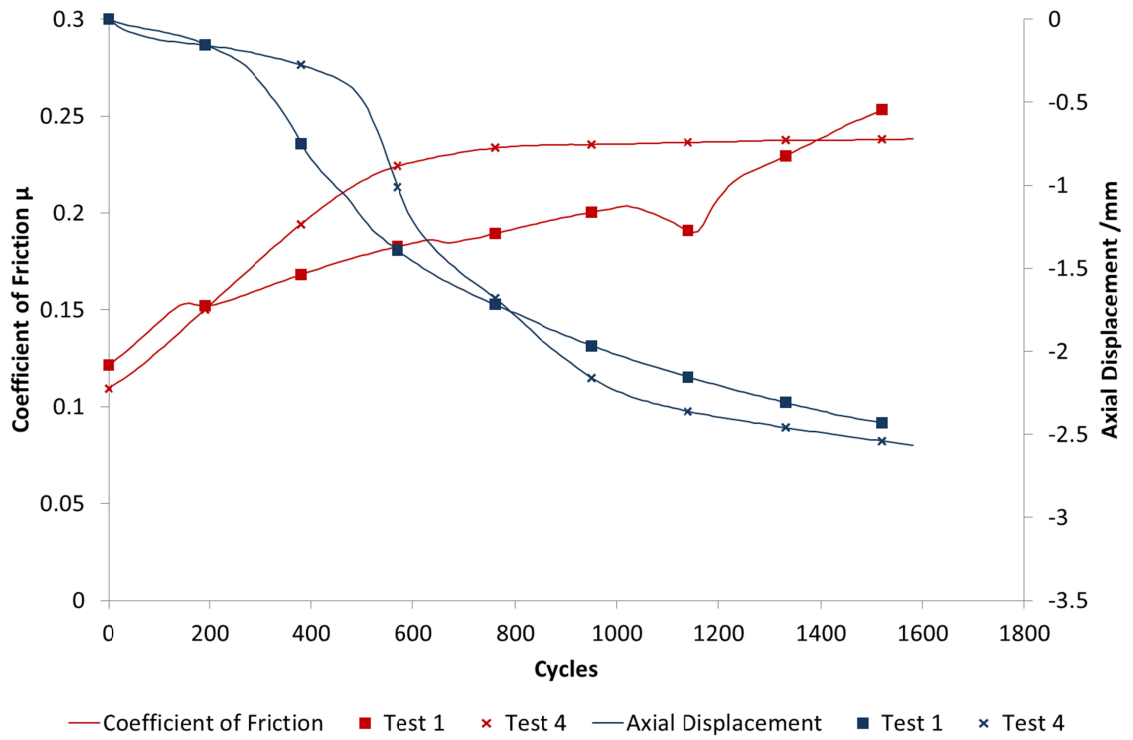


Figure 5.21 - Dynamic test results for unfilled PEEK tests 1 & 4

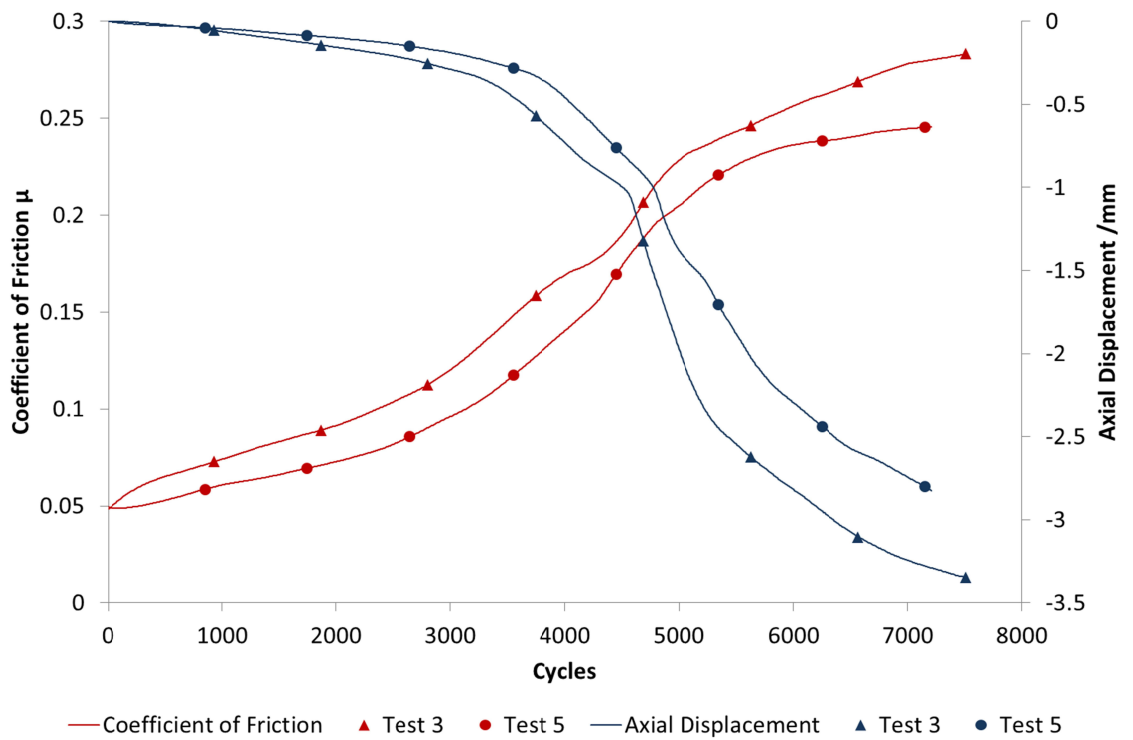
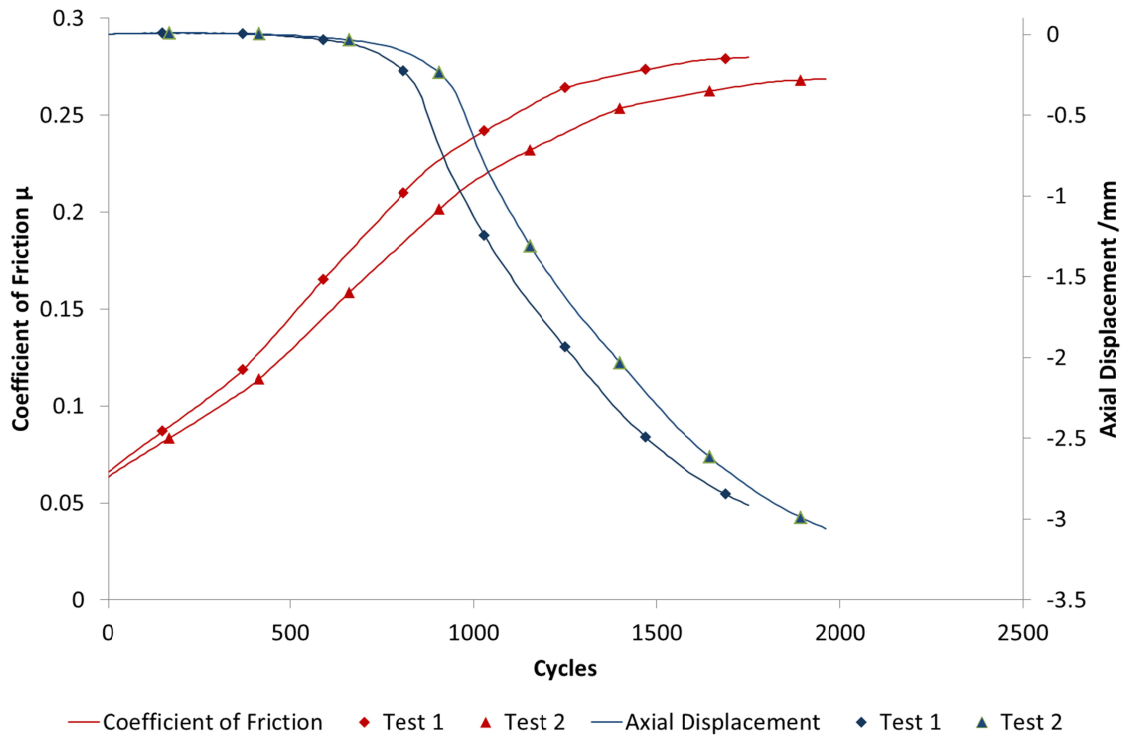


Figure 5.22 - Dynamic test results for unfilled PEEK tests 3 & 5

Figure 5.23 to Figure 5.26 shows the friction and wear data for glass fibre filled PEEK, PEK and PEKEKK respectively, at various glass fibre loadings. All graphs are shown on the same scales to enable straightforward comparison of results. For all glass fibre filled materials the coefficient of friction,  $\mu$ , follows a similar trend and evolution through the test. In all cases  $\mu$  starts at approximately 0.06 increasing to approximately 0.25 before levelling off to approximately 0.3 at maximum wear depth. The coefficient of friction levels off at the point where the wear rate begins to rapidly increase and then begins to fail. In all glass filled materials the wear evolution follows the characteristic trend observed in unfilled PEEK as seen in Figure 5.20. The magnitude of the friction coefficient is similar to that of unfilled PEEK and therefore the inclusion of glass fibres has little impact upon the friction coefficient.

PEEK filled with 15%w/w glass fibres, shown in Figure 5.23, exhibits a low steady state wear from the start of the test to approximately 650 cycles where the wear rate starts to increase rapidly. At the onset of rapidly increasing wear rate the coefficient of friction is approximately 0.18. The test ends at 3mm wear after 1750 cycles. When compared to unfilled PEEK the addition of 15%w/w glass fibres does not have a significant impact upon wear life, as the initial low wear region is approximately similar. The wear rate is higher than what is required for the material, therefore this material cannot be considered for the final composition.



**Figure 5.23 - Ring on disc test data for 15%w/w glass fibre filled PEEK**

For 30%w/w glass filled PEEK, Figure 5.24, initial steady state wear continues for 1100 cycles in test 1 and 500 cycles in test 2. The friction coefficient for test 2 is initially higher than in test 1, 0.09 compared to 0.06. The friction coefficients observed are approximately 10% higher than 15%w/w glass filled PEEK. Onset of rapid wear in both tests corresponds to a coefficient of friction of 0.25. Following the onset of rapid wear the test ends at 1740 and 1120 cycles respectively, with both tests having good correlation once rapid wear initiates. Whilst there is a significant spread in the results of the two tests it was not deemed necessary to make further repeat tests as this composition did not achieve the minimum wear standard in both tests. As for 15%w/w glass filled PEEK, the poor performance of this composition mean that it will not be carried forward as a suitable candidate material.

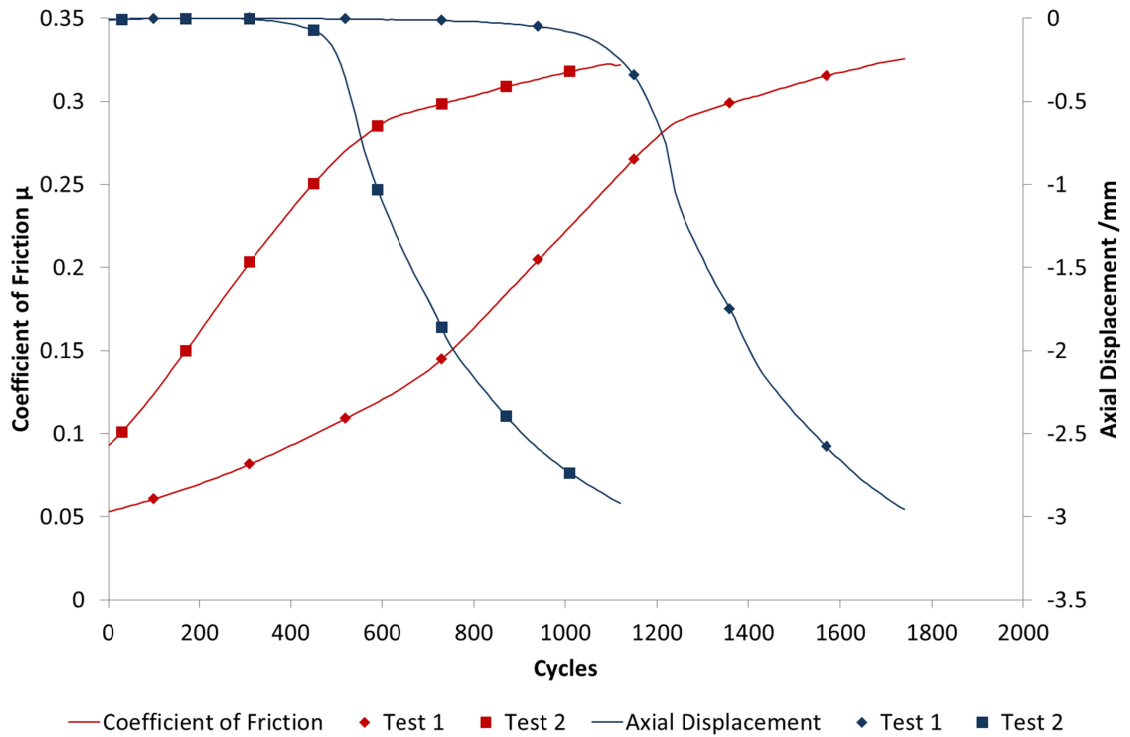


**Figure 5.24 - Ring on disc test data for 30%w/w glass fibre filled PEEK**

Figure 5.25 shows the friction and wear performance for 30%w/w glass filled PEK. PEK has a higher  $T_g$  and  $T_m$  than PEEK. Tests 1 and 2 show very good agreement, test 3 exhibits a higher number of wear cycles to failure. Again, wear rate is initially low before rapid wear onset is initiated. This occurs at 1000 cycles for tests 1 and 2 and 2200 cycles for test 3. When rapid wear occurs coefficient of friction is 0.22. The rapid wear region follows a similar trend to other glass filled materials tested. 3mm wear occurs after 2700 cycles in tests 1 and 2 and after 3600 cycles in test 3. Friction coefficient for this composition is comparable to that of unfilled PEEK and 15%w/w glass filled PEEK. This again implies that glass fibre fillers do not have a strong impact upon friction coefficient.

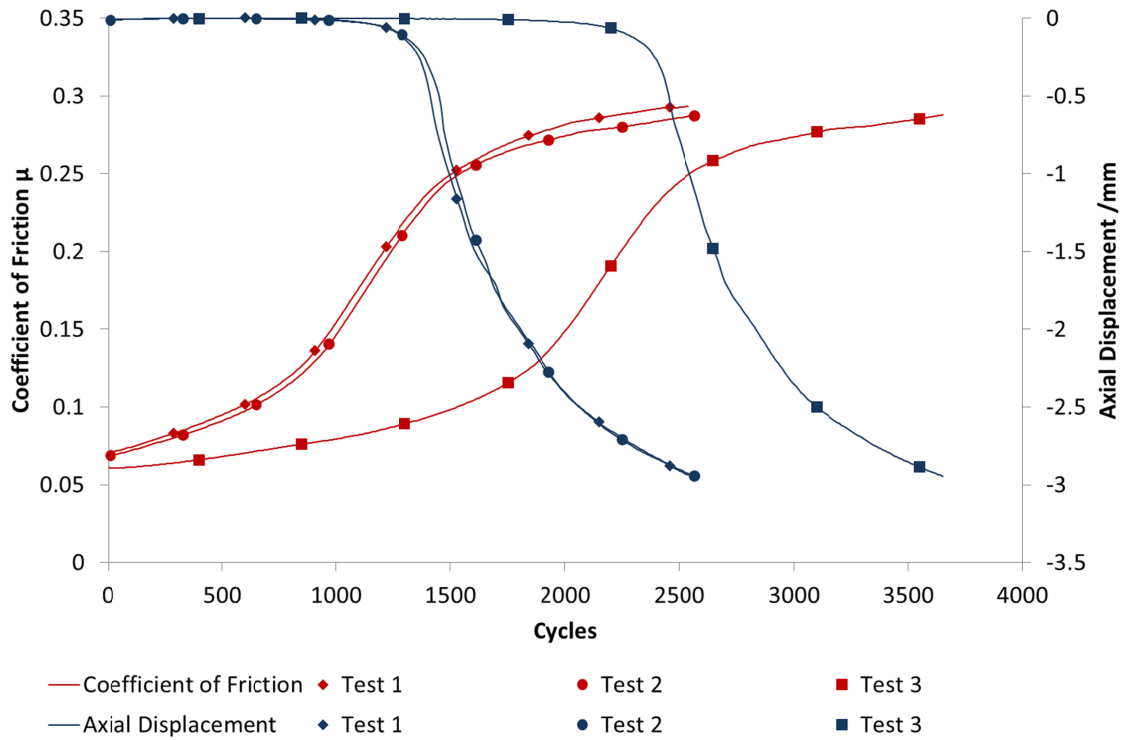
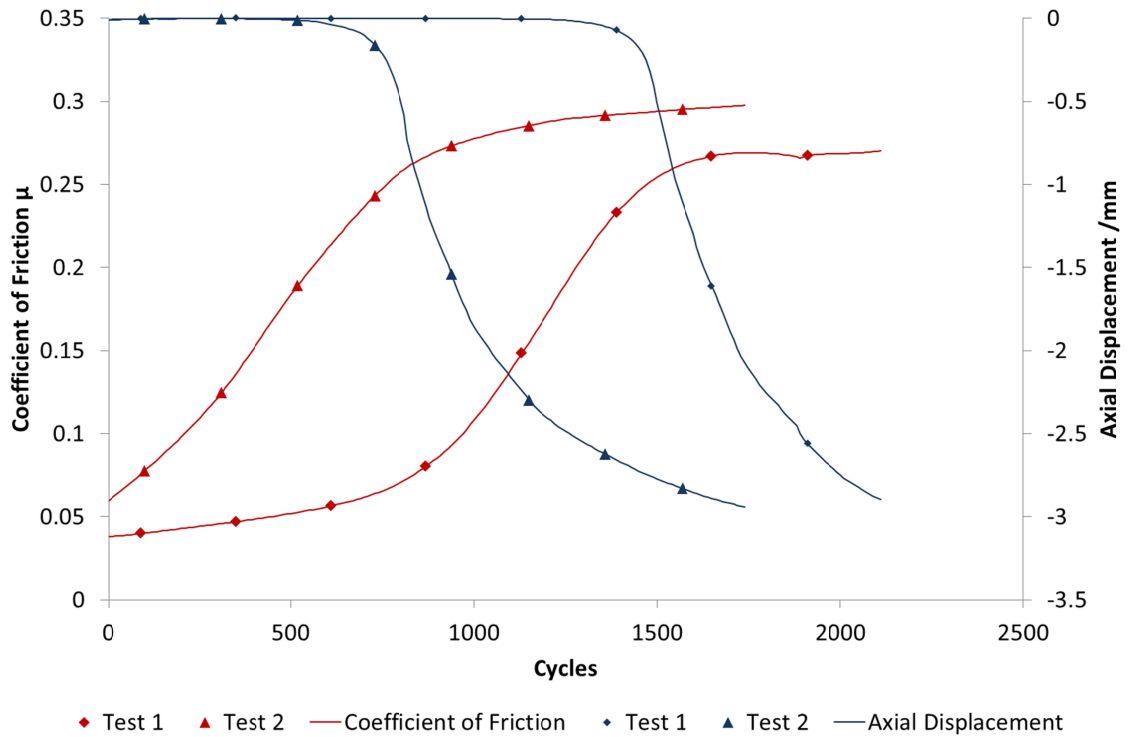


Figure 5.25 - Ring on disc test data for 30%w/w glass fibre filled PEK

Figure 5.26 shows results of three tests for 30%w/w filled PEKEKK, having a higher  $T_g$  and  $T_m$  than both PEEK and PEK. Both tests exhibit a low wear region followed by rapid wear initiates, as seen in unfilled PEEK. In test 1 this low wear region continues for 1700 cycles and in test 2 for 1000 cycles. The increasing wear rate corresponds to a coefficient of friction of approximately 0.24 in both tests. Wear to 3mm occurs after 2200 and 1750 cycles respectively.



**Figure 5.26 - Ring on disc test data for 30%w/w glass fibre filled PEKEKK**

Comparing PEEK, PEK and PEKK with 30%w/w glass fibre fillers, there is not a strong indication that increasing  $T_g$  and  $T_m$  contribute to an increase in performance. Coefficient of friction is marginally lower for PEK and PEKEKK, more comparable to a 15%w/w glass filled PEEK. PEK shows the highest performance in cycles to failure, however poor performance is observed for all compositions.

Each of the glass fibre filled materials a relatively consistent coefficient of friction can be observed at the point where rapid wear initiates. It would appear that the wear rate increases significantly when a critical friction value is reached, which is different for each composition. For 15%w/w glass fibre filled PEEK, onset of rapid wear coincides with a friction coefficient of 0.18, whereas for 30%w/w glass fibre filled PEEK, PEK and PEKEKK, this coincides with values of 0.25, 0.22 and 0.24 respectively. As has been shown in Figure 5.19, friction coefficient and contact temperature are directly proportional. Therefore, the critical friction value must correspond with a critical contact

temperature or bulk temperature as heat dissipates through the material. It is possible that the increasing friction coefficient from the start of the test is due to viscoelasticity at the sliding contact surface as the surface temperature exceeds the glass transition temperature. As the bulk material temperature increases as heat energy dissipates through the material, mechanical properties are reduced resulting in increasing plastic deformation as seen in unfilled PEEK. This agrees with the hypotheses suggested by Zhang et al (2008) and Tang et al (2010) in their studies on the tribological behaviour of PEEK.

Figures 5.27 and 5.28 show the friction and wear data against number of cycles for 30%w/w carbon fibre filled PEK and PEKEKK respectively. They are shown on the same scales to enable straightforward comparison. For both materials coefficient of friction at the start of the test is typically approximately 0.05, however this rapidly increases in the region of low wear. It then tends to plateau or slowly increase when wear rate accelerates, as seen in other PEEK composites. For both the PEK based composite, Figure 5.27, and the PEKEKK based composite, Figure 5.28, the coefficient of friction begins to level out at approximately 0.24. It slowly increases relative to number of cycles to within a range of 0.3 to 0.34.

Figure 5.27 shows good agreement between results for 30%w/w carbon fibre filled PEK with all tests following the same trend for both friction and wear. The rapid wear region initiates in all tests at approximately 2000 cycles with maximum wear of 3mm achieved after 13000 cycles. Friction coefficient is consistent with that observed in unfilled PEEK and glass fibre filled PEK. Wear performance is comparable to glass fibre filled PEK in the initial low wear region, however wear rate beyond the onset of rapid wear is much lower leading to a much higher sliding distance for wear to 3mm.

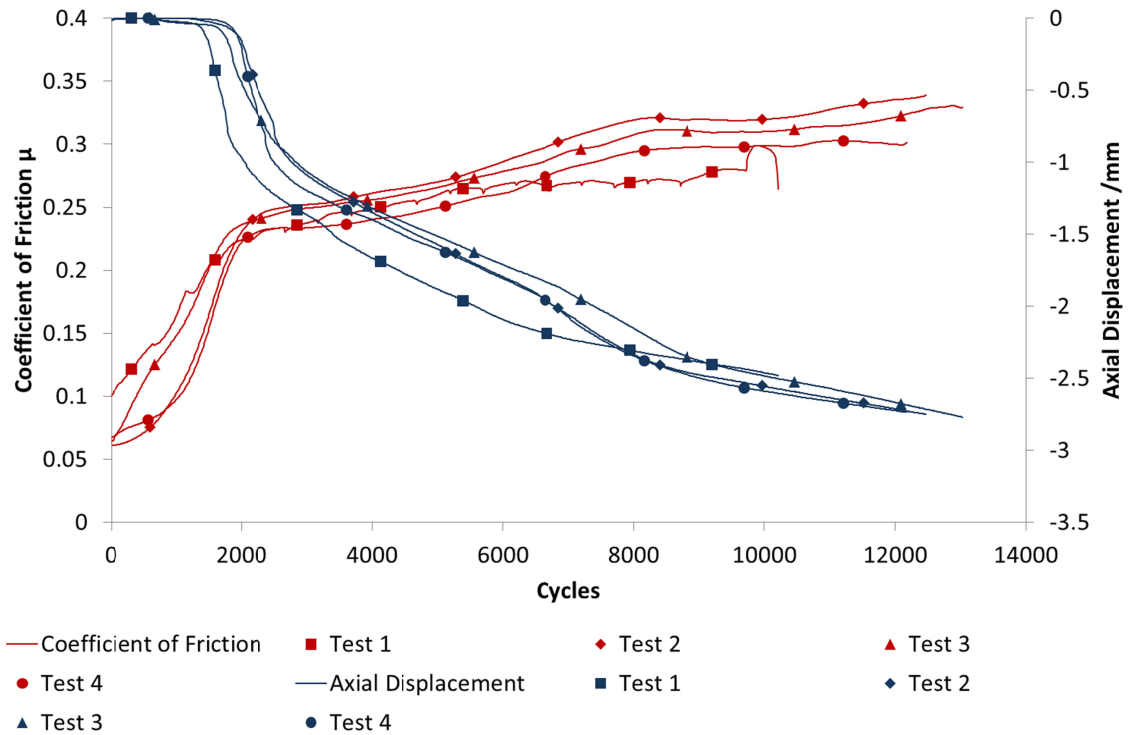


**Figure 5.27 - Ring on disc test data for 30%w/w carbon fibre filled PEK**

For 30%w/w carbon fibre filled PEKEKK, Figure 5.28 shows a spread in the number of cycles at which rapid wear initiates, test 1 at 4500 cycles, test 2 at 3000 cycles and test 3 at 2200 cycles. A lower friction coefficient of friction is indicated for test 1, however this is not an accurate value as there was a discrepancy in the calculated value in this test setup. It is displayed, however, to show the friction evolution through the test. Friction values are similar to those exhibited by carbon fibre filled PEK, unfilled PEEK and glass fibre filled PEKEKK. This indicates that inclusion of carbon fibres does not have a strong impact on friction coefficient for PEEK based composites. Flock et al (1999) and Lu and Friedrich (1995) observed a reduction in friction coefficient with increasing fibre content for CF-PEEK composites. Flock et al showed that with the inclusion of 30%w/w carbon fibres a reduction in friction coefficient of 25% was observed. Lu and Friedrich observed a reduction of approximately 40% with the same ratio of carbon fibres. For both experiments a contact pressure of 1MPa and sliding speed of 1m/s were used. The results from this experiment do not show agreement

with other literature, however the pressure velocity combination is significantly different so a difference is expected. The total cycles to failure are higher than those observed for carbon fibre filled PEK. The spread in the initial low wear region makes it difficult to conclude whether carbon fibre filled PEKEKK has improved wear performance compared to PEK. Nonetheless, the average number of cycles in this initial stage is approximately 4000 cycles for PEKEKK compared to 2000 for PEK, indicating some improvement. Friedrich et al (2005) indicated that specific wear rate was similar across PAEK based polymers, and therefore is in agreement with the results shown. It is indicated, however, that friction coefficient is lower for PAEKs with a higher ratio of ketone groups. This is not observed in the materials tested in this study.

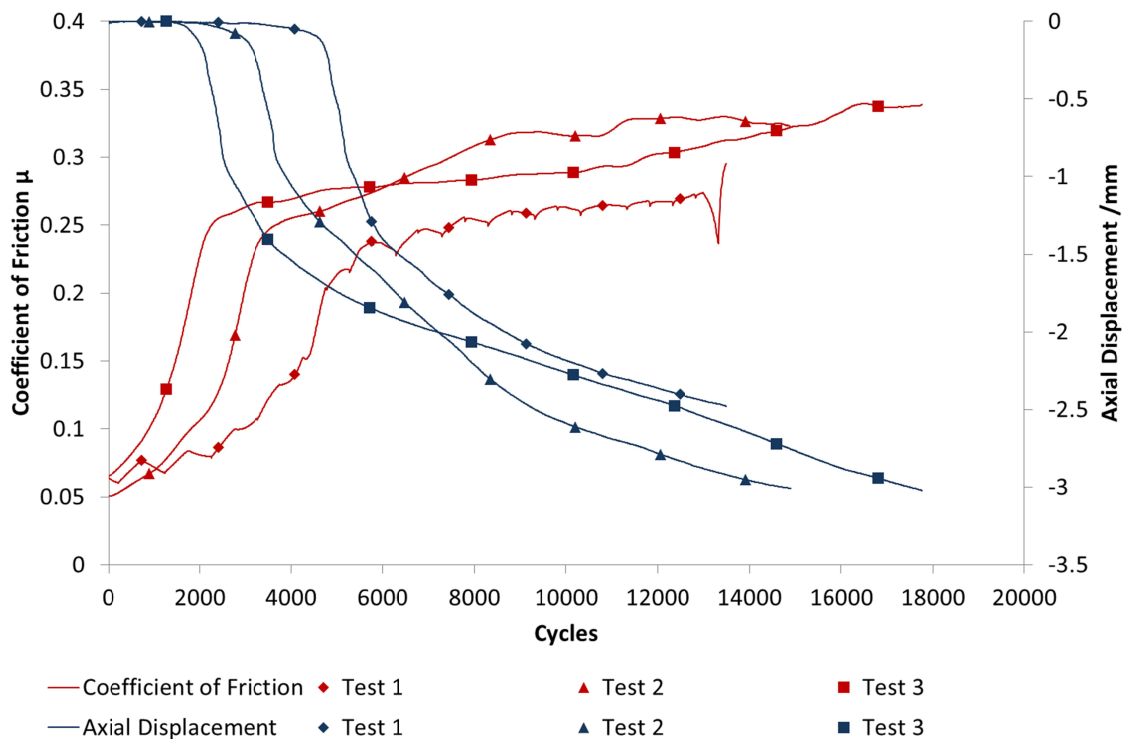


Figure 5.28 - Ring on disc test data for 30%w/w carbon fibre filled PEKEKK

Figure 5.29 shows the results for PEEK with 20% weight fraction PTFE. This composition has shown the highest level of wear resistance of all of the materials tested. All tests on this material have given less than 0.18mm wear for cycles in excess

of 500,000. None of the samples exhibited the characteristic plastic deformation failure seen in other composites and gave a stable wear rate. It is hypothesised that the very low friction coefficient coupled with a low thermal conductivity when compared to carbon fibre filled composites means that the temperature of the material remains low throughout the test. Therefore no significant plastic deformation failure is seen.

The initial coefficient of friction was approximately 0.025 to 0.03 for all materials, and decreased in the first 100,000 cycles to approximately 0.01 before increasing to a steady state friction coefficient of 0.02. This is significantly lower than the friction values seen in unfilled PEEK and glass and carbon fibre filled composites. The reducing friction coefficient can be attributed to the building up of a PTFE transfer layer on the counterface and running in of the mating face as shown in the work of Lancaster (1972) and Friedrich et al (1995).

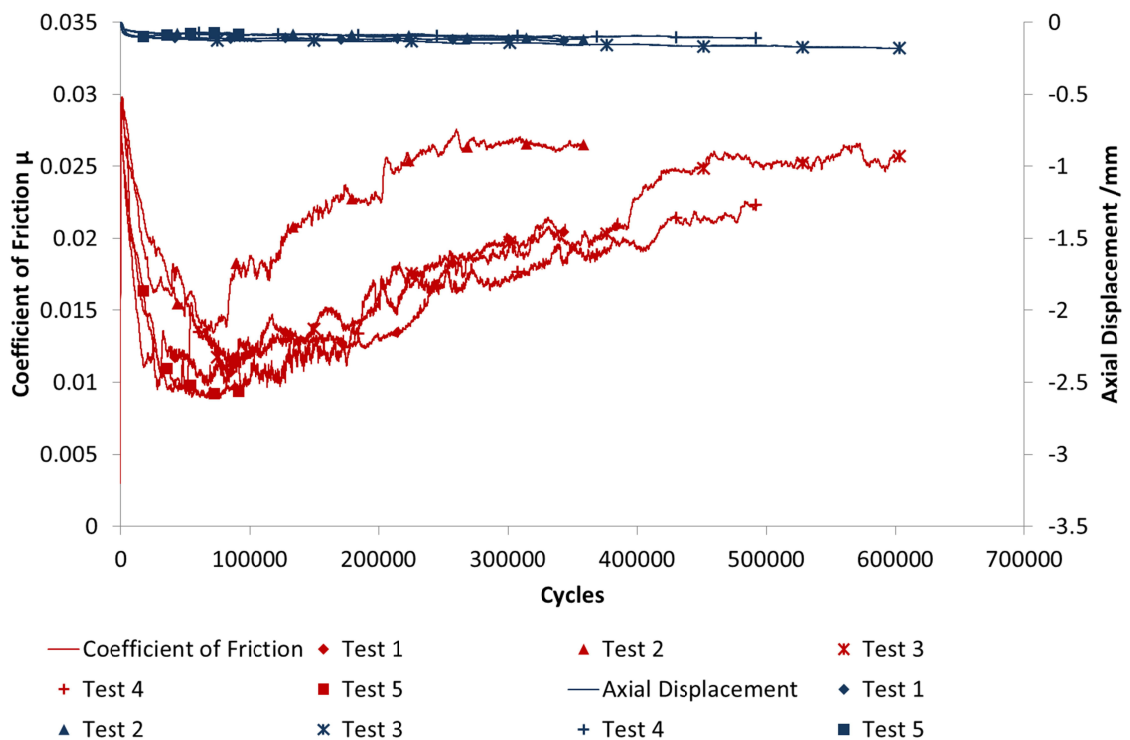


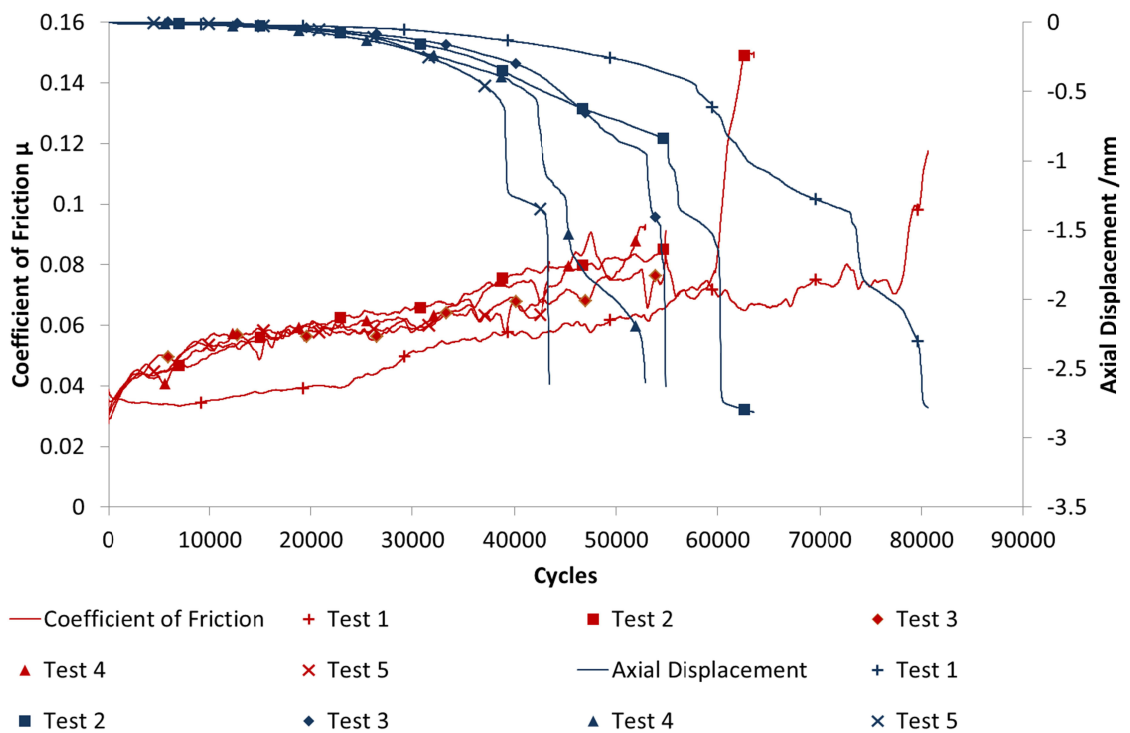
Figure 5.29 - Ring on disc test data for 20%w/w PTFE filled PEEK

Figure 5.30 shows the dynamic test results for PEEK filled with 10%w/w each of PTFE, graphite and carbon fibres. This material exhibited reasonably consistent friction results with low initial friction values at approximately 0.035 initially reducing to approximately 0.03 before rapidly increasing to approximately 0.06 after 10,000 cycles when the rate of friction increase reduces whilst wear rate remains relatively low. As the materials enter the phase of rapid wear acceleration the friction results become noisy and reach approximately 0.09 by the end of the test. In tests 1 and 2 the wear test continued to the point where they had worn through completely and the supporting metallic base came into contact with the counterface, which explains the spike in friction at the end of the test. The friction values are significantly lower than exhibited by unfilled PEEK, yet approximately twice those exhibited by 20%w/w PTFE filled PEEK. This is attributed to the inclusion of PTFE and graphite reducing the friction coefficient, whilst carbon fibre reinforcement thought to have no effect as discussed for carbon fibre filled composites, Figures 5.31 and 5.32.

Test 1 shows a different trend for coefficient of friction outside of the range of the other results. It does not show an initial decrease in friction coefficient and the rate of increase is lower than is seen for other materials, although interestingly onset of rapid wear occurs at a similar friction value. It can be considered an anomalous result.

The wear curves for all tests show initial agreement in the low wear region. Furthermore, all tests follow the characteristic wear curve exhibited by unfilled PEEK and the majority of other compositions with initially low wear followed by a rapid increase in wear rate. The onset of rapid wear varies considerably between tests. This could be linked to inconsistent dispersion and therefore local concentration of filler materials having an impact on local tribological properties within the test samples.

Due to the noise in the friction coefficient curves it is difficult to identify the critical value which coincides with onset of rapid wear, however it would appear that a value above 0.06 is detrimental to the wear rate of the material. This occurs at between 40,000 and 60,000 cycles for all tests. The minimum wear limit has been achieved by this material and therefore the composition should be considered for applications with similar load and sliding conditions. It will be considered when developing an optimised material composition.



**Figure 5.30 - Ring on disc test data for 10%w/w PTFE, 10%w/w carbon fibre and 10%w/w graphite filled PEEK**

Figure 5.31 shows the results for the Victrex composite WG101, a material marketed as ‘wear grade’ for its excellent friction and wear properties (Victrex 2011). The composition of this material is not published, however as it is recommended by Victrex as being most appropriate for applications where wear is an important consideration it was decided to use it as a baseline for wear performance of PEEK composites.

In line with the work done by Lancaster (1971) which aims to estimate the limiting 'pv' values for thermoplastic materials in dry sliding contact, Victrex discuss the limiting 'pv' of a selection of their composite materials and state that for 'WG101' this is 10-18 Mpa.ms<sup>-1</sup> compared to standard wear grades such as '450FC30' (10%w/w each of PTFE, carbon fibres and graphite) at 6-9 Mpa.ms<sup>-1</sup> and non-wear grade, reinforced composites such as '450CA30' (30%w/w carbon fibres) at 7 Mpa.ms<sup>-1</sup> (Victrex 2011). This data is given for high speed, low load conditions, for which the pressure and velocity is not given. However, in describing the high load, low speed condition, pressure is given as 20MPa and sliding velocity as 0.7ms<sup>-1</sup>. At these conditions all materials survived and therefore no limiting 'pv' was obtained. It is implied that the 'pv' product is the same in both scenarios. This indirectly supports the argument of Meng and Ludema (1995) that the 'pv' criterion is rarely useful for estimating bearing life and the work of Rhee (1970) which suggests that p and v are independently proportional to wear.

It is expected that this material should perform well in this high load, low speed configuration however, contrary to expectation, this material in fact has the lowest performance in terms of wear of all materials which have not failed by cracking due to overloading. The wear curves for all tests shown in Figure 5.31 do not show an initial low wear region prior to rapid wear onset. Wear of 3mm occurs after 800-1400 cycles. The absence of an obvious initial low wear region could be attributed to the resolution of the data plotted as there is one data point for every ten cycles.

Friction values are initially approximately 0.06 and increase to approximately 0.35 at 3mm wear.

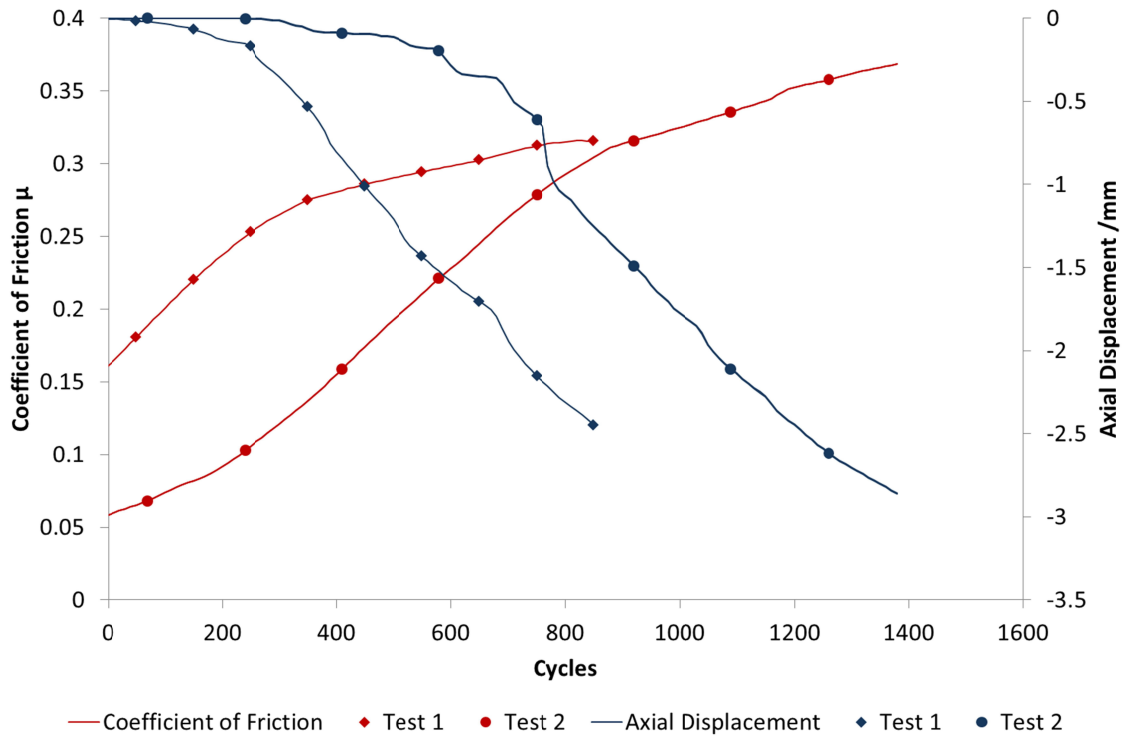
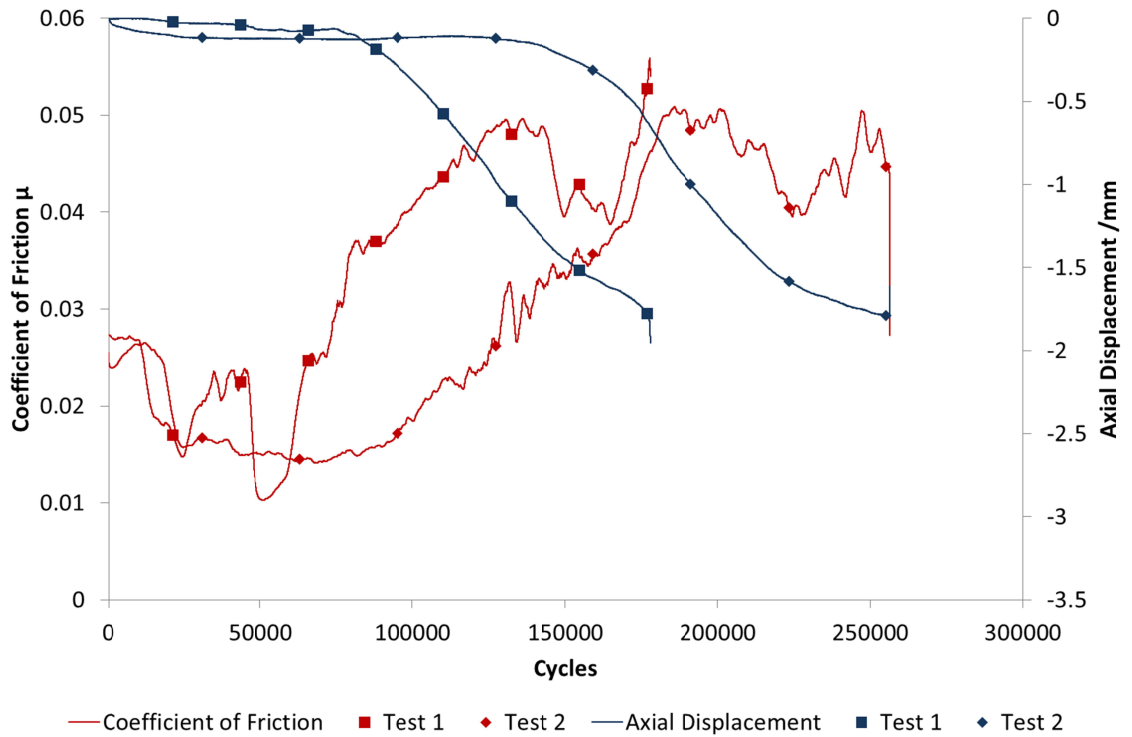


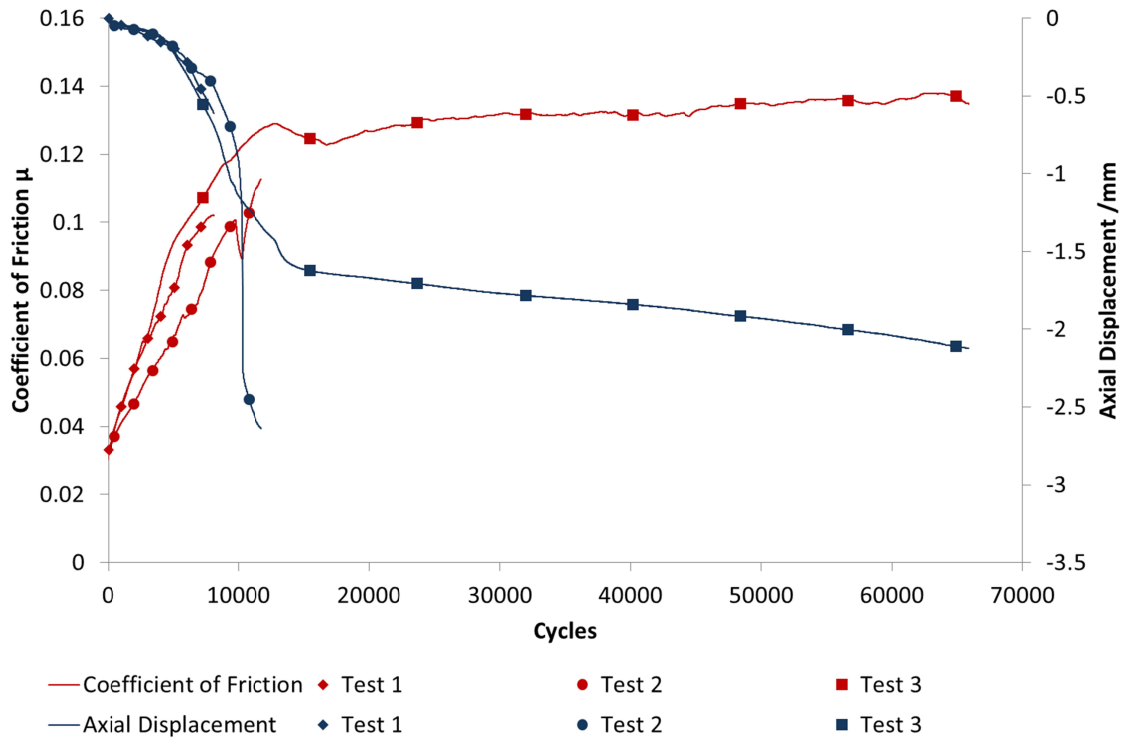
Figure 5.31 - Ring on disc test data for Victrex WG101 composite

Figure 5.32 shows the results for PEEK containing 10%w/w PTFE, 20%w/w Aramid fibres and 15%w/w MoS<sub>2</sub>. As for previously tested compositions, the results show that the material follows the characteristic friction and wear curves. Initially there is a low wear region with samples achieving 80,000 and 140,000 cycles before the onset of severe wear. 2mm of wear is achieved after 175,000 and 250,000 cycles respectively. Friction coefficient is initially 0.03 and reduces to 0.015 before increasing steadily to 0.05 at the end of the test. This is comparable to the friction values exhibited by 10% w/w PTFE, graphite and carbon fibre filled PEEK, whilst wear performance shows two to three fold improvement over this composition. Severe wear initiates as the coefficient of friction reaches 0.035.



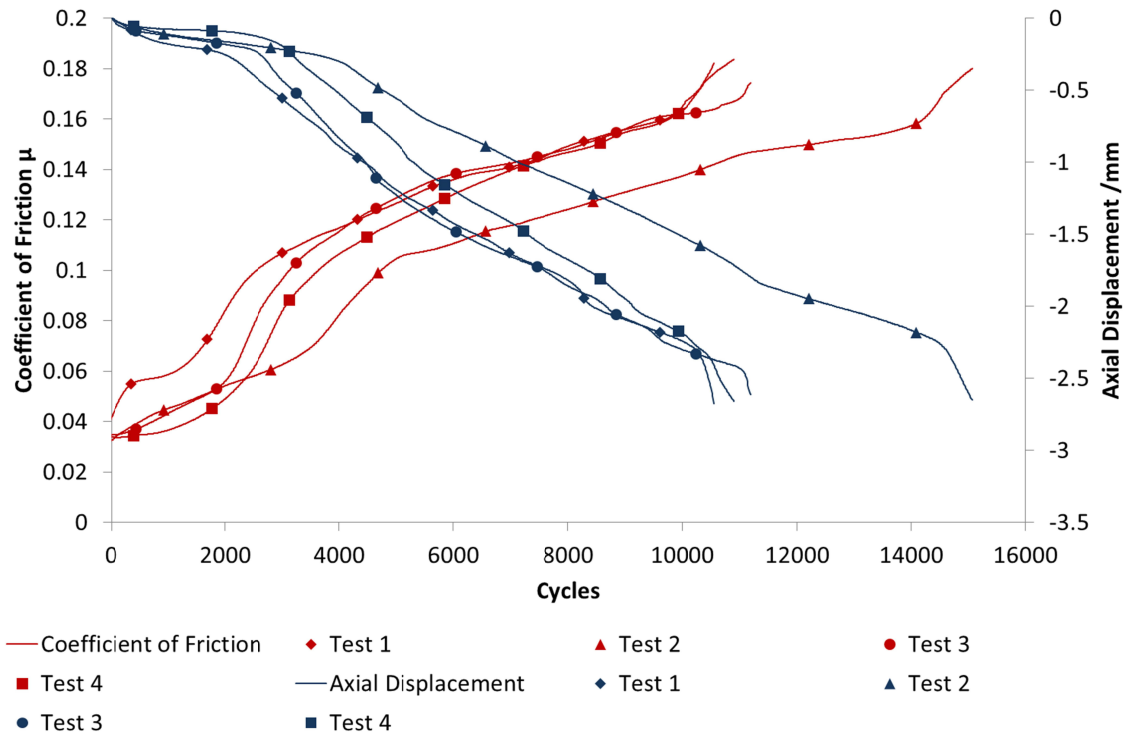
**Figure 5.32 - Ring on disc test data for 20%w/w Aramid fibre, 10%w/w PTFE and 15%w/w MoS<sub>2</sub> filled PEEK**

Figure 5.33 shows the results for PEEK containing 30%w/w Aramid fibres. There is low initial friction with  $\mu$  starting at 0.03 and increasing linearly over the first 10,000 cycles to approximately 0.13. This coincides with the point at which wear rate begins to rapidly increase. The friction values show an improvement over unfilled PEEK, and is approximately half of that observed for both 30%w/w glass and carbon fibre filled PEEK composites. The initial wear phase is characterised by an ever increasing wear rate, rather than a more steady low wear observed in glass and carbon fibre filled composites. Brittle failure was observed in all tests.



**Figure 5.33 - Ring on disc test data for 30%w/w Aramid fibre filled PEEK**

Figure 5.34 shows the results for PEEK containing 10%w/w Aramid fibres and 10%w/w PTFE. The results show good agreement for both friction and wear across the four tests. Coefficient of friction is 0.03 initially and increases to approximately 0.06 when the wear rate starts to increase rapidly. This occurs at 2,400 to 4,000 cycles across tests. Following this, test 4 shows the coefficient of friction increasing at a lower rate to 0.14 at test end. Due to the inclusion of PTFE it is expected that the friction coefficient would be lower and more comparable to that of 20%w/w aramid, 10%w/w PTFE and 15%w/w MoS<sub>2</sub>. This indicates that the inclusion of MoS<sub>2</sub> has a significant impact upon improving friction performance. Wear performance is poor and comparable to a 30%w/w carbon fibre filled composite. This composition will not be considered as a candidate material to carry forward.



**Figure 5.34 - Ring on disc test data for 10%w/w Aramid fibre and 10%w/w PTFE filled PEEK**

Figure 5.35 shows the results for PEEK filled with 40%w/w graphite and 10%w/w carbon fibres. The material achieved very few dynamic cycles. This was due to the material yielding as the 17.2 kN load was being applied; the failure of the test specimen was brittle in nature. This test was repeated three times upon samples from different batches in order to ensure that there were no external factors causing the failure. The same result was observed in each test.

The total loading of solid particles of 50% is particularly high and therefore it is hypothesised that the failure was caused by overloading of the matrix. It is expected that a poor adhesion between the PEEK and solid particles meant that the material failed in the PEEK regions of the material as there was increased stress at these points. This result has not been seen in materials highly loaded with carbon fibres, for example ST45CA30 and HT22CA30. There are two possible explanations for this, either a

combined overloading of the material between either graphite and carbon fibres, or that the interaction of high loading of graphite in PEEK causing the composite to become more brittle.

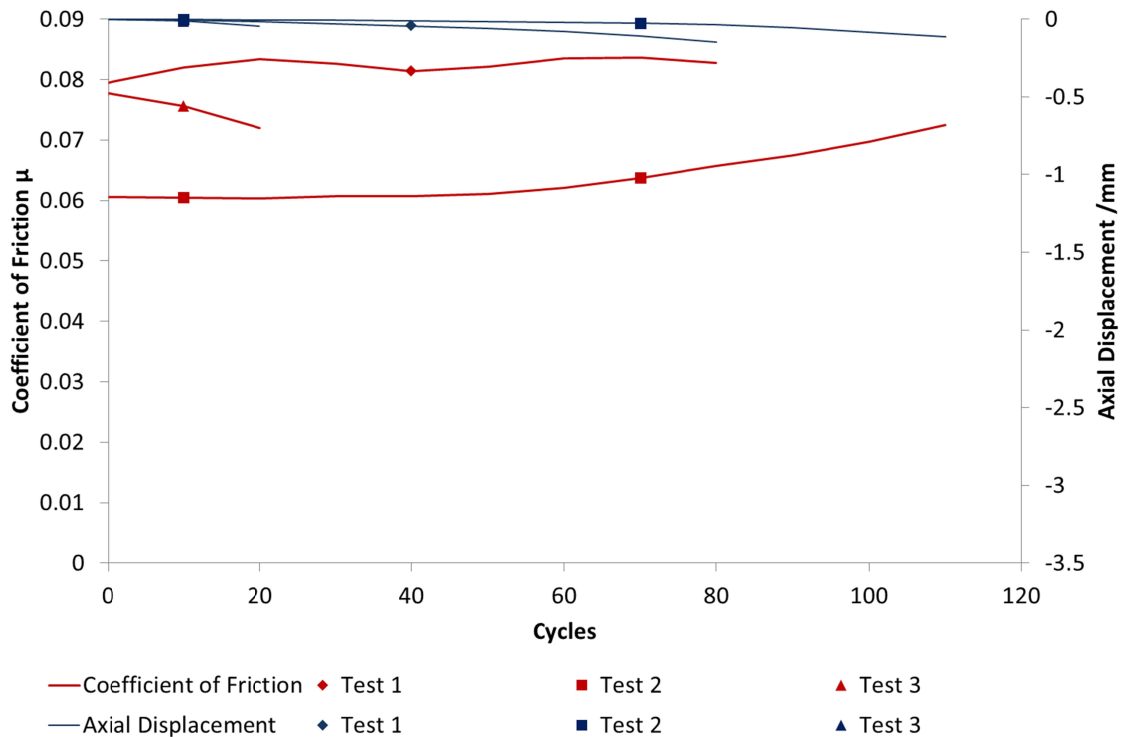


**Figure 5.35 - Ring on disc test data for 10%w/w carbon fibre and 40%w/w graphite filled PEEK**

Figure 5.36 shows the results for PEEK containing 30%w/w carbon fibres, 5%w/w graphite and 10%w/w PTFE. There is good agreement between the three data sets. There are two clear steady state wear regions, initially a very low wear rate over the first 2,000 cycles followed by an increased wear rate to test end at approximately 8,000 cycles. The characteristic wear curve is not seen in this material as there are two distinct wear regions. In other materials failure has occurred as wear rate has rapidly increased causing wear over a few hundred cycles. Figure 5.37 shows the specific wear rate against cycles for this material. The increase in wear rate can be clearly seen

in this plot and represents an order of magnitude increase in the specific wear rate across all tests. The specific wear rate increases from an average of  $2 \times 10^{-5}$  to  $1.5 \times 10^{-4}$ .

All tests ended with a brittle failure of the test specimen between 7,000 and 8,200 cycles after approximately 1mm of wear had taken place. Similarly to 10%w/w carbon fibre and 40%w/w graphite filled PEEK shown in Figure 5.35, this is thought to be due to the high loading of solid particle fillers.

Friction coefficient is initially low at 0.04 and is stable for the first 1,500 cycles. It then increases rapidly to 0.07, coinciding with the increase in wear rate at 2,100 cycles. It then remains stable for a further 2,000 cycles for samples 1 and 3, 3,500 cycles for sample 4, before increasing further towards 0.1. It is expected that frictional performance for this composition should be close to that of 10%w/w PTFE, graphite and carbon fibre filled PEEK as the composition is somewhat similar. The friction values observed for this composition are marginally higher than expected.

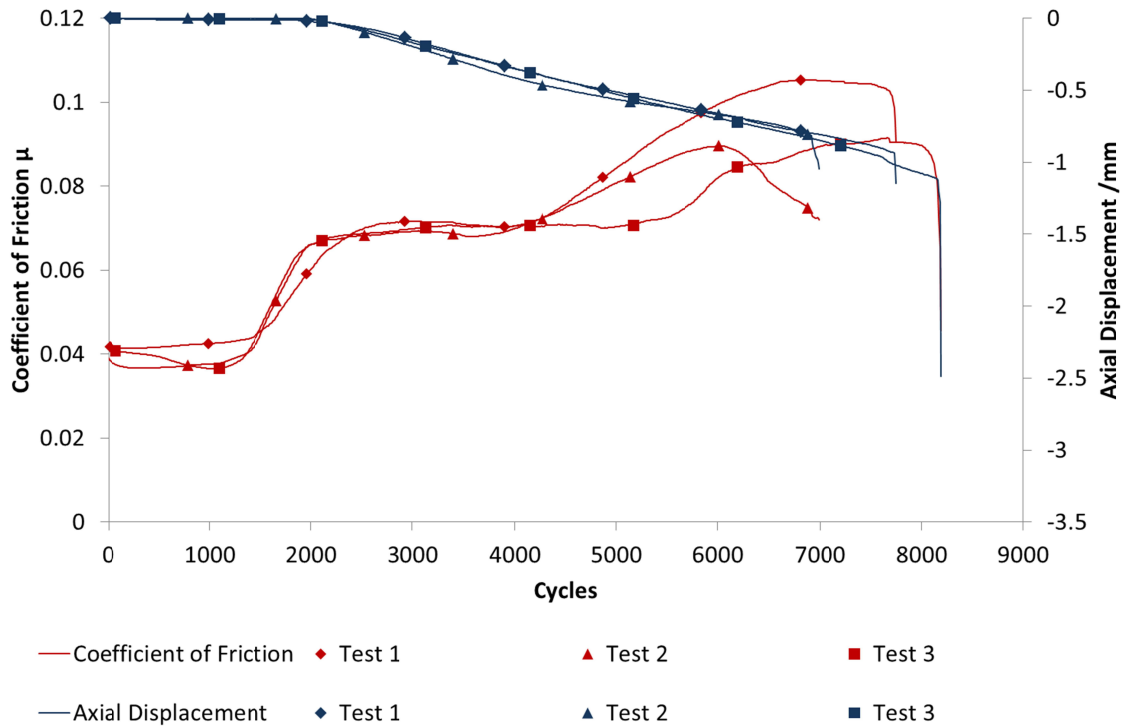
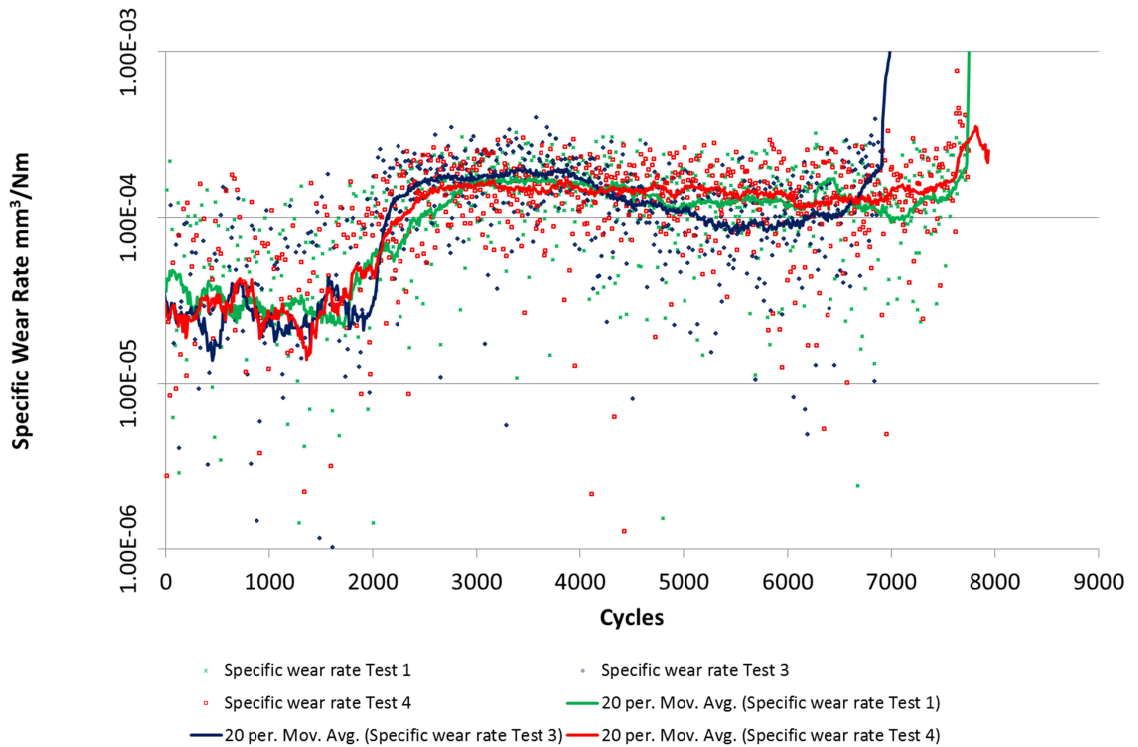


Figure 5.36 - Ring on disc test data for 30%w/w carbon fibre, 5%w/w graphite and 10%w/w PTFE filled PEEK



**Figure 5.37 - Specific wear rate for 30%w/w carbon fibre, 5%w/w graphite and 10%w/w PTFE filled PEEK**

Figure 5.38 shows the performance of PEEK filled with 15%w/w PTFE and 15%w/w graphite. Test 1 shows a good wear life with only 0.3mm at 240,000 cycles. Samples 2, 3 and 4 all exhibited brittle failure between 30,000 and 50,000 cycles. A significant increase in wear as has been observed in other material compositions was not seen in this material.

Friction coefficient was also low, starting at 0.03 and reducing initially. Test 1 shows the minimum coefficient of friction as approximately 0.02 at 100,000 cycles. Following this it again increases to 0.03. This is comparable to 20%w/w PTFE filled PEEK shown in Figure 5.29.

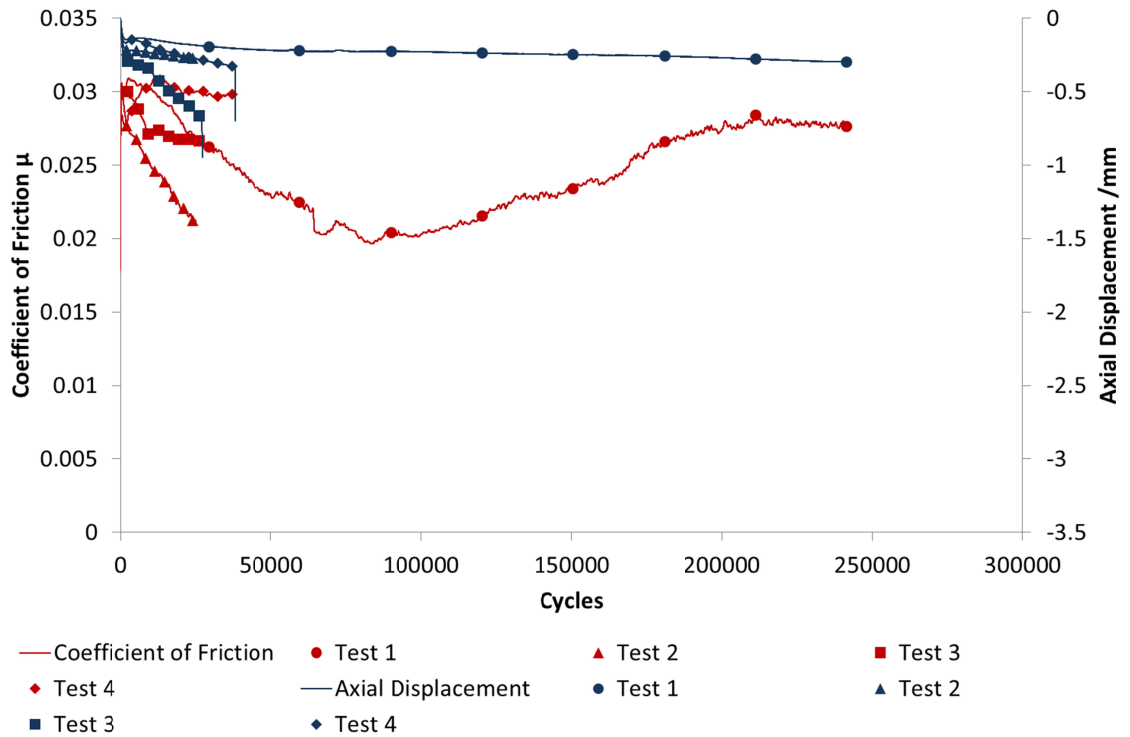


**Figure 5.38 - Ring on disc test data for 15%w/w graphite and 15%w/w PTFE filled PEEK**

Figure 5.41 shows the dynamic results for PEEK filled with 10%w/w carbon fibre, 10%w/w graphite and 20%w/w PTFE. The cycles to end of life are inconsistent with 1mm of wear occurring after 1,550, 600 and 200 cycles respectively. An initially low wear rate can be observed in samples 1 and 3, continuing for 1,220 and 190 cycles respectively. The observed friction coefficient started at approximately 0.03 and remained stable until the wear rate increased. Friction coefficient then increased to 0.035. These friction values are comparable to 20%w/w PTFE filled PEEK shown in Figure 5.29. The wear performance observed is poor, and much less than expected. The composition is very similar to that shown in Figure 5.30, with 10%w/w each of PTFE, graphite and carbon fibres. The wear performance, however, is significantly worse.

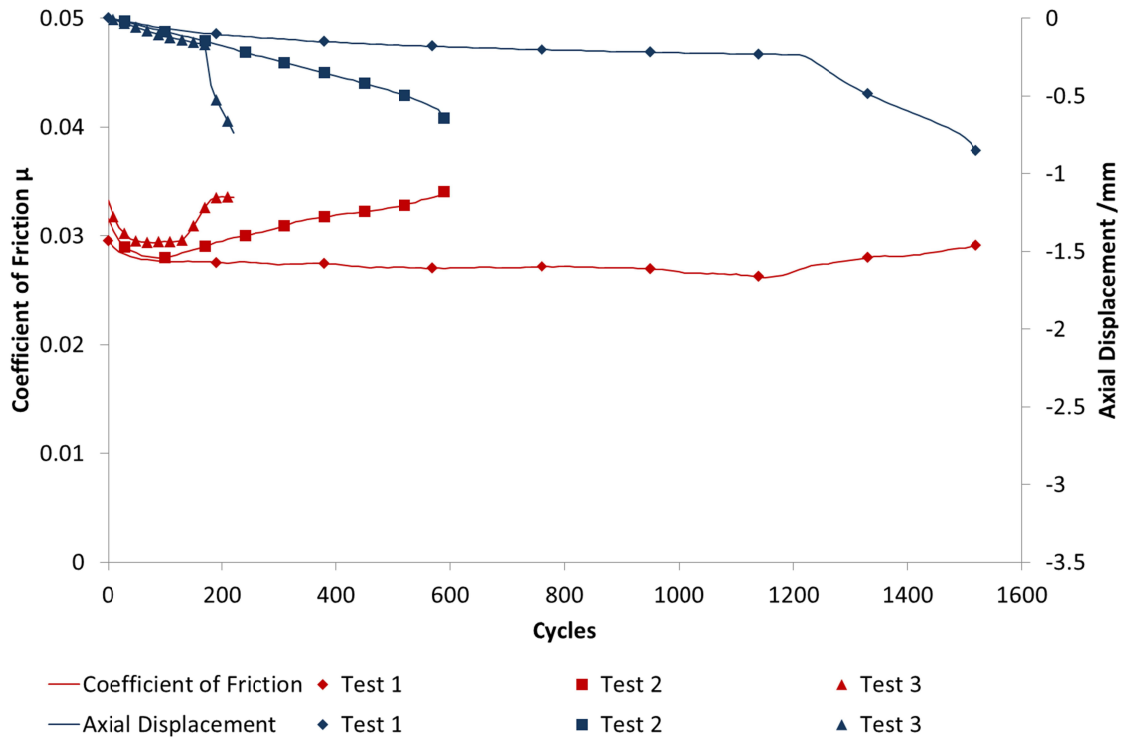


**Figure 5.39 - Ring on disc test data for 10%w/w carbon fibre, 10%w/w graphite and 20%w/w PTFE filled PEEK**

Figure 5.40 shows the test results for PEEK filled with 10%w/w carbon fibre, 10%w/w graphite, 15%w/w MoS<sub>2</sub> and 15%w/w PTFE. For all samples shown there is an indicative negative wear rate over the first 25,000 cycles. This is evidently not possible as material is not being generated at the contact. This can be explained by considering that the axial displacement measurement cannot completely isolate wear, therefore it is a composite of several factors, as described in Section 5.3. In this material, the thermal expansion of the test bench components is of the same order of magnitude as the wear of the sample material and initially slightly larger over the first few hundred cycles. This indicates a false negative wear reading. It can be said, however, that the initial wear rate is very low over the first 20,000 cycles. Wear rate then increases at approximately 22,000 cycles for samples 3 and 4. This is preceded by an increase in friction coefficient from 0.025/0/03 to .055 from 18,000 to 30,000 cycles. Samples 1 and 2 do

not show an increase in wear rate as the tests were stopped at 25,000 cycles. Tests 3 and 4 ended with brittle failure of the specimens.

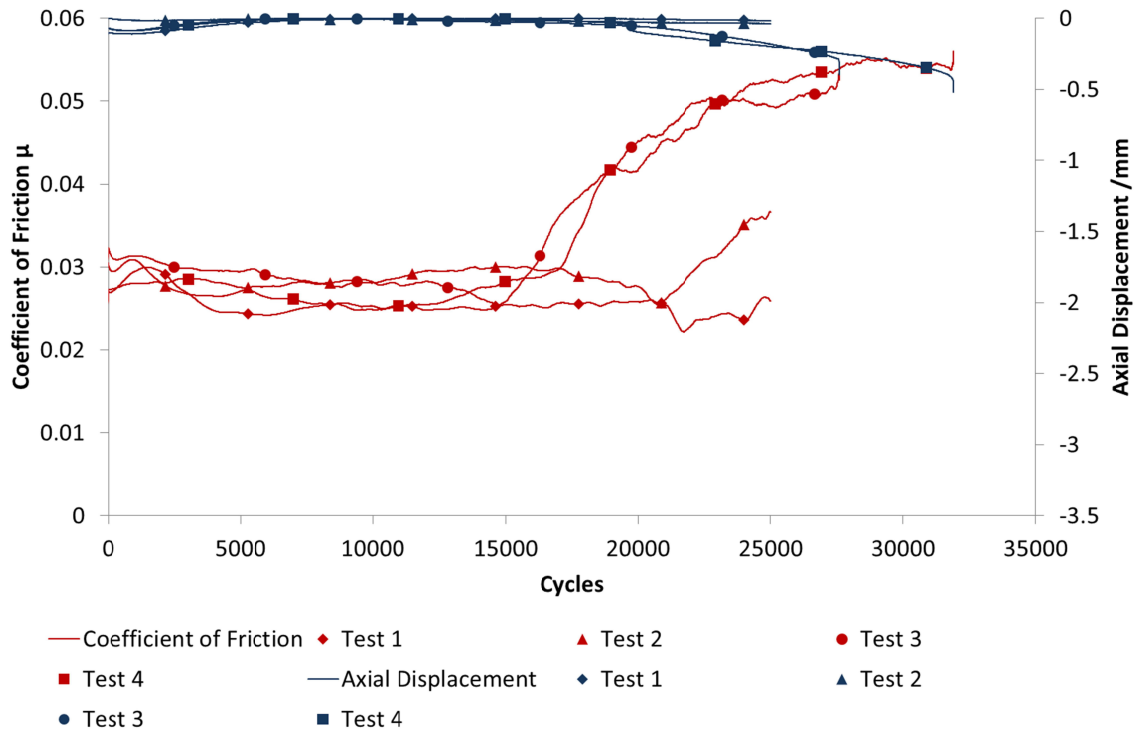


**Figure 5.40 - Ring on disc test data for 10%w/w carbon fibre, 10%w/w graphite, 15%w/w MoS<sub>2</sub> and 15%w/w PTFE filled PEEK**

Figure 5.41 shows the test data for PEEK filled with 15%w/w carbon fibres. This material exhibits an initially low wear region seen similar to that seen in other carbon fibre filled materials. In both samples there is inconsistency in both friction and wear. The initial low wear region continues for 3,000 cycles in sample 2 and 1,000 cycles in sample 3. Wear life is comparable to that observed in 30%w/w filled PEK and PEKEKK. It also shows a significant improvement when compared to 15%w/w glass filled PEEK. In both samples, coefficient of friction starts at approximately 0.04 and increases over the first 4,000 cycles. Sample 2 peaks at 0.09 whereas sample 3 peaks at 0.12. Both samples follow a similar trend for friction coefficient with two local maxima. As the wear rate in this region is in steady state it is assumed that the large variation in friction

coefficient is due to dispersion of fillers through the material thickness and breakout of these abrasive particles. The observed friction values are lower than those seen in unfilled PEEK and 30%w/w carbon fibre filled compositions, shown in Figures 5.31 and 5.32.

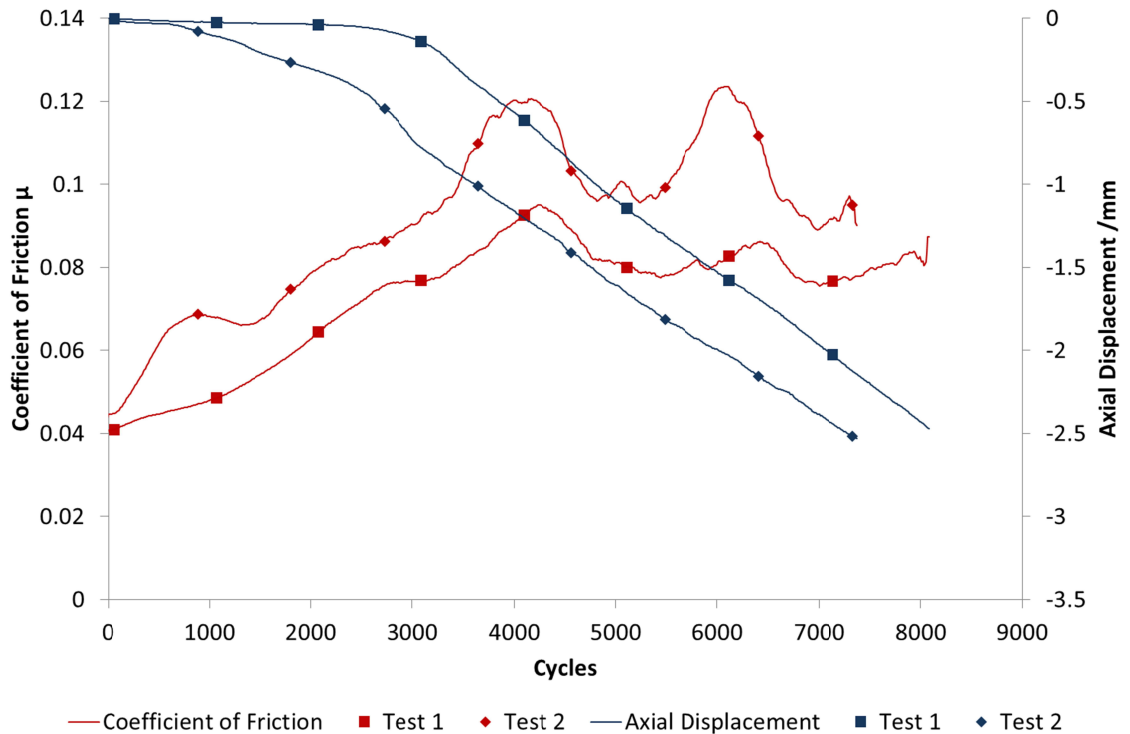


**Figure 5.41 - Ring on disc test data for 15%w/w carbon fibre filled PEEK**

Figure 5.42 shows the dynamic results for PEEK filled with 15%w/w MoS<sub>2</sub>, 15%w/w PTFE and 4%w/w silicone oil. This composition gives exceptional friction properties. Initially, friction coefficient is 0.04. It rapidly reduces over the first 15,000 cycles to 0.0125, the lowest friction coefficient of all materials tested. The reason for this significant reduction is assumed to be due to the gradual release of lubricant, particularly silicone oil, into the contact through the running in of the composite. Once the minimum friction coefficient is reached it increases to 0.025 over 300,000 cycles. The friction coefficient moves up and down through the test, this is assumed to be

where the lubricant is liberated locally at various stages. The friction values are comparable to that observed in 20%w/w PTFE filled PEEK.

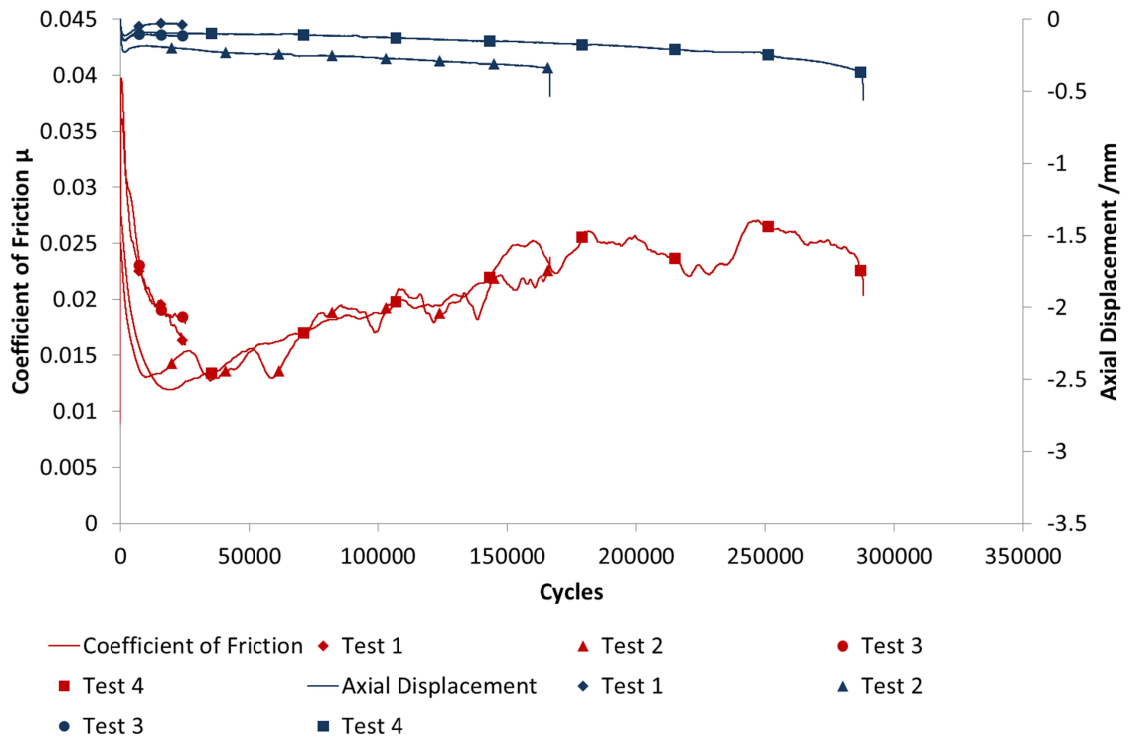


**Figure 5.42 - Ring on disc test data for 15%w/w MoS<sub>2</sub>, 15%w/w PTFE and 4%w/w silicone oil filled PEEK**

### 5.8. Conclusions

The results presented in Section 5.7 have shown that in general, PEEK composites are promising material choice as a self-lubricating sliding contact material. Compositions containing PTFE showed a significant improvement in friction coefficient, with minimum values of 0.01 and 0.012 for 20%w/w filled PEEK and 15%MoS<sub>2</sub>, 15%w/w PTFE and 4%w/w silicone oil filled PEEK respectively. This compares to a minimum friction coefficient for unfilled PEEK of 0.05, therefore a reduction of approximately 80%.

Compositions containing graphite have exhibited good friction properties, although in each case graphite has been coupled with PTFE. The only composition containing

graphite without PTFE contains 10%w/w carbon fibres and 40%w/w graphite. This composition suffered brittle failure under initial loading in all tests. It is therefore not possible to conclude the impact of graphite inclusion on friction performance. This is equally the case for wear performance as the improvement of wear properties is more heavily attributed to the addition of PTFE, and the lowering of friction coefficient preventing thermo-mechanical failure. The observed failure of 40%w/w graphite filled PEEK indicates that a high loading of stiff fillers is detrimental to the structure of the composite and leads to brittle failure. Brittle failure was also observed for PEEK filled with 10%w/w carbon fibres, 15%w/w PTFE, 10%w/w graphite and 15%w/w MoS<sub>2</sub>. This composition also has a high loading of stiff particles.

Similarly to graphite containing composites, compositions containing MoS<sub>2</sub> are coupled with the inclusion of PTFE. Compositions containing MoS<sub>2</sub> yield good results in both friction and wear, though it is unclear the impact which MoS<sub>2</sub> has on the performance. In order to isolate the impact of MoS<sub>2</sub> it has been included in a second composition described in Chapter 8.

Inclusion of glass fibres and carbon fibres as a structural filler showed no impact upon friction coefficient, whereas 30%w/w Aramid filled PEEK showed a reduction in peak friction coefficient of approximately 40% compared to unfilled PEEK. Glass fibres exhibit the poorest performance in wear, whilst carbon fibres alone show better performance than glass fibres. Aramid only filled PEEK exhibited the best wear performance with approximately 10,000 cycles completed before rapid wear initiated.

20%w/w PTFE filled PEEK gave the best wear performance at ambient temperature. Over 500,000 cycles were completed with only 0.18mm wear. The material did not exhibit a rapid increase in wear rate as seen in unfilled PEEK and many other compositions. As this composition has the lowest compressive strength, it is expected

that at high temperature the material would suffer mechanical failure due to reduction in mechanical properties.

The test method developed for this experiment has yielded good sets of performance data for all materials. During the early stages of the tests the axial displacement measurement, considered as the wear measurement, loses accuracy due to thermal expansion of the test rig components. This is due to frictional heating at the contact and heating of the test apparatus in dynamic motion. The accuracy improves as thermodynamic equilibrium is reached. It is suggested that for further experiments carried out using this apparatus, the wear measurement is made more accurate by removing sources of noise in the test rig.

## **6. Experimental methods – material characterisation**

A key assumption made in this thesis is that the fibres used in the composite materials are randomly oriented such that there is not a significant alignment of fibres in any one direction. Furthermore it has been assumed that the fibrous and particulate fillers are evenly distributed throughout the polymer matrix such that there is no localised concentration of fillers. These assumptions allow the material to be treated as an isotropic and quasi-homogeneous material. With equal properties in all directions, the mechanical properties and tribology of the material can be assumed to be consistent throughout the material. Thus any changes in tribology can be assumed to be due to some tribological phenomena rather than due to differences in the material in contact. This chapter seeks to establish the validity of this assumption and identify where the assumption can no longer be made.

### *6.1. Optical microscopy*

In order to understand the effect of fibre loading, orientation and dispersion upon the three dimensional material properties, a methodology to view the micro-structure of the materials was developed.

In terms of evaluating the tribological performance of the composite materials, it has been assumed that the dispersion of the fillers is consistent and that there are not areas which are densely or sparsely populated with such filler materials. It has also been assumed that there is a complete randomness to the orientation of the fibres. By taking this assumption of the micro-structure of the materials, it allows the material can be treated as having bulk properties and as such is homogeneous and isotropic. This idealised view can be tested against the real case by use of imaging techniques.

The equipment used was a Reichert-Jung Polyvomet microscope, shown in Figure 6.1, with objective lenses ranging from 5x to 50x magnification, an intermediate lenses offering magnification from 0.8x to 2x and an eyepiece magnification of 6.3x. This gives a compounded total magnification ranging from 25.2x to 630x. In order to capture images of the specimen a CCD camera was used. The device used was a 5MPixel digital camera connected to a PC. The microscope and camera were not ideally matched and so the image was projected onto the CCD such that the field of view of the camera was much smaller that of the eyepiece. The magnification of the image was therefore much higher than expected, as illustrated in Figure 6.2.



**Figure 6.1 - Reichert Jung Polyvar Met optical microscope**

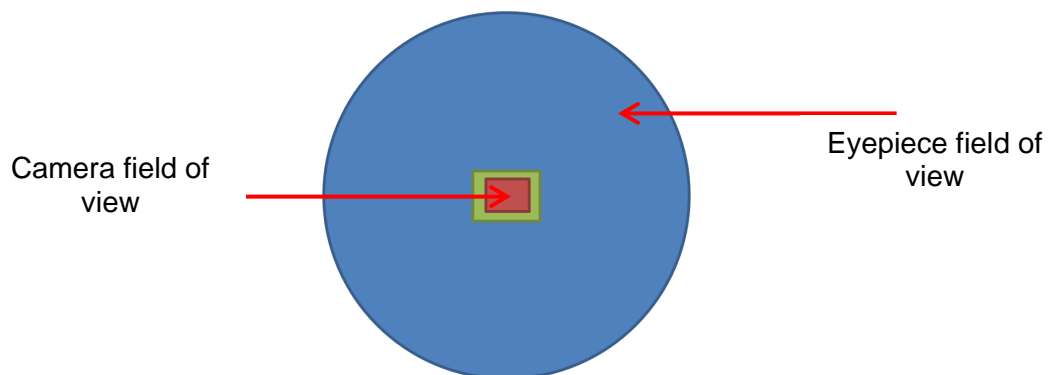


**Figure 6.2 - Microscope eyepiece field of view compared with camera field of view**

In order to analyse the composite structure, size and orientation of the fillers the materials were prepared from injection moulded samples. The samples were polished

to remove asperities and give a reflective surface. Without removing these asperities the sample would give a diffuse reflection. This would mean that microscopic features could not be determined. Each specimen was polished using a rotating base grinding/polishing machine. Initially water lubricated, coarse grit silicon-carbide paper was used followed by several intermediate grit papers, finally using a P2000 fine grit for final finishing.

In order to establish the three dimensional dispersion and orientation of the filler materials, initial samples were evaluated on the top surface and through the material cross section. To view the cross section of the sample a specimen was mounted in amounting resin. The resin used was a room temperature curing two part epoxy sample mounting resin. The sample was then polished using a rotating base grinding/polishing machine as described above.

Typical microscope images are shown in Figures 6.10 to 6.13, represented at 160x, 320x, 650x and 1700x magnification respectively. The fibre fillers can be clearly observed within the PEEK matrix as the lighter coloured long strands.

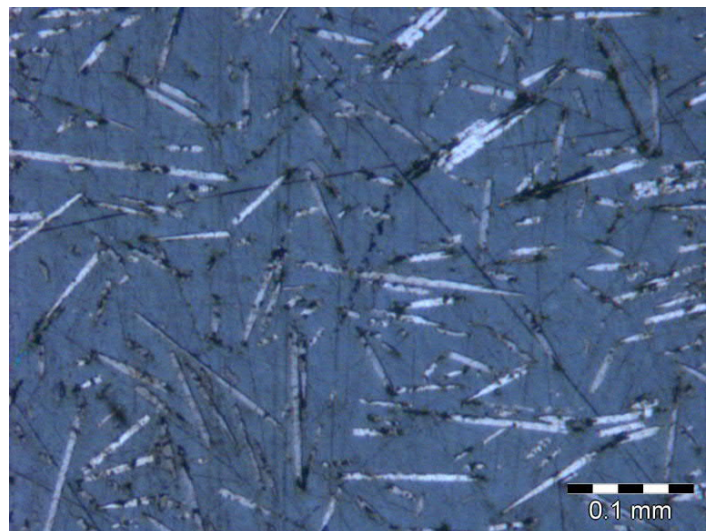


**Figure 6.3 – Optical microscope image of carbon fibre filled PEEK at 160x magnification**

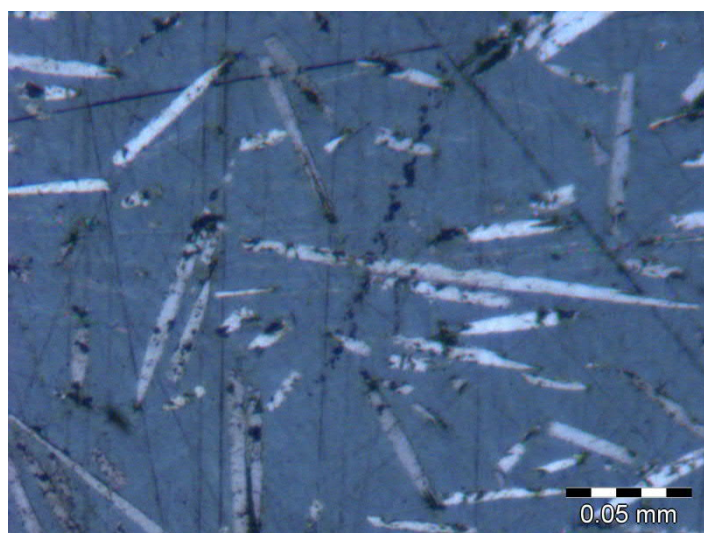


**Figure 6.4 – Optical microscope image of carbon fibre filled PEEK at 320x magnification**

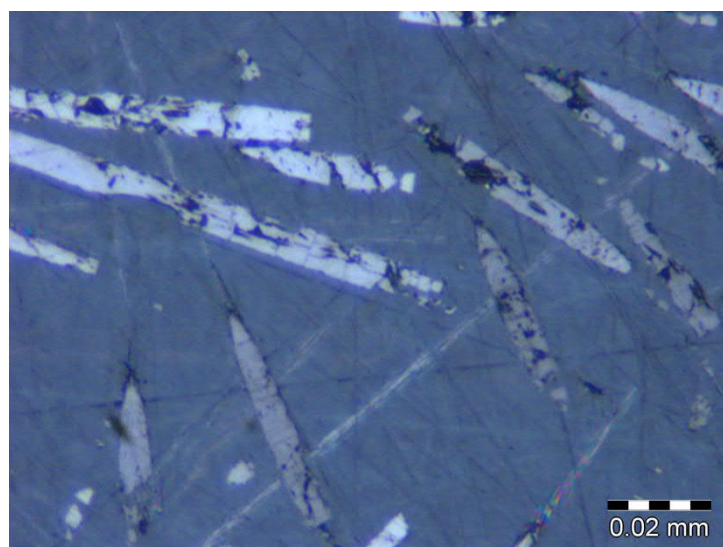


**Figure 6.5 – Optical microscope image of carbon fibre filled PEEK at 650x magnification**

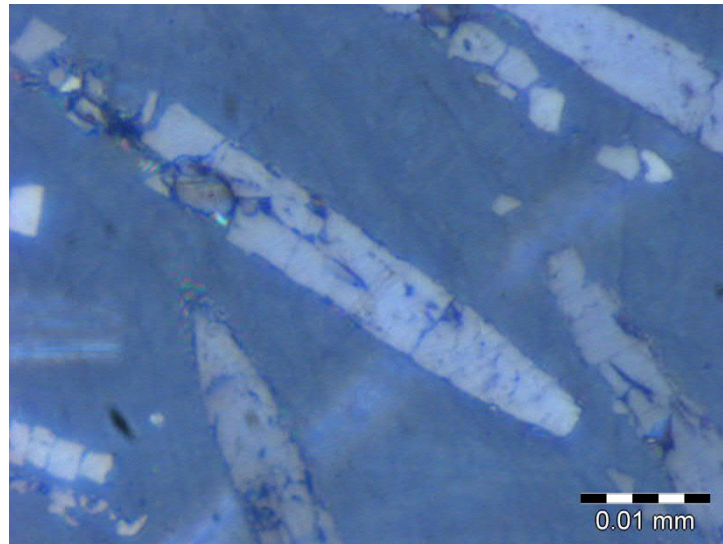


**Figure 6.6 – Optical microscope image of carbon fibre filled PEEK at 1700x magnification**

It is expected that a boundary layer where fillers do not reach the surface of the composite will be observed, and as such there will be a thickness of pure peek before reaching the filler materials. It has been assumed that there is a random orientation and even dispersion of fillers through the composite, however it is expected that some local alignment and agglomeration of fibres will occur. If generally there is a random orientation and dispersion of fillers, this will support the assumption that the composite materials can be considered isotropic and homogeneous on the macro scale, and thus considered as having bulk properties.

## **6.2. Results and discussion**

This section presents and discusses the results from the optical microscopy. The discussion seeks to give answers to the questions raised in Section 5.1 and develop new hypotheses relating to the composite structure and influence on bulk properties of the material.

Section 5.1 discusses the influence of fibre orientation and dispersion upon the local and bulk properties of the composite material. Whilst it may be more ideal to tailor the

properties of the composite liner in each plane by deliberate fibre alignment or placement of fibres in different points in the cross section, this type of engineered solution would require advanced manufacturing techniques and tooling design which are outside of the scope of this project. That said, it is important to understand the microstructure of the materials in order to give an additional context to the results from the static and dynamic testing presented in Chapters 5 and 7. It is possible that there is a degree of anisotropy in the composites tested which is inherent to the materials and the manufacturing processes used which this section seeks to understand.

For the purposes of this study the most ideal condition would be that of an isotropic material which can be considered to have bulk properties and treated as such as a bulk material. For this to be the case it would require that on a micro scale the filler materials have a random orientation. i.e. fibres which are not aligned in the same plane, and good dispersion, i.e. no concentration of fillers in particular areas as discussed in Section 5.1. Furthermore, it is necessary to understand any change in the microstructure through the thickness of the material as this can impact significantly the tribological characteristics of the composite. Alignment of fibres parallel to the surface *at* the surface will give different properties to the core if the fibres tend away from being parallel, as discussed by Voss and Friedrich (1987). Also, if there is a boundary layer at the surface where only the bulk material exists, it will behave as the unfilled bulk material would behave until the wear depth reaches the filler materials. The thickness of this boundary layer would define the initial wear phase characteristics.

Figures 6.14 to 6.23 show the microscope images for PEEK composites at 160x optical magnification. The scale for each is shown in the bottom right hand corner.

Figure 6.7 shows the microscope image of unfilled PEEK at 160x magnification. It is possible to see scratches on the surface from the polishing process. The image shows

the material as having a consistent colour with no other obvious features. This is as expected for an unfilled material.

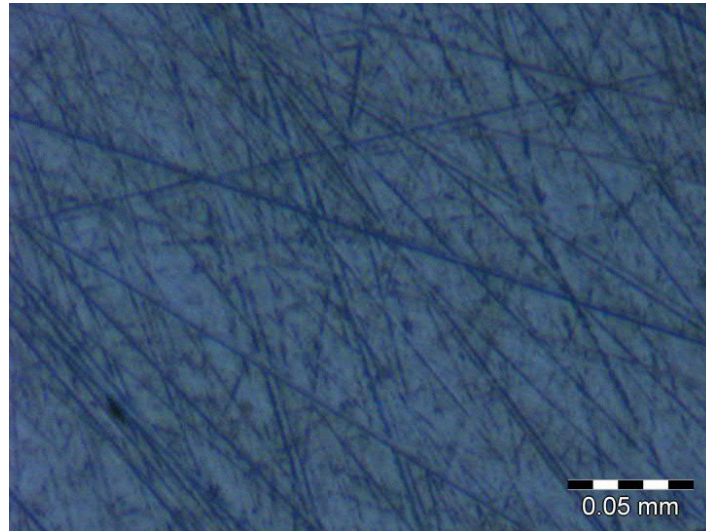
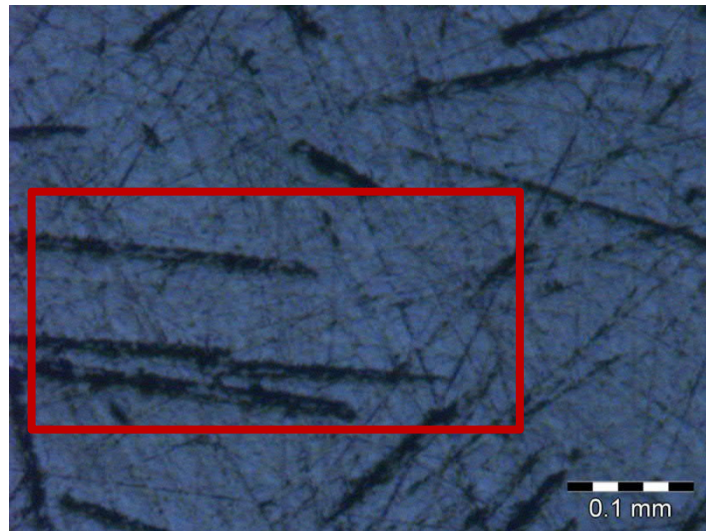


**Figure 6.7 - Optical microscope image of unfilled PEEK at 160x magnification**

Figure 6.8 shows PEEK filled with 15% by weight glass fibres, approximately 8% by volume. The glass fibres show up as the dark features in the image and are distinct from the surface scratches from polishing.

The maximum fibre length observed is approximately 250 $\mu$ m with a diameter of approximately 15 $\mu$ m. There is a clear variation in fibre lengths within the composite. There are two reasons for this: firstly there is an inherent distribution in fibre geometries as can be naturally expected; secondly the two dimensional nature of the image only shows the part of the fibre which is exposed at the surface. For fibres which are not parallel to the surface and therefore only partially exposed they appear to be shorter than they are in reality. This has also been observed by Mlekusch et al (1999) and Rasheva et al (2010).

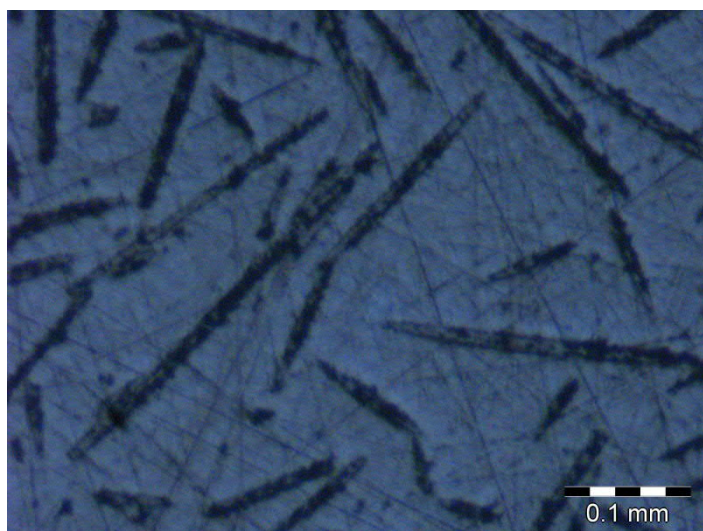
The area highlighted in the red box show that there is fibre alignment in some areas, however there appears to be an otherwise random orientation in other areas. There is also a reasonably good distribution of fibres.



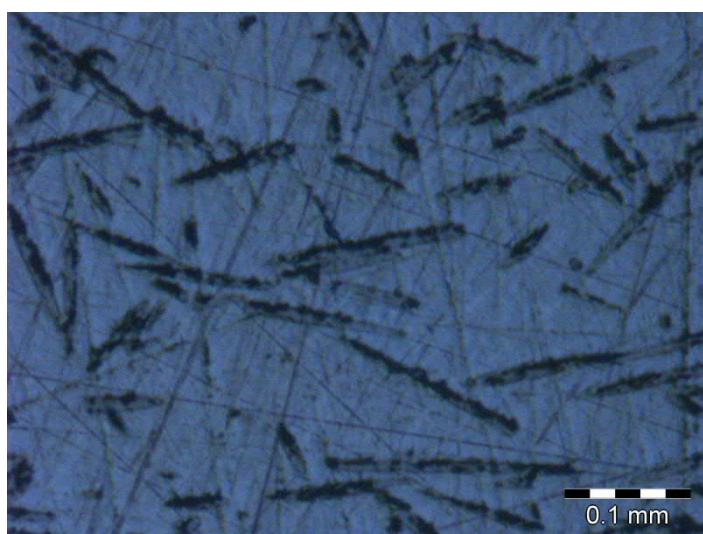
**Figure 6.8 - Optical microscope image of 15% w/w glass fibre filled PEEK at 160x magnification with aligned fibres highlighted**

Figures 6.16, 6.17 and 6.18, 30%w/w glass fibre filled PEEK, PEK and PEKK respectively, approximately 18% by volume. The bulk resins are different forms of PAEK as presented in Chapter 3. The images show no distinction between PEEK, PEK and PEKEKK. As expected, the fibres represent a larger area of the images due to the increase in the volume fraction of the fillers when compared to Figure 6.8.

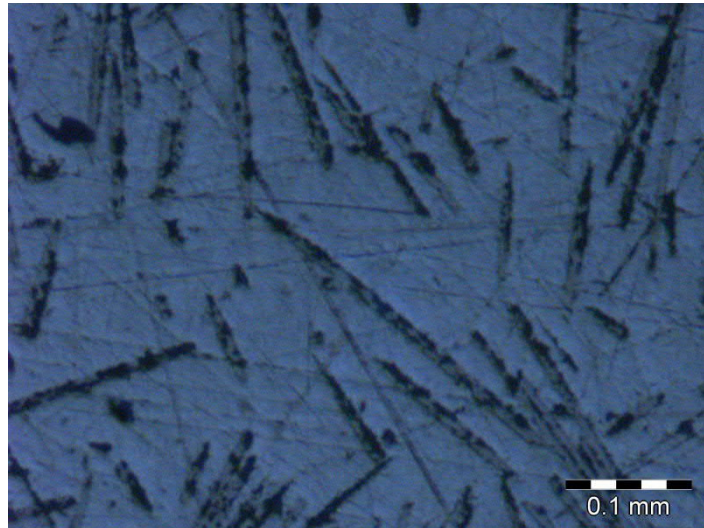
Figure 6.9 and 6.18 indicate an even dispersion of fibres; fibre orientation is random with some alignment of fibres in close proximity, similar to that seen in Figure 6.8. Figure 6.10 appears to have a lesser degree of alignment.



**Figure 6.9 - Optical microscope image of 30% w/w glass fibre filled PEEK at 160x magnification**



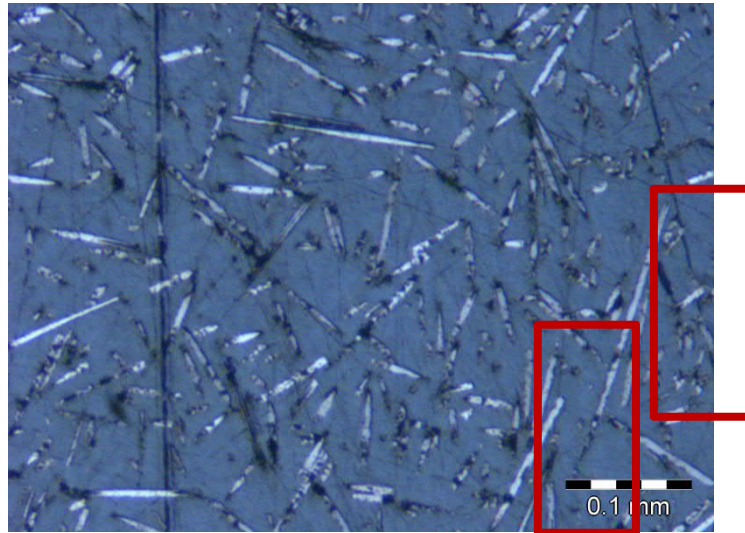
**Figure 6.10 - Optical microscope image of 30% w/w glass fibre filled PEK at 160x magnification**



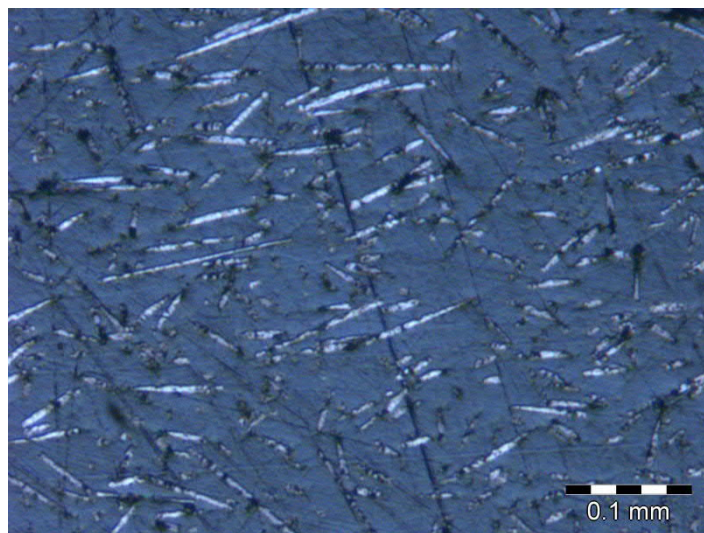
**Figure 6.11 - Optical microscope image of 30% w/w glass fibre filled PEKEKK at 160x magnification**

Figure 6.12 and 6.20 show PEK and PEKEKK filled 30% by weight carbon fibres. This represents a volume fraction of approximately 24%, a third greater than that of the 30% weight fraction glass fibre filled composite. The area fraction of fillers in each image reflects this. Conversely to glass fibres, the carbon fibres show as a lighter feature as compared to the bulk material. The maximum observed length of the carbon fibres is approximately 150 $\mu\text{m}$  and the diameter is approximately 10 $\mu\text{m}$ . It can be seen that the carbon fibre geometry is smaller than that of the glass fibres.

Figure 6.12 again shows even dispersion of the fibres with some fibre alignment in the areas highlighted in red. There is, however, a predominantly random orientation of fibres. Figure 6.13, conversely, shows a greater degree of fibre alignment whilst remaining well dispersed. In both materials it is again the case that alignment occurs where fibres are in close proximity.



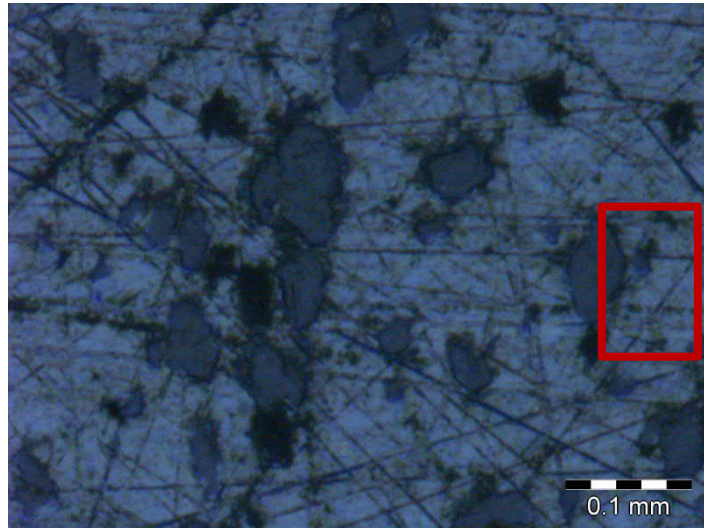
**Figure 6.12 - Optical microscope image of 30% w/w carbon fibre filled PEK at 160x magnification with aligned fibres highlighted**



**Figure 6.13 - Optical microscope image of 30% w/w carbon fibre filled PEKEKK at 160x magnification**

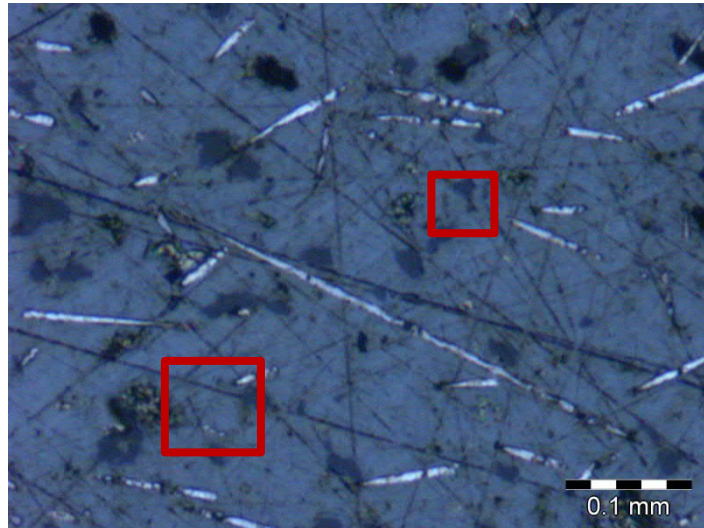
Figure 6.14 shows PEEK with 20% weight fraction of PTFE, equivalent to approximately 12.5% volume fraction. The PTFE regions show as darker areas compare to the PEEK bulk material, as highlighted. The particle size appears to be somewhat inconsistent with some approaching 100 $\mu$ m diameter. Similarly to the fibre fillers this can be due to the two dimensional nature of the image whereby the exposed

area is smaller than the true diameter, where the maximum diameter is below the surface or has been removed in the polishing process. There is also a degree of agglomeration visible in the left hand portion of the image.



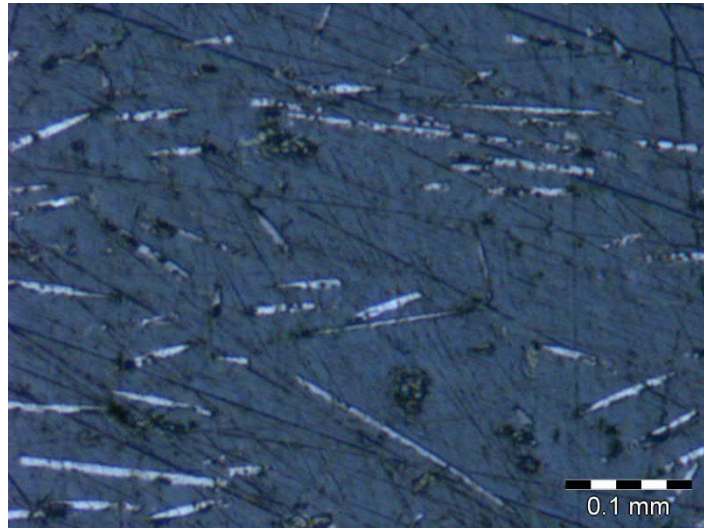
**Figure 6.14 - Optical microscope image of 30% w/w PTFE filled PEEK at 160x magnification**

Figure 6.15 shows PEEK with 10% weight fraction each of PTFE, carbon fibres and graphite particles. The volume fractions are approximately 6.5% PTFE, 8.5% carbon fibres and 6.5% graphite particles. The image shows an even dispersion of fibres and fillers in the matrix with a random orientation of the carbon fibres. It is possible to distinguish the carbon fibres however it is more difficult to distinguish between the PTFE and graphite particles. The particle sizes are similar, however the graphite is less contrasting against the PEEK bulk and has a mottled appearance as highlighted. It can be seen that the PTFE particle size appears to be smaller in this composite than for the composite shown in Figure 6.21.



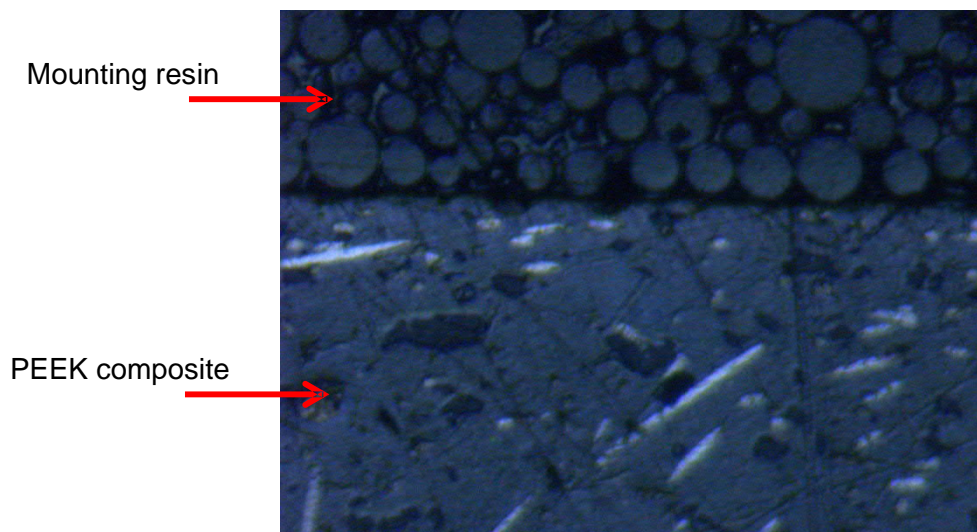
**Figure 6.15 - Optical microscope image of 10% w/w PTFE, graphite and carbon fibre filled PEEK at 160x magnification**

Figure 6.16 shows a PEEK composite manufactured by Victrex and marketed as Wear Grade 101. The fillers and their weight fractions are not available from literature. The nature of the fibrous filler appears to be the same as that of the carbon fibres seen in other composites. Manufacturer literature states that this composite blend does not contain PTFE however does exhibit low friction properties (Victrex 2011). The particles that can be seen have a similar appearance to that of the graphite. It is therefore suggested that graphite has been included as a friction reducing component. It is also possible that these particles could be another mineral based solid lubricant such as  $\text{MoS}_2$ . The glass transition temperature of  $143^\circ\text{C}$  and melting point of  $343^\circ\text{C}$  suggest that the bulk resin is PEEK which cannot be determined by optical microscopy.



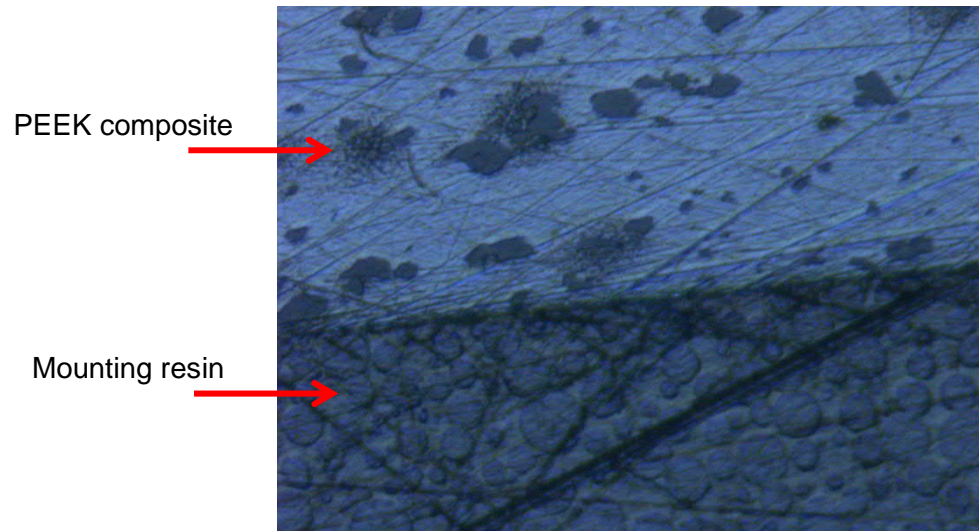
**Figure 6.16 - Optical microscope image of Victrex WG101 PAEK at 160x magnification**

Figure 6.17 shows a cross section of 10%w/w PTFE, graphite and carbon fibre filled PEEK at the surface of the moulding. The mounting resin can be observed and as light circles within a darker matrix. The PEEK composite shows fillers reaching the surface of the material. There is some alignment of fibres parallel to the material surface, which can be seen close to the interface. This is expected, and is agrees with the hypothesis of Voss and Friedrich (1987) who observed alignment of fibres parallel to the surface from injection moulding.



**Figure 6.17 - Optical microscope image of 10% w/w PTFE, graphite and carbon fibre filled PEEK at 160x magnification**

Figure 6.18 shows a cross section of 20%w/w PTFE filled PEEK. For this composite PTFE is evenly dispersed and reaches the surface of the material. There does not appear to be a boundary layer whereby PEEK is the only constituent.



**Figure 6.18 - Optical microscope image of 20% w/w PTFE filled PEEK at 160x magnification**

Across all compositions there is not a significant amount of fibre alignment. The fibres aligned with the surface, those which appear longest, show some local alignment where fibres are in close proximity. There are also fibres which are not aligned parallel to the surface, those which appear shortest and have an oval shape, as shown in Figure 6.24. Some alignment parallel to the surface has been observed close to the moulded surface of the composite, which is expected. This could impact the initial wear stages for fibre filled materials, although the effect of fibre alignment has been shown not to have a large impact on wear rate (Zhang et al. 2010)



**Figure 6.19 - Optical microscope image of 30%w/w carbon fibre filled PEEK at 320x magnification showing fibre alignment**

### 6.3. Conclusions

Agglomeration of fibres and fillers has not been generally observed. There is some local agglomeration, however fillers appear evenly dispersed in all compositions. The orientation of fibres and dispersion of fillers generally support the hypothesis that the materials tested in this study can be considered isotropic. Fibre filled materials may see some impact of surface alignment in tribological tests, however the effect of this is expected to be small.

## 7. Experimental Methods - Mechanical testing

This chapter investigates the mechanical performance of the PEEK composites described in Chapter 3. Mechanical properties have been derived from manufacturer data and are presented to allow comparison between compositions and infer any impact of the various structural fillers upon mechanical performance. Thermoplastic polymers are particularly susceptible to creep, therefore a creep test at loads representative of aerospace test and application conditions has been carried out. The results for this experiment are presented and discussed.

### 7.1. Mechanical properties of selected compositions

Chapter 3.1 describes the performance criteria upon which candidate materials must be selected when being considered as liner materials for aerospace plain bearings. One key aspect is their load carrying capability, as dynamic contact pressures in excess of 100MPa are not uncommon. Moreover, qualification tests are carried out at contact pressures exceeding 250MPa in order to accelerate failure (SAE 2008). It is therefore necessary to understand the mechanical performance of the materials selected in Chapter 3 in conditions that are representative of these high loads.

The selected composite bulk material, PEEK, offers good base mechanical performance when compared to alternative thermoplastics (Friedrich et al. 1995). As described in Chapter 3.2.2, the mechanical performance of PEEK can be enhanced by the inclusion of structural filler material and, depending upon their individual mechanical properties, the inclusion of solid lubricants. The values for compressive strength, tensile strength and elastic modulus are shown in Table 7.1 (Matweb 2016; Victrex 2011). The values for compressive strength are not provided for Luvocom materials, however tensile strength and elastic modulus are shown. The values for

compressive strength are higher than those given for tensile strength, which is commonly observed in polymers.

**Table 7.1 - Mechanical properties of selected PEEK composites**

Composite	Compressive Strength (Mpa)	Tensile Strength (MPa)	Tensile Modulus (GPa)
450G	120	100	3.7
450GL15	130	140	7.5
450GL30	250	180	11.8
HT22GL30 (PEK)	290	200	12
ST45GL30 (PEKEKK)	290	200	12
HT22CA30 (PEK)	300	260	26
ST45CA30 (PEKEKK)	310	270	25
150FC30	170	150	12.8
450FE20	105	78	2.9
WG101	230	180	19
1105-8783		90	8.5
1105-8487		90	5
1105-8403		-	-
1105-8165		90	22
1105-0699		220	26
1105/GR/15/TF/15-2		70	4
1105-8613		-	-
1105-7760		130	12
1105/XCF/15-S		235	17
1105-7714-WE		75	4

Figure 7.1 shows the tensile strength against elastic modulus for the materials selected in Chapter 3. It can be observed that materials without structural fillers tend to populate

the lower left hand portion of the graph and offer very similar performance to unfilled PEEK. Addition of PTFE causes the compressive strength, tensile strength and elastic modulus of the composite to be lower than that of unfilled PEEK. This is because PTFE has worse mechanical properties than PEEK, and by applying the rule of mixtures, the properties of the composite are expected to be worse. Addition of Aramid fibres offers some improvement to elastic modulus, however tensile strength is reduced. 1105-8783 (20%w/w Aramid fibre, 10%w/w PTFE and 15%w/w MoS<sub>2</sub> filled PEEK) shows a much larger enhancement of elastic modulus and tensile strength compared to 30%w/w Aramid fibre filled PEEK, 1105-8487. The proportion of Aramid fibres is lower in this composition and as the inclusion of PTFE lowers the elastic modulus, it can be inferred that MoS<sub>2</sub> has a significant positive impact upon mechanical performance. Inclusion of glass fibres has a much larger positive impact upon mechanical properties than Aramid fibres when comparing 30%w/w glass fibre filled (450GL30, HT22GL30 and ST45GL30) and Aramid fibre filled composites (1105-8487). Inclusion of carbon fibres has the most positive impact upon mechanical properties. 15%w/w carbon fibre filled PEEK, 1105/XCF/15-S, offers a 30% improvement in tensile strength and a 44% improvement in elastic modulus compared to 30%w/w glass fibre filled PEEK, 450GL30. It is worth noting that the volume fraction of carbon fibre and glass fibre fillers in these compositions is 11% and 18% respectively. This means that a much lower filler volume can achieve far superior mechanical properties when using carbon fibres as a structural filler. The superiority of carbon fibres with respect to mechanical performance has been suggested in many studies, including those of Flock et al (1999) and Yamamoto and Hashimoto (2004). This, coupled with the superior tribological performance of carbon fibre fillers compared to glass shown in Chapter 5, suggests that carbon fibre is the most appropriate structural filler for the final liner material. This agrees with the work of Davim and Cardoso (2009), Lu and Friedrich (1995) and Voss and Friedrich (1987).

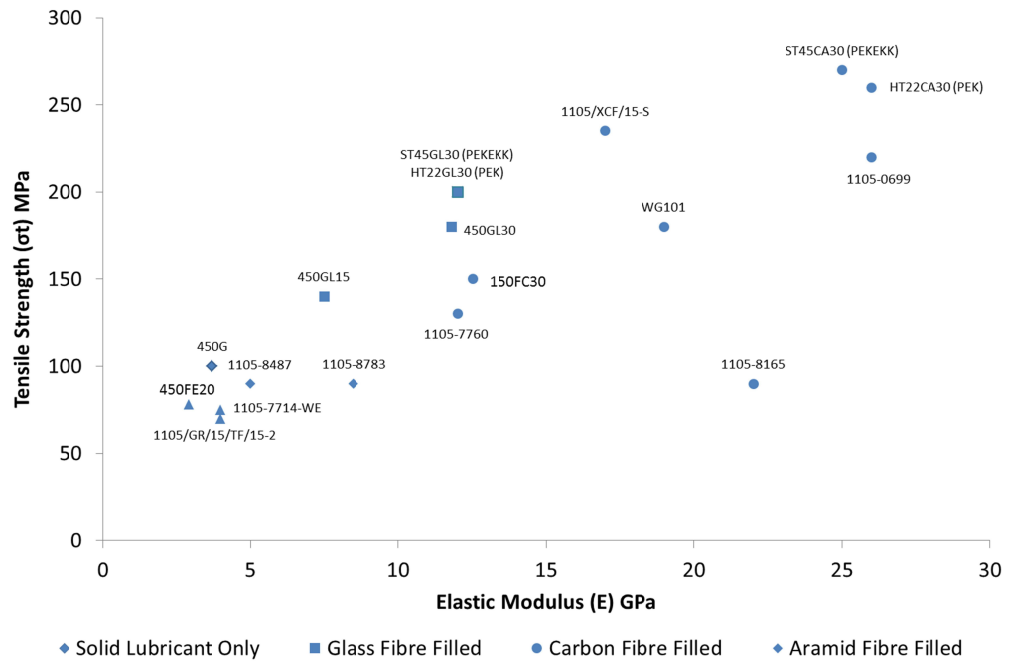


Figure 7.1 - Tensile strength against elastic modulus for selected PEEK composites

Figures 7.2 and 7.3 compare tensile strength with weight and volume fraction of structural fillers for the PEEK composites selected for testing. For the same loading by weight for the various structural fillers, a trend can be observed for the ranking of materials for their impact upon the tensile strength. As previously discussed, carbon fibres offer the best enhancement of mechanical performance compared to glass and Aramid fibres. Naturally, with increasing weight and volume fraction of structural fillers an increasing tensile strength can generally be observed.

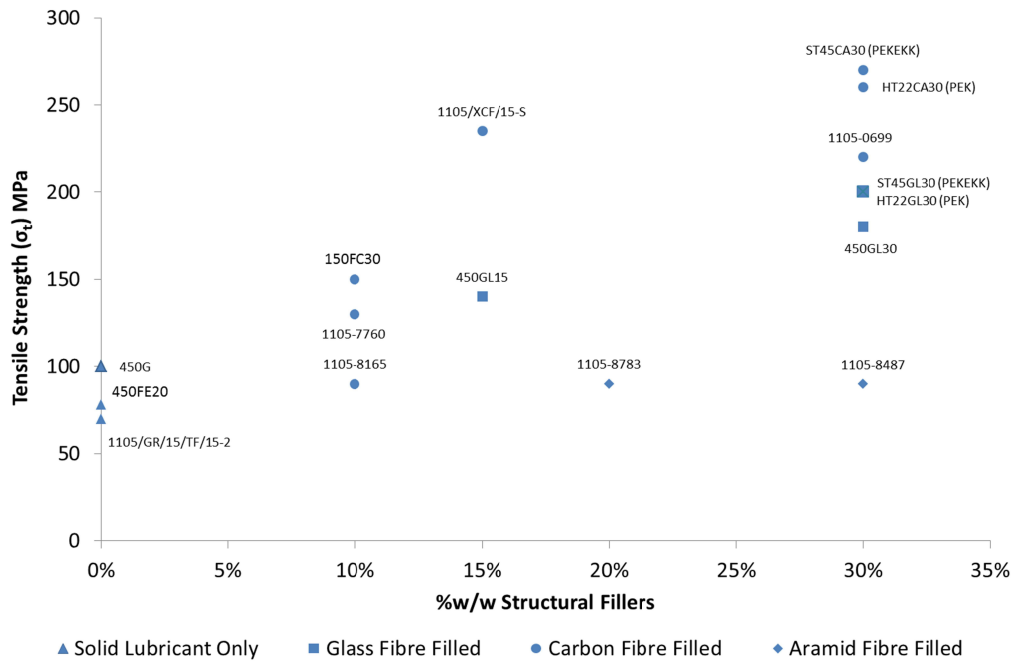


Figure 7.2 - Tensile strength against weight fraction structural fillers for selected PEEK composites

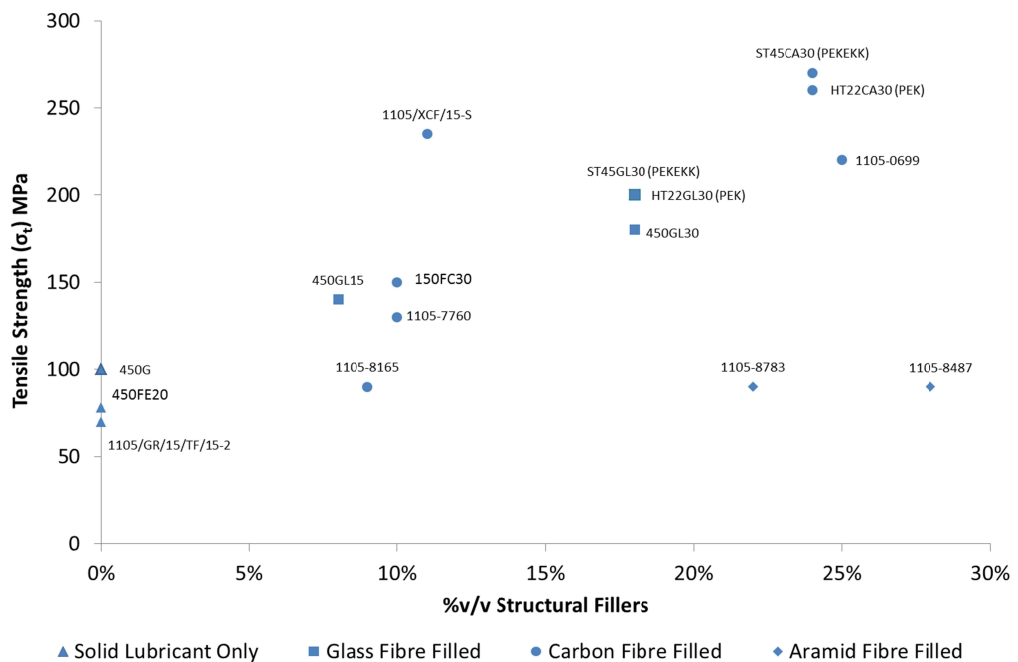


Figure 7.3 - Tensile strength against volume fraction structural fillers for selected PEEK composites

Thermoplastic materials are known to have poor creep resistance compared to thermosets such as epoxy and phenolic resins (Flöck et al. 1999). Creep is the time dependent permanent deformation of a material under constant load (Callister 2006). Thermoplastic materials, including PEEK, behave in a viscoelastic manner and exhibit viscoelastic creep. Incorporation of short fibre fillers serve not only to improve the pure mechanical properties of PEEK, but also to improve the viscoelastic properties as discussed by Zhang et al (2004).

In order to quantify the mechanical and viscoelastic response of the PEEK composites selected in Chapter 3, a series of tests was carried out as described in the following sections.

## *7.2. Static load testing method*

During dynamic testing it was identified that the axial displacement measurement was not a single measure of wear. Rather, the axial displacement was a composite value consisting of the following measurements:-

- Wear
- Instantaneous strain of the composite material
- Creep (time dependent strain) of the composite material
- Thermal expansion of the composite material
- Strain compliance of the test apparatus loaded metallic components
- Thermal expansion of the test apparatus components

This test method seeks to understand the instantaneous strain and creep characteristics of each of the composite materials, and the effect of the different fillers on these characteristics.

In order to understand the impact of initial strain and creep on the axial displacement measurement a series of tests were undertaken for a selection of the materials. To ensure that the measurements could be consistent with the dynamic tests, the test apparatus described in Chapter 5 was used, shown in Figure 7.4. The test method was consistent with the dynamic tests, however the dynamic aspect was removed to create a static load test. The counterface remained the same giving a contact area of  $100.53\text{mm}^2$ . The applied load was 17.2kN giving a contact pressure of 172Mpa. The dynamic test method states that the applied load of 17.2kN is held for 15 minutes in order to allow for creep displacement to reach a steady state. In this test the load was held for 60 minutes in order to determine the steady state characteristics of the material. All creep tests were carried out at ambient temperature. Load and displacement were recorded at 1Hz through the loading phase and for the duration of the experiment. For justification of the overall test rig design, refer to Chapter 5.

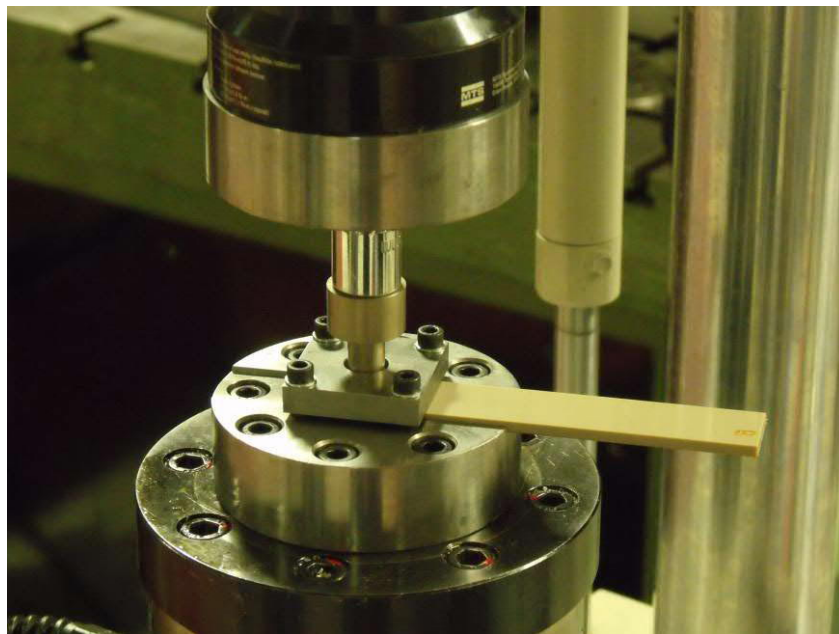


**Figure 7.4- Test rig for compressive load and creep tests**

## Methodology

- 1) Secure top and bottom plates on test rig
- 2) Locate socket and ring counterface head on the top plate
- 3) Identify test areas on sample
- 4) Insert sample into recess
- 5) Lower the top arm
- 6) Apply the required load of 17.2kN
- 7) Hold the load at 17.2kN for 60 minutes
- 8) Record parameters throughout the test using the MTS multipurpose testware PC based software.

### *7.3. Results and Discussion*

This section presents and discusses the results obtained from the static testing described. The results comprise the two aspects tested, the instantaneous strain characteristics and the creep characteristics of the composites. The discussion examines the influence of the various filler materials tested upon the mechanical properties and links these findings back to the mechanical properties given in Section 7.1, which are from published material data from the raw material supplier.

Of particular interest is the time required for the strain exhibited under the high load of 17.2kN (172 MPa contact pressure) to reach a steady state. This is compared with literature to gain an understanding of whether the creep properties at these loads are comparable to those shown at lower loads.

Only the results for Victrex materials are shown. The tests for the Luvocom materials were carried out on a different test bench as the test bench used for Victrex materials had broken down. The recorded axial displacement for these tests was subsequently found to not be accurate due error in the test setup.

Figure 7.5 shows the axial displacement measurements against time for the various PEEK compositions. The graph shows the displacement over the duration of the test of 1 hour (3600 seconds). An initial large displacement can be observed over the first 10 seconds as the load is ramped up to 17.2kN. This represents the instantaneous strain for each material. Subsequently, all materials exhibit further axial displacement, i.e. strain, over the rest of the test duration. Those materials with the lowest initial displacement tend to plateau early on in this period, whereas those with the greatest initial strain exhibit time dependent strain continuing to the end of the test. The displacements observed are large when compared to the wear measurements observed in Chapter 5. For example, 20%w/w PTFE filled PEEK shows a 280 $\mu$ m axial displacement due to elastic deformation and creep alone. In dynamic tests, however, the initial strain and creep observed over the first 15 minutes of the test described in Chapter 5 is not included in the wear measurement, i.e. the axial displacement measurement is zeroed at the point when dynamic motion begins. After the first 15 minutes of static loading, a maximum variation of 9.92 $\mu$ m and 7.29 $\mu$ m is observed in 450G and 450FE20 respectively. This is small compared to the wear observed in tests, and accounts for an error of approximately 0.4% at a wear depth of 3mm.

The values shown in Figure 7.5 do not account for the sample thicknesses, and therefore the axial displacement must be converted to strain to accurately compare composites.

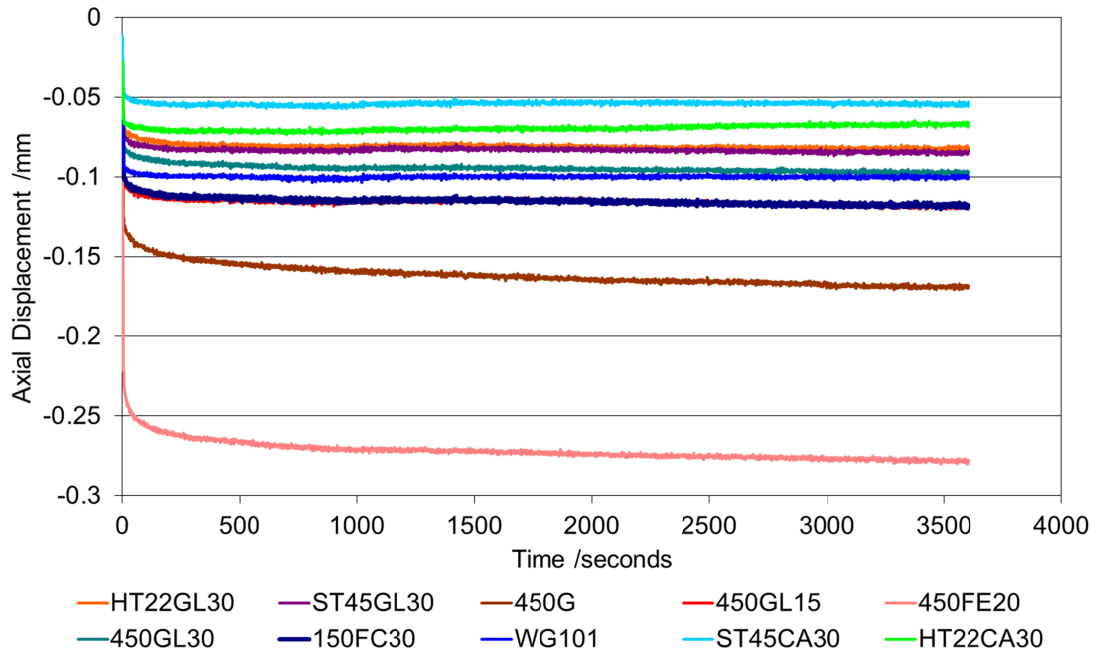


**Figure 7.5 – Axial displacement against time to 3600 seconds for Victrex PEEK composites**

Figure 7.6 shows strain against time for the selected PEEK composites. The results show that the carbon fibre filled composites exhibit the best performance, with 30%w/w carbon fibre filled PEEK (ST45CA30) reaching a maximum strain of 1.45 after 900 seconds. Glass filled materials perform well compared to unfilled PEEK (450G). 15%w/w PEEK (450GL15) reaches a maximum strain of 2.9% compared to unfilled PEEK at 4%. Increasing the filler weight fraction improves both initial strain and creep response with 30%w/w glass fibre filled PEEK (450GL30) achieving 2.4% strain. The specimen containing 20%w/w PTFE filled PEEK (450FE20) had a thickness of 6mm, compared to 4mm for unfilled PEEK. When converting the values of axial displacement shown in Figure 7.5 to strain, the large difference in axial displacement of 450FE20 compared to 450G becomes much closer to the values observed. This shows that addition of PTFE has minimal impact upon the compressive and viscoelastic properties of the PEEK matrix.

Overall, the magnitude of strain observed in all materials is relatively low. The AS81820C specification allows for a maximum moulded liner thickness of 550 $\mu\text{m}$ . For the worst performing materials, 450G and 450FE20, this would mean an expected deformation of 22 $\mu\text{m}$  at ambient temperature. This would be acceptable from a design perspective.

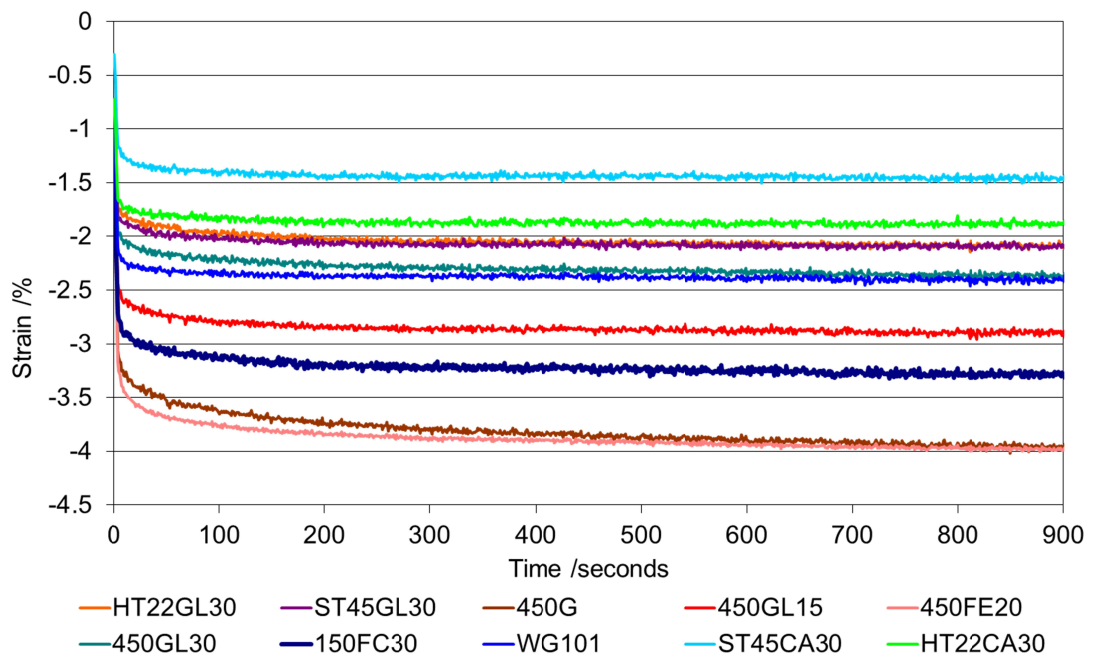


**Figure 7.6 - Strain against time to 900 seconds for Victrex PEEK composites**

Figure 7.7 shows the maximum strain at 60 minutes against weight fraction of structural fillers for the PEEK composites tested. As expected, increasing the weight fraction of structural fillers leads to a lower magnitude of strain and viscoelastic creep. The results agree with mechanical performance from literature and rank the filler materials in the same order. Again, carbon fibre fillers show a significant performance enhancement compared to glass fibre fillers.

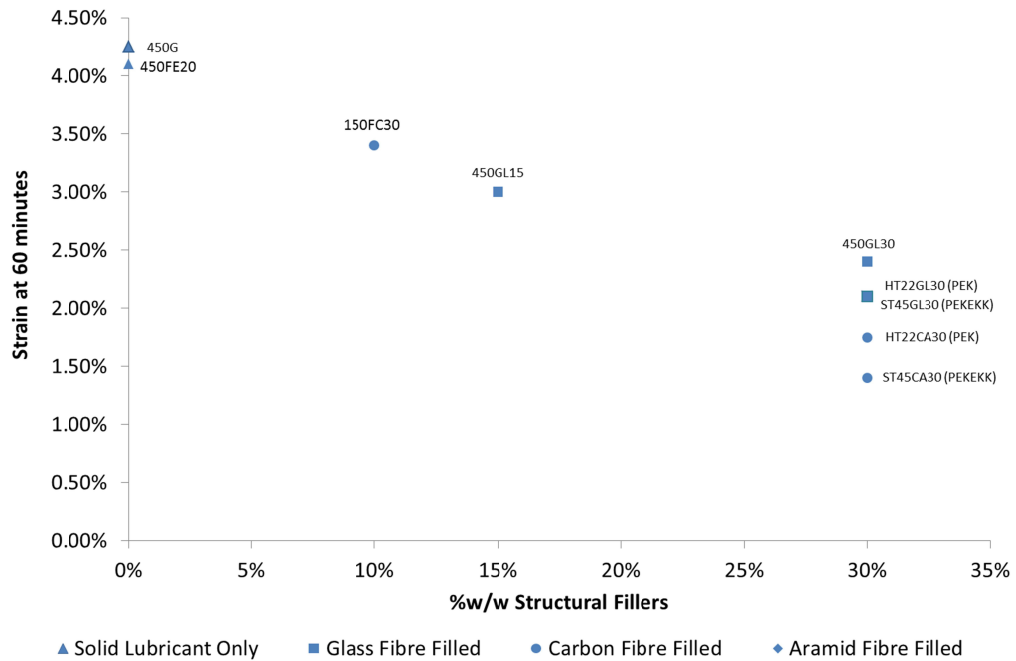


**Figure 7.7 - Strain at 60 minutes against weight fraction of structural fillers for PEEK composites**

Whilst the selected composite materials supplied by Luvocom did not yield accurate test data for analysis, failure of some of the composites was observed. Compositions 1105-8165 (10%w/w carbon fibre and 40%w/w graphite filled PEEK) and 1105-8613 (10%w/w carbon fibre, 20% PTFE and 10% graphite filled PEEK) exhibited brittle failure as the load was applied. Composition 1105-8613 failed catastrophically in compression, whereby the material shattered into small pieces leaving a fine powder residue. This was indicative of poor cohesion of the PEEK matrix and the filler materials. This is likely as the loading of solid particles was very high, 50% by weight and 38% by volume, the highest of all the selected materials. Composition 1105-8613 failed by cracking only. This could be due to poor alignment of the counterface causing a high initial contact pressure leading to local material yield.

#### *7.4. Conclusions*

The mechanical performance of the PEEK composites investigated show that inclusion of glass and carbon fibres have a positive impact upon tensile strength. Carbon fibres give the best improvement in mechanical performance compared to glass and Aramid fibres for a significantly lower volume fraction of fillers. Aramid fibres do not improve the tensile strength of the composite however they do give an improvement in elastic modulus, though less than that of carbon and glass fibres.

Creep tests show that materials with good tensile strength exhibit good creep resistance. The ranking of materials for creep resistance follows that of tensile strength. Carbon fibre filled composites exhibit the best creep resistance, then glass fibre filled materials, whilst composites without structural fillers performed the worst.

It is recommended that carbon fibres are used as the structural component in any future composite development.

## 8. Developing PEEK composite blends

Previous chapters have focussed on characterising and understanding the tribological and mechanical performance of PEEK composites as a self-lubricating material in high load, low speed conditions. This chapter provides a summary discussion bringing together the experimental chapters and describes how this knowledge has been used to develop two composite materials. The materials have been developed to give good friction and wear performance whilst having mechanical properties suitable for the high load being exerted upon the material. One material incorporates molybdenum disulphide ( $\text{MoS}_2$ ) firstly as it was expected that it would give a higher performance enhancement than the addition of graphite, but also to compare it directly against the same material combination without  $\text{MoS}_2$  present.

### 8.1. Summary discussion of experimental work

Chapters 5 to 7 have presented the experimental work undertaken to develop an understanding of PEEK composites in tribology, morphology and mechanical performance. Each chapter has considered the performance with respect to each aspect individually, whereas in order to identify material compositions capable of meeting the performance requirements for the application, all aspects must be considered together.

The conclusions drawn from the tribological tests suggest that inclusion of PTFE is necessary to ensure good friction performance. This performance then translates to good wear performance due to low frictional heating causing mechanical failure of the composite. This is evident from the exceptional performance of 20%w/w PTFE filled PEEK (Viktrex 450FE20). Chapter 7 shows that inclusion of PTFE has a small negative impact upon mechanical performance of the composite. Viktrex 450FE20 give the

worst mechanical performance with the highest level of strain and creep. The tensile strength and elastic modulus of this composition is the lowest of all of the compositions, with 78MPa and 2.9GPa respectively. At high temperature, 163°C, this composition is unable to carry the test load of 172MPa and fails due to plastic deformation. It is therefore necessary to include a structural component in order to enhance the mechanical performance of the composite.

In order to enhance the mechanical performance of the composite, the inclusion of structural fillers is necessary. Aramid fibres exhibit significantly better tribological performance than both carbon fibres (CF) and glass fibres (GF). The observed friction coefficient is approximately half that of both carbon and glass filled compositions. Wear life shows improvement with the inclusion of Aramid fibres compared to unfilled and CF and GF reinforced composites. The wear life of 30%w/w Aramid fibre filled PEEK (1105-8487) is approximately 10,000 cycles to 1mm wear depth, whereas the average for 30%w/w CF and GF filled composites are 4000 and 1000 cycles respectively. The results of Chapter 7, however, show that the worst performance with respect to the mechanical and creep properties of the composite is exhibited by Aramid fibres. The best performance derives from the inclusion of carbon fibre fillers. The performance of composites containing only structural fillers without solid lubricants is not at the level required for the application discussed. It is therefore necessary to include structural fillers into the final composition. By combining carbon fibre fillers with PTFE, it is expected that optimum performance with respect to mechanical and tribological performance can be achieved, balancing both properties. This is generally found to be the case for the testing at low contact pressures and high sliding velocities presented in literature.

Zhang et al (2004) conclude that a composite of PEEK containing 10%v/v PTFE, 10%v/v graphite and 20%v/v carbon fibres offer optimal wear performance.

Furthermore, they conclude that the wear performance has a slight dependence upon the mechanical properties of the composite. They carried out tests at 1MPa contact pressure and 1m/s sliding velocity in a block-on-ring set up. The high contact pressures used seen in this study lead to a much higher dependence of wear performance upon mechanical properties of the composite.

Lu and Friedrich (1995) conclude that addition of PTFE improves the wear performance to a minimum in the range of 5%w/w to 40%w/w. They also concluded that the inclusion of up to 20%w/w carbon fibres improves the friction performance.

The conclusions drawn by Rasheva et al (2010) illustrate the balance of mechanical and tribological performance shown in this thesis. They conclude that low solid lubricant content and high short carbon fibre content tends to exhibit higher wear rates, however suggest that the higher CF content is good for mechanical performance of the composite. Higher solid lubricant content and lower CF content gives the most stable wear behaviour. At the testing conditions described in Chapter 5, the very high contact pressures of 172MPa mean that there is larger impact of this balance of properties.

## *8.2. PEEK composite blends*

***This section has been removed for copyright reasons and/or confidentiality reasons***

***This section has been removed for copyright reasons and/or  
confidentiality reasons***

***This section has been removed for copyright reasons and/or  
confidentiality reasons***

***This section has been removed for copyright reasons and/or  
confidentiality reasons***

***This section has been removed for copyright reasons and/or  
confidentiality reasons***

***This section has been removed for copyright reasons and/or  
confidentiality reasons***

## 9. Conclusions and future work

### 9.1. Summary of conclusions

The design of experiments undertaken described in Chapter 4 for injection moulding of thermoplastic materials gave an indication of the most influential factors on final part geometry. When considering the final mass of the part produced, holding pressure had the biggest impact. Injection pressure and barrel temperature gave a small impact for all materials. Barrel temperature was insignificant for all materials except polystyrene. This is due to the sensitivity of the material to the melt temperatures selected for the experiment. The injection flow did not have a significant impact upon mould filling. Comparison between materials shows a correlation between factors with significant and insignificant impact. Selection of parameter values were arbitrarily chosen for each material, with some more appropriate than others. It is therefore difficult to draw analogies between materials. Holding pressure is the most significant factor across materials.

The design of experiments method proved to give a good indication of the impact of each parameter for all materials.

PEEK composites have been shown to be a promising choice for self-lubricating sliding contacts in high load aerospace applications. Compositions containing PTFE showed significant reduction of friction coefficient. Frictional heating causes a reduction in mechanical properties due to softening of the PEEK matrix, so by reducing the friction coefficient, premature mechanical failure can be avoided. 20%w/w PTFE filled PEEK showed the best friction and wear performance across all composites. Compositions containing MoS<sub>2</sub> and graphite showed good performance, though in all cases this was coupled with the inclusion of PTFE. Testing in Chapter 8 showed that the inclusion of

MoS<sub>2</sub> reduced wear performance and had no impact on friction performance and mechanical properties.

Inclusion of glass and carbon fibres had no impact upon friction coefficient, whilst Aramid fibres reduced this by approximately one half. Glass fibres exhibited the worst wear performance, whilst carbon fibres show better performance than glass. Aramid only filled PEEK exhibited the best wear performance with approximately 10,000 cycles completed before rapid wear initiated.

The test method developed in Chapter 5 gave good comparative performance results for all materials. The accuracy of measurements can be improved, especially at the start of the tests when thermal expansion clouds the wear measurement. It is suggested that bearing tests are carried out with a selection of the materials to validate whether the same ranking of performance is observed, thus validating the test method.

One of the key assumptions made in this work is that there is a random orientation and good dispersion of fibres and fillers. This leads to the assumption that the materials tested can be considered homogeneous and isotropic for both mechanical and tribological properties. The analysis carried out in Chapter 6 validates this assumption. It is suggested that a full three dimensional analysis of fibre and filler orientation and distribution is carried out in order to quantify the degree of alignment and therefore anisotropy of the composites. Fibre filled materials may see some impact of surface alignment in tribological tests, however the effect of this is expected to be small as fillers reach the surface and alignment parallel to the surface is minimal.

***This section has been removed for copyright reasons and/or confidentiality reasons***

## ***9.2. Future Work***

Alternative materials should be investigated, such as thermoset materials, as their performance has been proven by both traditional bearing solutions as well as commercially available technologies from Kamatics.

It is recommended to perform a deeper investigation into the injection moulding process to include material morphology and fibre and filler orientation and dispersion.

It is recommended to explore alternative manufacturing processes for the developed technologies, as the nature of high volume injection moulding is not necessarily aligned with the small batch nature of high performance aerospace parts.

As the testing carried out in this work has been on a coupon scale, materials need to be incorporated into a full bearing design so that performance can be validated in conditions more representative of the application conditions.

## 10. References

Altan, M. 2010. Reducing shrinkage in injection moldings via the Taguchi, ANOVA and neural network methods. *Materials & Design* 31(1), pp. 599–604.

Arburg GmbH 2016. Arburg Allrounder 370E [Online] Available at: [https://www.arburg.com/fileadmin/redaktion/bilder/presse\\_300dpi/arburg\\_30206\\_allrounder\\_370e.jpg](https://www.arburg.com/fileadmin/redaktion/bilder/presse_300dpi/arburg_30206_allrounder_370e.jpg) [Accessed: 29 March 2016].

Archard, J. 1953. Contact and rubbing of flat surfaces. *Journal of applied physics* 24(8), pp. 981–988.

Archard, J.F. and Hirst, W. 1956. The wear of metals under unlubricated conditions. In: *Proceedings of the Royal Society of London A: Mathematical, Physical and Engineering Sciences*. The Royal Society, pp. 397–410.

ASTM International 2007. *Terminology for Composite Materials*. ASTM International.

Basil, L. 2011. Private Communication.

Bell, A. 2009. *ARD511: Wear Hypothesis for SKF Airframe Self-lubricating Bearing Technology*. SKF Ltd.

Bhushan, B. 2000. *Modern Tribology Handbook, Two Volume Set*. CRC Press.

Booser, R.. 1988. *CRC Handbook of Lubrication. Theory and Practice of Tribology, Volume II: Theory and Design*. CRC Press.

Bowden, F.P. et al. 1951. The friction and lubrication of solids. *American Journal of Physics* 19(7), pp. 428–429.

Callister, W.D. 2006. *By William D. Callister - Materials Science and Engineering: An Introduction*. 7th Edition edition. John Wiley & Sons.

Campbell, F.C. 2003. *Manufacturing Processes for Advanced Composites*. Elsevier.

Davim, J.P. and Cardoso, R. 2006. Tribological behaviour of the composite PEEK-CF30 at dry sliding against steel using statistical techniques. *Materials & Design* 27(4), pp. 338–342.

Davim, J.P. and Cardoso, R. 2009. Effect of the reinforcement (carbon or glass fibres) on friction and wear behaviour of the PEEK against steel surface at long dry sliding. *Wear* 266(7–8), pp. 795–799.

De, S.K. and White, J.. 1996. *Short Fibre-Polymer Composites*. Woodhead Publishing.

Dowson, D. 1998. *History of tribology*. 2nd ed. London: Professional Engineering Publishing.

DuPont 2012. Fluoropolymer Comparison - Typical Properties [Online] Available at: [http://www2.dupont.com/Teflon\\_Industrial/en\\_US/tech\\_info/techinfo\\_compare.html](http://www2.dupont.com/Teflon_Industrial/en_US/tech_info/techinfo_compare.html) [Accessed: 1 April 2012].

Engelbach, R. 1923. *The Problem of the Obelisks: From a Study of the Unfinished Obelisk at Aswan*. TF Unwin, limited.

Erzurumlu, T. and Ozelik, B. 2006. Minimization of warpage and sink index in injection-molded thermoplastic parts using Taguchi optimization method. *Materials & Design* 27(10), pp. 853–861.

Flöck, J. et al. 1999. On the friction and wear behaviour of PAN- and pitch-carbon fiber reinforced PEEK composites. *Wear* 225–229, Part 1, pp. 304–311.

Friedrich, K. 1985. SHORT FIBER/THERMOPLASTIC MATRIX COMPOSITES. In: pp. 197–207.

Friedrich, K. et al. 1995. Recent advances in polymer composites' tribology. *Wear* 190(2), pp. 139–144.

Friedrich, K. et al. 2005. Effects of various fillers on the sliding wear of polymer composites. *Composites Science and Technology* 65(15–16), pp. 2329–2343.

Gay, R. 2013. Friction and wear behaviour of self lubricating bearing liners. Cardiff University.

Gay, R. 2014. Heat Generated at Contact - Ring on Disc.

Geim, A.K. and Novoselov, K.S. 2007. The rise of graphene. *Nature materials* 6(3), pp. 183–191.

Giltrow, J.P. 1973. Friction and wear of self-lubricating composite materials. *Composites* 4(2), pp. 55–64.

Goodship, V. ed. 2004. *Arburg Practical Guide to Injection Moulding*. Shawbury: Smithers Rapra Technology.

Häger, A.M. et al. 1993. Selected thermoplastic bearing materials for use at elevated temperatures. *Wear* 162–164, Part B, pp. 649–655.

Hedayati, M. et al. 2012. Tribological and mechanical properties of amorphous and semi-crystalline PEEK/SiO<sub>2</sub> nanocomposite coatings deposited on the plain carbon steel by electrostatic powder spray technique. *Progress in Organic Coatings* 74(1), pp. 50–58.

Hexcel 2016. as4.pdf [Online] Available at: <http://www.hexcel.com/resources/datasheets/carbon-fiber-data-sheets/as4.pdf> [Accessed: 29 March 2016].

Hutchings, I.M. 1992. *Tribology: Friction and Wear of Engineering Materials*. Edward Arnold.

Jost, H.P. 1966. *Lubrication: Tribology; Education and Research; Report on the Present Position and Industry's Needs (submitted to the Department of Education and Science by the Lubrication Engineering and Research) Working Group*. HM Stationery Office.

Lancaster, J.K. 1971. Estimation of the limiting PV relationships for thermoplastic bearing materials. *Tribology* 4(2), pp. 82–86.

Lancaster, J.K. 1972. Polymer-based bearing materials: The role of fillers and fibre reinforcement. *Tribology* 5(6), pp. 249–255.

Lancaster, J.K. 1979. Accelerated wear testing of PTFE composite bearing materials. *Tribology International* 12(2), pp. 65–75.

Layard, A.H. 1853. *Discoveries in the Ruins of Nineveh and Babylon: With Travels in Armenia, Kurdistan and the Desert*. John Murray.

Lu, Z.P. and Friedrich, K. 1995. On sliding friction and wear of PEEK and its composites. *Wear* 181–183, Part 2, pp. 624–631.

Matweb 2016. Online Materials Information Resource - MatWeb [Online] Available at: <http://www.matweb.com/index.aspx> [Accessed: 23 March 2016].

Meng, H.C. and Ludema, K.C. 1995. Wear models and predictive equations: their form and content. *Wear* 181, pp. 443–457.

Mlekusch, B. et al. 1999. Fibre orientation in short-fibre-reinforced thermoplastics I. Contrast enhancement for image analysis. *Composites Science and Technology* 59(4), pp. 543–545.

National Research Council 1996. *Accelerated Aging of Materials and Structures: The Effects of Long-Term Elevated-Temperature Exposure*. Washington, D.C.: National Academies Press.

Newberry, P.E. et al. 1893. El Bersheh, Part 1,(The tomb of Tehuti-Hetep). . Available at: <http://www.researchonline.mq.edu.au/vital/access/manager/Repository/mq:100> [Accessed: 28 February 2016].

Park, K. and Ahn, J.-H. 2004. Design of experiment considering two-way interactions and its application to injection molding processes with numerical analysis. *Journal of Materials Processing Technology* 146(2), pp. 221–227.

Petrie, E. 2012. *Extreme High Temperature Thermoplastics - Gateway to the Future or the Same Old Trail?*

Pötsch, G. and Michaeli, W. 2008. *Injection Molding: An Introduction*. Carl Hanser Publishers.

Prime, B. An Introduction to Thermosets. . Available at: [www.primethermosets.com/introtothermosets.pdf](http://www.primethermosets.com/introtothermosets.pdf) [Accessed: 13 December 2011].

Ralph, C. et al. 2015. *Mechanics of Composite and Multi-functional Materials, Volume 7: Proceedings of the 2015 Annual Conference on Experimental and Applied Mechanics*. Springer.

Rasheva, Z. et al. 2010. A correlation between the tribological and mechanical properties of short carbon fibers reinforced PEEK materials with different fiber orientations. *Tribology International* 43(8), pp. 1430–1437.

Rhee, S.K. 1970. Wear equation for polymers sliding against metal surfaces. *Wear* 16(6), pp. 431–445.

Rutland Plastics Ltd 2016. Moulding Machine Ig.jpg (JPEG Image, 1094 x 595 pixels) [Online] Available at: <http://www.rutlandplastics.co.uk/images/Moulding%20Machine%20Ig.jpg> [Accessed: 29 March 2016].

SAE 2008. *Bearings, Plain, Self-Aligning, Self-Lubricating, Low Speed Oscillation*. SAE.

Sha, B. et al. 2007. Investigation of micro-injection moulding: Factors affecting the replication quality. *Journal of Materials Processing Technology* 183(2–3), pp. 284–296.

Tang, Q. et al. 2010. Tribological behaviours of carbon fibre reinforced PEEK sliding on silicon nitride lubricated with water. *Wear* 269(7–8), pp. 541–546.

Tang, S.H. et al. 2007. The use of Taguchi method in the design of plastic injection mould for reducing warpage. *Journal of Materials Processing Technology* 182(1–3), pp. 418–426.

Unal, H. et al. 2004. Sliding friction and wear behaviour of polytetrafluoroethylene and its composites under dry conditions. *Materials & Design* 25(3), pp. 239–245.

Victrex 2011a. Injection Moulding Guide.

Victrex 2011b. *Materials Properties Guide*. Victrex.

Voss, H. and Friedrich, K. 1987. On the wear behaviour of short-fibre-reinforced peek composites. *Wear* 116(1), pp. 1–18.

Williams, J. 1994. *Engineering Tribology*. New York: Oxford University Press.

Wu, Y.. *How short aramid fiber improves wear resistance*.

Yamamoto, Y. and Hashimoto, M. 2004. Friction and wear of water lubricated PEEK and PPS sliding contacts: Part 2. Composites with carbon or glass fibre. *Wear* 257(1–2), pp. 181–189.

Zhang, G. et al. 2008. Effects of sliding velocity and applied load on the tribological mechanism of amorphous poly-ether–ether–ketone (PEEK). *Tribology International* 41(2), pp. 79–86.

Zhang, G. et al. 2010. Friction and wear variations of short carbon fiber (SCF)/PTFE/graphite (10 vol.%) filled PEEK: Effects of fiber orientation and nominal contact pressure. *Wear* 268(7–8), pp. 893–899.

Zhang, Z. et al. 2004. Wear of PEEK composites related to their mechanical performances. *Tribology International* 37(3), pp. 271–277.

# APPENDIX A

